Metal Complexes as Catalysts/Moderators for Polymerization Reactions

Christophe Fliedel, Samuel Dagorne, Erwan Le Roux

Metal Complexes as Catalysts/Moderators for Polymerization Reactions

Christophe Fliedel*
LCC-CNRS, Université de Toulouse, CNRS, 205 route de Narbonne, 31400 Toulouse, France
christophe.fliedel@lcc-toulouse.fr
+33 561 333 166

Samuel Dagorne*
Institut de Chimie (UMR CNRS 7177), Université de Strasbourg, 4 rue Blaise Pascal, 67000 Strasbourg, France
dagorne@unistra.fr
+ 33 368 851 530

Erwan Le Roux*
Chemistry Department, University of Bergen, Allégaten 41, N5007, Bergen, Norway
Erwan.LeRoux@uib.no

* Corresponding author

Abstract
This chapter highlights the most representative results on the use of coordination compounds in polymerization reactions, since the version of the *Comprehensive Coordination Chemistry II* by Gibson and Marshall (2003). Noteworthy developments of more efficient catalysts and related significant advancements in coordination polymerization of olefins, radical polymerization, lactide and related cyclic esters polymerization and CO_2/epoxides polymerization are discussed therein.

Keywords
Coordination polymerization – Radical Polymerization – Ring-opening polymerization – Ethylene – Olefin – Lactide – Cyclic esters – Carbon dioxide – Epoxides – Transition metals – Group 3 metals – Group 4 metals – Group 13 metals – Lanthanides – Metallocenes

Abbreviations

AGET	Activators generated by electron transfer
AIBN	2,2‘-Azobis(isobutyronitrile)
ARGET	Activators regenerated by electron transfer
ATRP	Atom transfer radical polymerization
BD	1,3-Butadiene
BDE	Bond dissociation energy
Bipy	2,2’-Bipyridine
CCT	Catalytic chain transfer
CHO	Cyclohexene oxide
1,4-CHDO	1,4-Cyclohexadiene oxide

Cp	Cyclopentadienyl
Cp*	Pentamethylcyclopenadienyl
CPO	Cyclopentene oxide
CPC	Cyclopropylene carbonate
CGC	Constrained geometry catalyst
Đ	Dispersity (M_w/M_n)
DMAP	4-(Dimethylamino)pyridine
DT	Degenerative transfer
EBiB	Ethyl 2-bromoisobutyrate
EBP	Ethyl 2-bromopropionate
EBrPA	Ethyl 2-bromophenylacetate
EDG	Electron-donating group
EWG	Electron-withdrawing group
GPE	Glycidyl phenyl ether
Hex	1-Hexene
IP	Isoprene
LAM	Less activated monomer
MAM	More activated monomer
MA	Methyl acrylate
Me_6TREN	Tris(2-(dimethylamino)-ethyl)amine
MMA	Methyl methacrylate
MVE	Methyl vinyl ether
MW	Molecular weight
*n*BA	*n*-Butyl acrylate
NHC	*N*-heterocyclic carbene
NVP	*N*-vinylpyrrolidone
OMRP	Organometallic mediated radical polymerization
PCHC	Poly(cyclohexene carbonate)
PCHDC	Poly(1,4-cyclohexadiene carbonate)
PCHO	Poly(cyclohexene oxide)
P_{CO2}	Pressure of CO_2
PCPC	Poly(cyclopentene carbonate)
PEBr	1-Phenylethyl bromide
PLA	Poly(lactic acid) or polylactide
PO	Propylene oxide
PPC	Poly(propylene carbonate)
PPN	Bis(triphenylphosphine)iminium
PRE	Persistent radical effect
PTHFC	Poly(3,4-tetrahydrofuran carbonate)
RDRP	Reversible deactivation radical polymerization
ROP	Ring-opening polymerization
RT	Reversible termination
SARA	Supplemental activator and reducing agent
SO	Styrene oxide

SR&NI	Simultaneous reverse and normal initiated
St	Styrene
T	Temperature
taa	Tetraazaannulene
TOF	Turnover frequency
TMP	Tetramesitylporphyrin
TPMA	Tris(2-pyridylmethyl)amine
V-70	2,2'-Azobis(4-methoxy-2,4-dimethyl valeronitrile)
VAc	Vinyl acetate
VC	Vinyl chloride
v-CHO	Vinyl-cyclohexene oxide
VF	Vinyl fluoride

1. Introduction

Today, metal-mediated polymerization reactions offer access to a wide range of polymeric materials, such as polyolefins, polyacrylates, polyesters and polycarbonates, with complex architectures and specific properties, that can be produced from petrochemical- or renewable-resources. Everything started with the seminal work of Ziegler and Natta (Nobel prize in 1963) that paved the way to many developments in the field of coordination polymerization of olefins, which is now performed with (pre)catalysts of various metals and applied to numerous polar and apolar monomers.

In the last decades, several other polymerization techniques that make use of a coordination compound as catalyst or moderator, such as radical polymerization and ring-opening polymerization, were developed, improved and are now commonly used in industrial processes.

The present chapter focuses on recent and significant developments in the fields of coordination polymerization of olefins, metal-mediated radical polymerization, cyclic esters polymerization and CO_2/epoxide copolymerization, with a special emphasis in (pre)catalysts design and polymerization performances.

2. Coordination Polymerization of Olefins

2.1. Introduction

Due to the increasing demand of polymeric materials, especially high-added value polymers for high-tech applications, the development of highly efficient metal catalysts is still a very active field of research. The objective of the present section is to provide an overview of notable classes of olefin polymerization catalysts, to introduce recent, representative and significant examples and to guide the readers towards selected and/or specific reviews for more details or critical discussions.

2.2. Metallocene, *ansa*-Metallocene and Constrained Geometry Catalysts

Since the pionneering studies showing the applicability of $[Cp_2MX_2]$ (M = Ti, Zr and X = Br, Cl) complexes to ethylene polymerization, a large variety of rare-earth and Group 4 metallocene catalysts were developed and applied to the polymerization of ethylene and various α-olefins. All these advances were already well-reviewed (**2.1**, Figure 2.1).[1-4]

Following the discovery of the metallocene catalysts, considerable efforts have been dedicated to the development of stereoselective catalysts to control the microstructure of the resulting polymeric material. It was found that the main factor influencing the tacticity of the final polymer was the symmetry of the metallocene. As a result, many investigations were oriented to related *ansa*-metallocenes of rare-earth, Group 4 and Group 5 metals, which are related compounds where the two arenes (Cp, fluorenyl, indenyl and derivatives) are linked by a bridging moiety that can be a single atom (C, Si, Ge, Sn) or a longer chain (**2.2**, Figure 2.1). The resulting catalysts, with *e.g.* C_2-, C_1-, C_s-symmetry, effectively produced polyolefins with high tacticity (isotactic or syndiotactic), and this important breakthrough was well-summarized and discussed in several reviews.[1-2, 4-7] In particular, Wang examined how the nature of the bridging group in such *ansa*-metallocenes affects the activity and stereoselectivity of the catalysts.[5] Recently, a series of allyl *ansa*-lanthanidocenes were shown to act as single-component catalysts for the polymerization of styrene (St), producing highly syndiotactic polySt ($[r]^5$ = 63–88%; T_m up to 260 °C),[8] and the syndioselective copolymerization of St

with ethylene ([*r*][5] = 71%, 1-15 mol% ethylene content).[9] Sterically congested complexes or those based on small ionic radius metals (yttrium or scandium) were poorly or not active under the studied polymerization conditions.

Constrained geometry catalysts (CGCs) were further developed with the aim of improving the thermal stability of the catalysts and the production of higher MW polymers (**2.3**, Figure 2.1). CGCs exhibited great performances in ethylene polymerization and copolymerization with higher α-olefins, which were attributed to a more open coordination sphere, a small ligand bite-angle and a reduced tendency to undergo chain transfer, compared to metallocenes.[2, 4, 10-12] Recently, a series of rare-earth metal dialkyl CGCs, based on a pyridyl-methylene-fluorenyl ligand, exhibited high activity and remarkable to perfect syndioselectivity for the polymerization of St,[13] *ortho*-fluorostyrene,[14] and 1-phenyl-1,3-butadiene (high 3,4-regioselectivity).[15]

The aforementioned classes of catalysts were subjected to extensive patenting, triggering new research directions in the field, such as the development of post-metallocene catalysts (see following sections).[16]

Noteworthy, metallocenes and derivatives were not limited to the polymerization of ethylene and non-polar α-olefins and were found to be efficient catalysts for the polymerization of polar monomers, such as (meth)acrylates and (meth)acrylamides, and their copolymerization with non-polar olefins.[17]

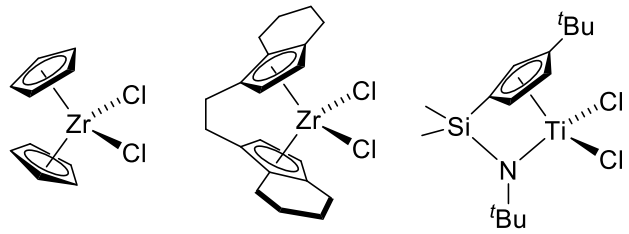

2.1 Metallocene | **2.2** *ansa*-Metallocene | **2.3** Constrained geometry catalyst (CGC)

Figure 2.1. Examples of metallocene, *ansa*-metallocene and constrained geometry catalysts used in olefin polymerization.

2.3. Post-Metallocene Catalysts

Comprehensive overviews of the research activities accomplished until the end of the 2000's in the fields of metal-catalyzed polymerization, *via* coordination polymerization mechanisms, of polar[17] and apolar olefins are available,[2, 18-19] and therefore the following sections will focus on more recent significant coontributions.

2.3.1. Rare-Earth Metal Catalysts

Rare-earth metal complexes of C,C,C-pincer bis-NHC ligands (**2.4**, Figure 2.2) exhibited high activity and *cis*-1,4-selectivity (up to 99.6%) for isoprene (IP) polymerization upon activation with AlR_3 (R = Me, Et, ^{i}Bu) and $[Ph_3C][B(C_6F_5)_4]$.[20]

The NHC-amidino lutetium dialkyl complex **2.5** (Figure 2.2) polymerized IP with high activity, 3,4-regioselectivity (up to 99.3%), affording polymeric materials with low MWDs, high glass-transition temperatures and moderate syndiotacticity.[21] The livingness of the process allowed further chain-

extention *via* ROP of ε-CL, to produce poly(3,4-IP)-*b*-polycaprolactone block copolymers with controllable molecular weight and narrow dispersity.

The rare-earth dialkyl complexes of OMe- and Ph_2PO-functionalized amidinate-type ligands (**2.6**, Figure 2.2) exhibited high activities in IP polymerization (organoborate and Al^iBu_3 cocat.), affording the corresponding polymeric materials with good *trans*- and *cis*-1,4-selectivity (≈ 96%), respectively.[22-23]

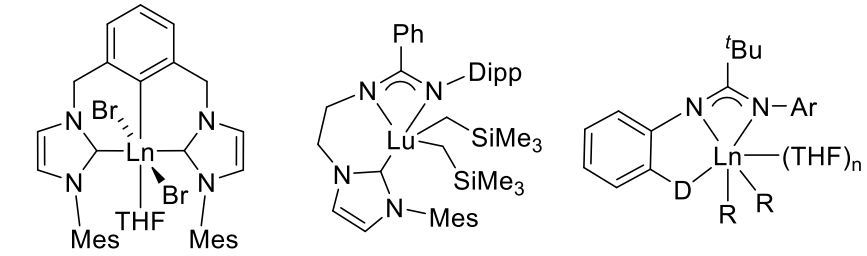

2.4
Ln = Y, Nd, Gd, Dy, Ho

2.5

2.6
Ln = Y, Er, Lu
R = CH_2SiMe_3
D = OMe, $(O)PPh_2$

Figure 2.2. Rare-earth metal complexes of NHC-based ligands used in IP polymerization.

A series of rare-earth metal complexes of bis- and tris(pyrazolyl)-based ligands were developed for applications in polymerization reactions (**2.7**-**2.10**, Figure 2.3). While complexes **2.7**, activated with MAO, exhibited only moderate activities in ethylene polymerization,[24] the other heteroscorpionate bis(pyrazolyl)-based complexes (**2.8**-**2.9**) and the tris(pyrazolyl)borate complex **2.10** showed high activities (up to 3.2 x 10^6 g mol^{-1} h^{-1} atm^{-1}) when activated with MAO and $[Ph_3C][B(C_6F_5)_4]$, respectively.[25-26]

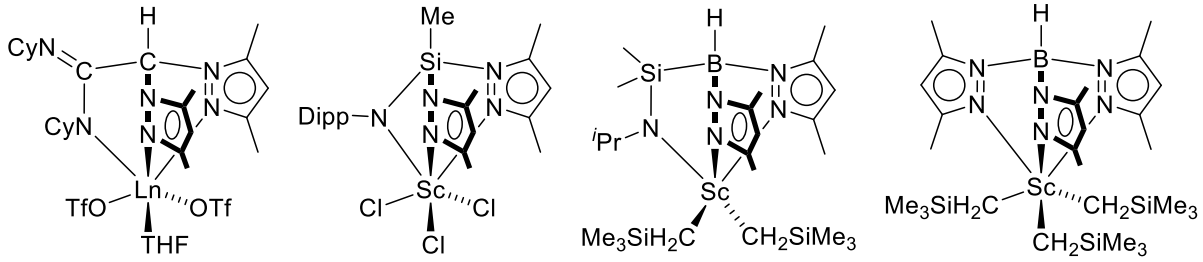

2.7
Ln = Sc, Y, La,
Nd, Sm, Dy, Yb

2.8

2.9

2.10

Figure 2.3. Rare-earth metal complexes of bis- and tris(pyrazolyl)-based ligands used in ethylene polymerization.

The dicationic scandium complex of a C_3-chiral tris(oxazoline) ligand, *in-situ* generatd from the trialky precursor (**2.11**, Figure 2.4) and 2 equiv. $[Ph_3C][B(C_6F_5)_4]$, exhibited high activity (up to 3.6 x 10^7 g mol^{-1} h^{-1}) for the polymerization of 1-hexene (Hex), producing high molecular weight polymeric materials (up to 7.5 x 10^5 g mol^{-1}) with narrow to moderately broad dispersities (*Đ* = 1.18-2.36) and high degree of isotacticity ([*mmmm*] = 90%).[27] The corresponding, *in-situ* generated, dicationic thulium complex was found to promote the isospecific ([*mmmm*] = 89-95%) polymerization of Hex, 1-heptene and 1-octene with high activities.[28] After activation with 1 equiv. of a borate, the rare-earth metal complexes of a chiral bis(oxazoline)amido ligand (**2.12**, Figure 2.4) showed good to high

activities (up to 2.0 x 10^5 g mol^{-1} h^{-1}) and remarkable *trans*-1,4-selectivity (up to 100%) for the polymerization of IP, affording polyIP with moderate MW and narrow to moderately broad MWDs (*Đ* = 1.14-2.66).[29]

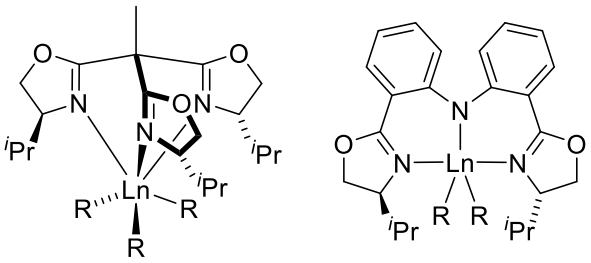

2.11
Ln = Sc, Tm
R = CH_2SiMe_3

2.12
Ln = Sc, Lu
R = CH_2SiMe_3

Figure 2.4. Rare-earth metal complexes of bis- and tris(oxazoline)-based ligands used in polymerization.

Combinations of rare-earth metal complexes of N,N,N-tridentate pyrrolyl-based ligands (**2.13**) and $[Ph_3C][B(C_6F_5)_4]$ activator were evaluated in the IP polymerization.[30] While the lutetium derivatives initiated atactic IP polymerization, the scandium ones showed high 3,4-selectivity (87%) and one yttrium complex, a dinuclear species bridged by two ligands that coordinate in mixed η^5:η^5/κ^1:κ^1 coordination modes, exhibited high activity and produced polyIP with high *cis*-1,4-selectivity (94.1%).

In the presence of a borate and an organoaluminum as cocatalysts, dialkyl scandium and lutetium complexes of a 1,3-bis(2-pyridylimino)isoindoline were found to polymerize IP with high activity (up to 1.9 x 10^6 g mol^{-1} h^{-1}) and remarkable *cis*-1,4-selectivity, to afford the corresponding PIP with high MW (up to 6.1 x 10^5 g mol^{-1}) and narrow to moderate MWDs (*Đ* = 1.26-2.08).[31]

Upon activation with an organoborate, such as $[Ph_3C][B(C_6F_5)_4]$ or $[PhNMe_2H][B(C_6F_5)_4]$, scandium and yttrium alkyl complexes of various N,N,N-tridentate azacycloalkane-based ligands (**2.14**) were reported to be highly active catalysts for the polymerization of ethylene (up to ≈ 1 x 10^6 g mol^{-1} h^{-1}).[25, 32-34]

The lutetium (**2.15**, Al^iBu_3 and organoborate cocat.) and neodymium (**2.16**, Mg^nBu_2 and borane or organoborate cocat.) complexes of phosphinimidic-aminopyridine-based ligands were found to be active catalysts for the 3,4- and *trans*-1,4-selective polymerizations of IP, respectively (Figure 2.5).[35] In contrast, upon activation with $[Ph_3C][B(C_6F_5)_4]$ and Al^iBu_3, the $(N,N)_2$-bis-chelate rare-earth metal complexes of a phosphine-aminopyridinyl derived ligand (**2.17**, Figure 2.5) were highly *cis*-1,4-selective (up to 97%). Further studies have shown that the nature of the Ln atom, the steric bulk around it and the presence/absence of the pyridyl donor have strong influence on the 3,4-selectivity with complexes of type **2.15**.[36]

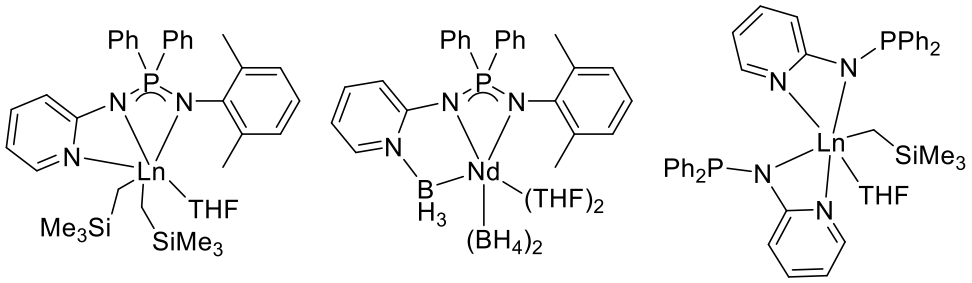

2.15
Ln = Lu, Sc, Y, Er

2.16

2.17
Ln = Sc, Y, Lu

Figure 2.5. Rare-earth metal complexes of phosphinimidic-aminopyridine-based ligands used in IP polymerization.

Upon activation with $[Ph_3C][B(C_6F_5)_4]$ and AlR_3, rare-earth metal complexes of N,C,N-bis(imine)benzene-type ligands (**2.18**, Figure 2.6) were found to be active catalysts for the *cis*-1,4-selective polymerization of dienes, such as butadiene (BD) (up to 99.9%) and IP (up to 98.8%).[37] While the nature of the Ln element had nearly no effect on the selectivity, the latter was influenced by the bulkiness of both the *ortho*-substituent of the *N*-aryl ring of the ligands and the R group of the alkylaluminum cocatalyst.

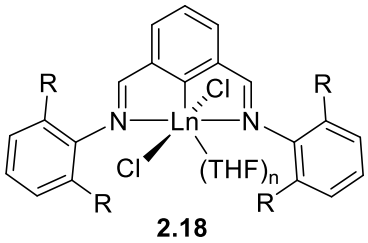

2.18
Ln = Y, La, Nd, Gd, Tb, Dy, Ho, Lu
R = Me, Et, ^{i}Pr,

Figure 2.6. Rare-earth metal complexes of bis(imine)benzene-type ligands applied to the *cis*-1,4-selective polymerization of dienes.

The neutral dialkyl rare-earth metal complexes of bis(phosphino)amido-type ligands (**2.19**, Figure 2.7), in combination with $[Ph_3C][B(C_6F_5)_4]$, $[PhNMe_2H][B(C_6F_5)_4]$ or $B(C_6F_5)_3$, or their corresponding isolated monoalkyl cations, exhibited high activities in the *cis*-1,4-selective polymerization of IP (up to 99.6%), BD (99%) and their copolymerization (>99% *cis*-1,4-PIP, 99% *cis*-1,4-PBD), leading to polymeric materials formed with narrow MWDs ($Đ$ < 1.15).[38] Upon activation with $Ph_3C][B(C_6F_5)_4]$, the related complexes **2.20** (Figure 2.7) also perfomed well in the *cis*-1,4-selective polymerization and random copolymerization of IP and BD.[39]

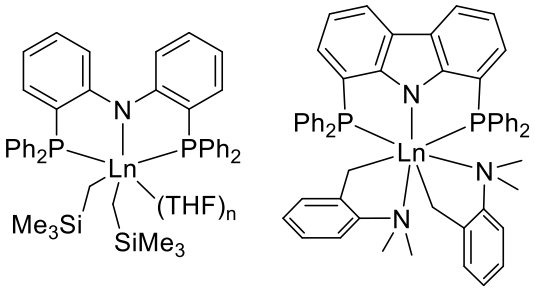

2.19
Ln = Sc, Y, Lu

2.20
Ln = Sc, Y, Er

Figure 2.7. Rare-earth metal complexes of bis(phosphino)amido-type ligands applied to the *cis*-1,4-selective polymerization of dienes.

Recent reports highlighted the efficiency of rare-earth metal complexes of various ligand architectures (**2.21**-**2.26**, Figure 2.8) for the highly isotactic or syndiotactic polymerization of the challenging 2-vinylpyridine, which cannot easily be achieved *via* other polymerization techniques.[40-44]

In a very recent review, Marks and coworkers also provided a comprehensive state of the art, including (pre)catalysts structures, range of applications (monomers) and mechanistic considerations, of the copolymerization of olefins and polar monomers mediated by early transition metal-based catalysts (rare-earth and Group 4 metals).[45]

In complement to the present section, interested readers may refer to more specific and detailed reviews dealing with the use of rare-earth metal complexes in coordination polymerization.[4, 46]

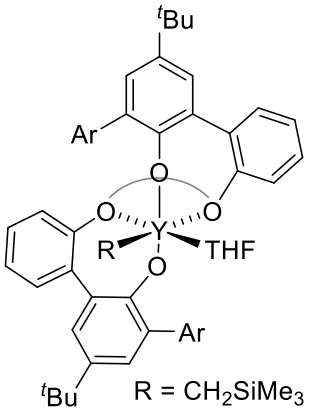

2.21

$Lu(CH_2SiMe_3)_3(THF)_x(Py)_{2-x}$

2.22

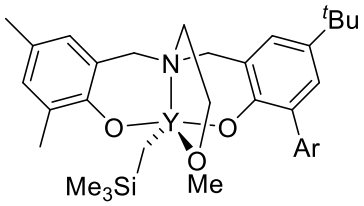

2.23

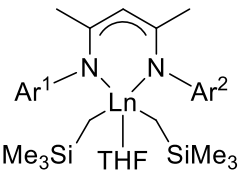

2.24
Ln = Y, Lu

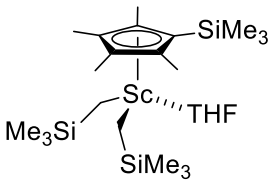

2.25

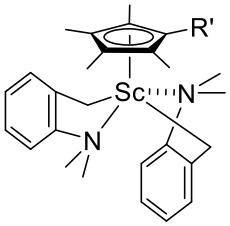

2.26
R' = $SiMe_3$, CH_3

Figure 2.8. Recent examples of rare-earth metal-based catalysts for the isotactic or syndiotactic polymerization of 2-vinylpyridine.

2.3.2. Group 4 Metal Catalysts

Post-metallocene Group 4 metal complexes are major compounds for the coordination polymerization of olefins. Most of them are supported by polydentate N-based ligands, such as amido-, imido-, β-diketiminate (BDI), amidinate or phenoxy-imine-type ligands, and were found to

be successful (pre)catayst for the (co)polymerization of ethylene, α-olefins, and copolymerization of olefins and polar monomers.[45-50]

Group 4 metal complexes of ligands composed of nitrogen donors only were extensively studied in the 90's and 2000's and exhaustive analyses of their performances in (co)polymerization of olefins were already provided in several comprehensive reviews.[46-47, 51]

Relevant achievements in the field of Group 4 metal-catalyzed olefin polymerization could be attributed to phenoxy-imine (N,O) complexes, also called FI catalysts (Figure 2.9). Due to the straightforward synthesis and tunable properties of the proligands, a large variety of catalysts could be easily obtained and structure/activity rationalization was made possible. This topic was comprehensively discussed by Fujita and coworkers in several review articles.[48-50] The following selected examples will highlight the claim that such FI catalysts may still have impact in this field. Marks and coworkers have recently shown that the nature of the σ-ligand(s) in FI catalysts, usually halide or alkyl group(s), may strongly affect their performances in (co)polymerization reactions. Indeed, upon sequential activation with $AlMe_3$ and $[Ph_3C][B(C_6F_5)_4]$, the zirconium bis(amido) derivative of a phenoxy-imine ligand (**2.27**, Figure 2.9) exhibited high activity and good 1-octene content (up to 7.2%) in the ethylene/1-octene copolymerization, whereas the dichloride derivative was totally inactive.[52] In a recent contribution, it was shown that the particular environment created by a cyclic bis(phenoxy-aldimine) ligand around the titanium dichloride center in complex **2.28** (Figure 2.9) resulted in exceptional regio- and isoselectivity in the polymerization of propylene.[53]

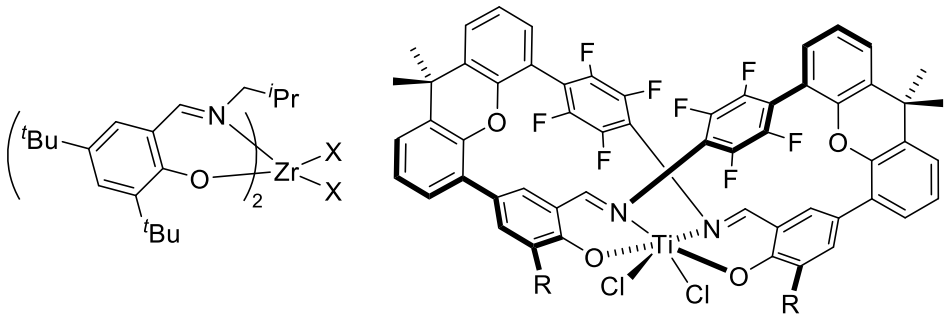

2.27
X = Cl, Me, Bn, NMe_2

2.28
R = Me, ^{t}Bu

Figure 2.9. Examples of Group 4 metal complexes of phenoxy-imine-type ligands (FI catalysts).

The following paragraphs summarize a selection of recent studies dealing with the use of Group 4 metal complexes of ligands composed of other donor sets than N_n and N,O, which exhibited remarkable performances in polymerization reactions. Upon activation with $[Ph_3C][B(C_6F_5)_4]$ or $[PhNMe_2H][B(C_6F_5)_4]$ the hafnium dimethyl complex (**2.29**, Figure 2.10) of C,N,N-pincer pyridylamido-based ligand showed high activity in ethylene polymerization and ethylene/1-octene copolymerization, though the dinuclear analog (**2.30**, Figure 2.10) exhibited much higher activities and produced polyethylene with 5.7 times higher MW and poly(ethylene-co-1-octene) with 2.4 times higher MW and 1.9 times greater 1-octene content.[54]

For interested readers, a comprehensive overview of the performances towards olefin polymerization of titanium (pre)catalysts supported by tridentate ligands, including half-titanocenes, CGCs, C,N,X, O,P,N, O,S,N, O,N,N, O,N,O, N,C,N, N,N,S and bis-aryloxide derivatives, was recently provided by Sun and coworkers.[55]

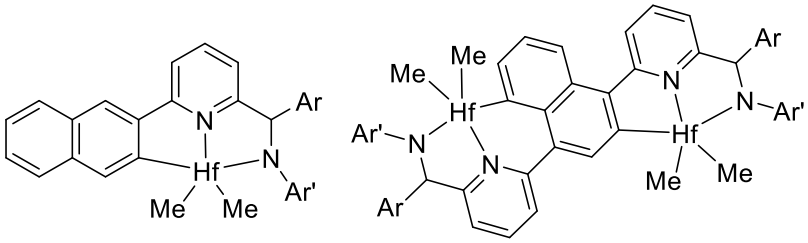

2.29 **2.30**

Figure 2.10. Tridentate mono- and dinuclear hafnium complexes exhibiting high activities in ethylene polymerization and ethylene/1-octene copolymerization.

A series of titanium trichloride complexes of O,N,D-pincer (D = P, S, O) ligands (**2.31**, Figure 2.11), in combination with MMAO, showed high activities (best results obtained with thioether derivatives) in the copolymerization of ethylene and functionalized olefins, such as 9-decen-1-ol, producing the corresponding copolymers with reasonable MWDs (*Đ* = 1.5-3.8) and up to 8.8 mol % functionalized olefin contents.[56]

Group 4 dibenzyl complexes of O,N,C-tridentate phenoxy-pyridine-based ligands (**2.32**, Figure 2.11) with variable σ-F functionalization on the aryl moiety (R^1, R^2, R^3) were evaluated as catalysts for ethylene polymerization (MAO cocat.).[57] The CF_3-functionalized titanium derivative exhibited the highest activity (6.8 x 10^5 g mol^{-1} h^{-1}) within this series, affording high MW polyethylene with relatively narrow MWD (*Đ* = 2.6). The Zr analogues were all found less active than their Ti analogues.

Various Group 4 metal halide or alkyl complexes of bis(phenolate)-NHC ligands (NHC precursors **2.33**-**2.34**, Figure 2.11) were evaluated in polymerization of ethylene and/or Hex and exhibited variables activities and selectivities, which were summarized in [46].

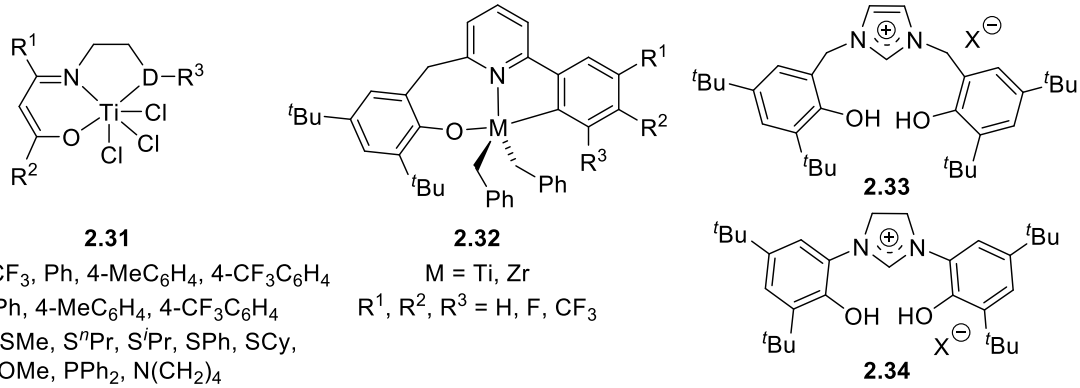

2.31

R^1 = Me, CF_3, Ph, 4-MeC_6H_4, 4-$CF_3C_6H_4$
R^2 = Ph, 4-MeC_6H_4, 4-$CF_3C_6H_4$
D-R_3 = SMe, S^{n}Pr, S^{i}Pr, SPh, SCy, OMe, PPh_2, $N(CH_2)_4$

2.32

M = Ti, Zr
R^1, R^2, R^3 = H, F, CF_3

2.33

2.34

Figure 2.11. Group 4 metal complexes (**2.31**-**2.32**) supported by ligands composed of mixed-donors and phenoxy-NHC precursors (**2.33**-**2.34**) applied to olefin polymerization.

In addition to N-based ligands, Group 4 metal complexes of tri- (O,S,O, **2.35**) and tetra-dentate (O,S,S,O, **2.36**) thio-bis(phenolate) ligands (Figure 2.12) were shown to be active catalysts for the (stereoselective) polymerization of olefins, and their performances were summarized and discussed in comprehensive reviews.[58-59] In particular, upon activation with aluminum-based or borate cocatalysts, some Group 4 metal catalysts of the type **2.36** exhibited high activities and stereoselectivities for the (co)polymerization of olefins such as St, ethylene, propylene and Hex.[58]

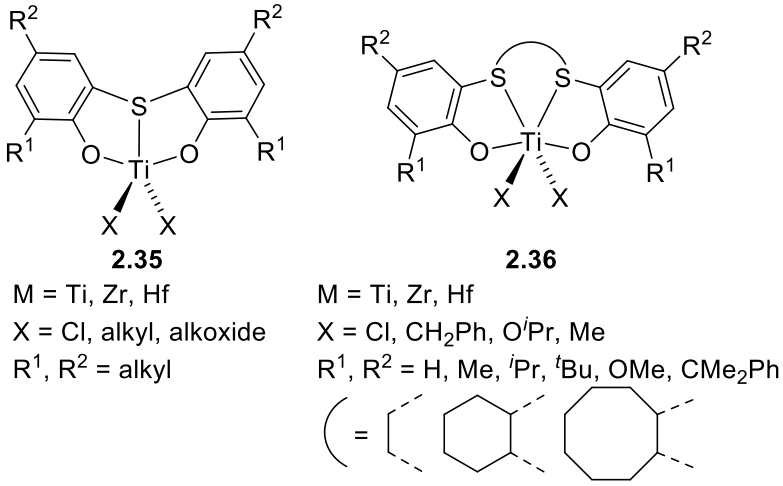

2.35 **2.36**

Figure 2.12. Representative examples of (O,S,O)- and (O,S,S,O)-supprted Group 4 catalysts for olefin polymerization.

2.3.3. Group 5 to Group 10 Metal Catalysts

The development of vanadium-based catalysts for olefin polymerization has attracted much attention over the last 20 years. Vanadium (pre)catalysts of different oxidation states, ranging from +III to +V, and supported by ligands of various denticity (from 1 to 5) and composition of donor atoms/sets (N, O, P and combinations) were reported (Figure 2.13). Even if these species do not exhibit higher activities than their Group 4 counterparts, they are generally better at producing (ultra)-high molecular weight polyethylene and syndiotactically-enriched polypropylene. Vanadium catalysts also perform better in ethylene/α-olefin copolymerization, with higher comonomer incorporation, and permit the production of synthetic rubbers based on ethylene/propylene or ethylene/propylene/diene copolymers. The progresses in design of vanadium-based (pre)catalysts and in their performances in olefin (co)polymerization were regularly and comprehensively reviewed.[60-62]

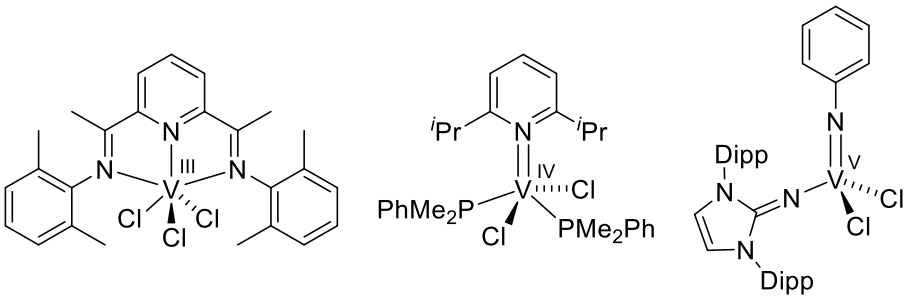

2.37 **2.38** **2.39**

Figure 2.13. Examples of V^{III} (**2.37**), V^{IV} (**2.38**), V^{V} (**2.39**) used as precatalysts for the polymerization of olefins.

Due to the industrial interest in linear α-olefins (LAOs), such as 1-butene, hex, and 1-octene, which are valuable building blocks for the generation of detergents, surfactants and lubricants, the development of selective ethylene oligomerization catalysts became an intense field of investigation, both in industrial and academic laboratories. Chromium-based complexes rapidly emerged as the most active and selective compounds to achieve this, and the different aspects of

this research area, *i.e*. catalyst development, polymerization performances, structure/activity balance and mechanistic considerations were comprehensively and periodically reviewed.[63-65] Figure 2.14 summarizes some of the most efficient precatalysts for selective ethylene oligomerization. Much efforts have been devoted over the last ten years to understand/rationalize the action of the organoaluminum cocatalyst in Cr-mediated ethylene oligomerization and we discussed this aspect in a recent contribution.[66]

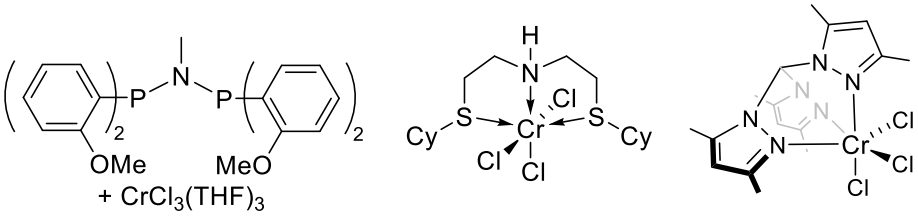

Figure 2.14. Typical Cr-based precatalysts for the selective oligomerization of ethylene.

Due to its high abundance, low cost and environmental impact, and good tolerance to heteroatom-functionalized groups, iron attracts significant interest for the development of olefin polymerization catalysts. Iron(II) or iron(III) halide complexes of polydentate neutral nitrogen-containing ligands were found to be the most successful catalysts for ethylene oligo-/poly-merization (see e.g. **2.43**, Figure 2.15).[67-68] It was shown that the steric hindrance of the *ortho*-groups of the aryl imine moiety in bis(imino)pyridine-type ligands, as well as the presence/absence of EWGs or the rigidity of the ligand backbone may influence catalytic activity and selectivity.[67] Other neutral bidentate N,N (**2.44**, Figure 2.15), neutral tridentate ligands with different donor sets, e.g. N,N,P or N,N,S (**2.45**, Figure 2.15), or anionic ligands were positively applied to Fe-catalyzed ethylene oligo-/poly-merization. Recent comprehensive reviews summarize the latest and significant catalyst developments, and discuss their performances towards the polymerization of ethylene and conjugated dienes, together with mechanistic considerations.[67-68]

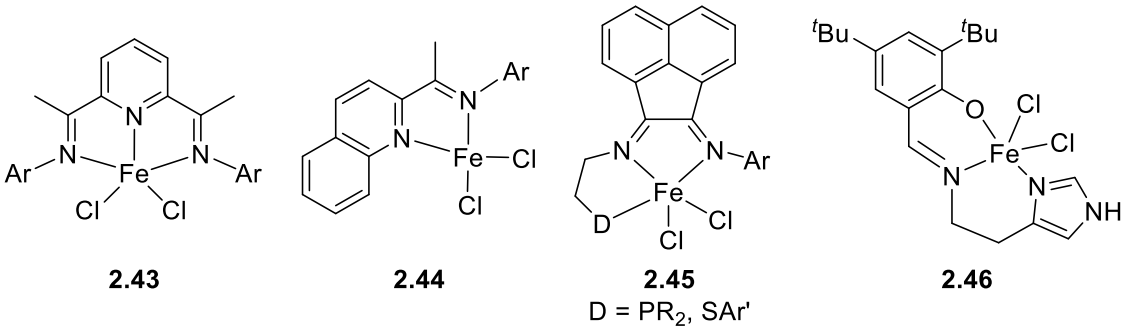

Figure 2.15. Representative Fe-based precatalysts for ethylene oligo-/polymerization.

Since the discovery of the Shell Higher Olefins Process (SHOP) for oligomerization of ethylene in the 1980's, using P,O-nickel(II) complexes, nickel-catalyzed olefin oligomerization remains an important field of research. To date, several tens of ligand scaffolds were designed for the development of more active and selective nickel catalysts. The huge library of reported ligands includes neutral (mono- to tri-dentate) and monoanionic (bi- and tri-dentate) ones, of a wide range of donors (N, P, O) or donor sets, such as N,N, P,P, P,N, P,S, P,O, O,NHC etc (Figure 2.16). It was

shown that subtle changes in the ligand/catalyst structure and/or the nature of the cocatalyst may strongly influence both activity and selectivity of the nickel catalysts.[69-73]

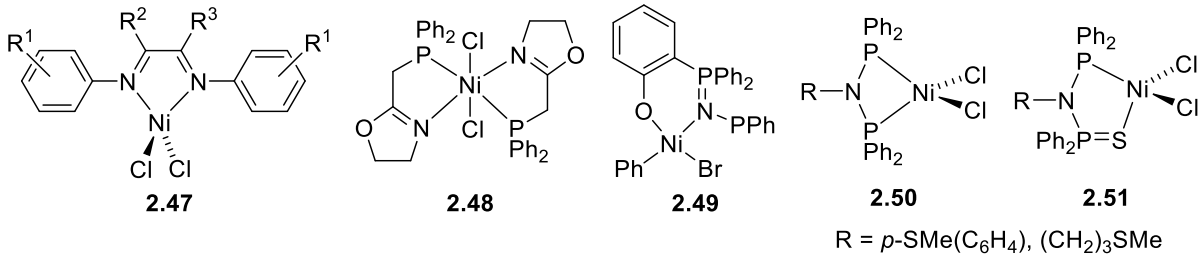

Figure 2.16. Representative Ni-based precatalysts for ethylene oligo-/polymerization.

3. Radical Polymerization

3.1. Introduction

Conventional or free radical polymerization (FRP) is used at the industrial scale to produce hundreds of tons of polymers annually, essentially because of its easy implementation and high tolerance to various functional groups.[74] However, this technique suffers from the tendency of radicals to undergo irreversible bimolecular terminations that prevent the production of well-defined materials.

Control over the radical propagation was gained by the development and improvement of reversible deactivation radical polymerization (RDRP) techniques over the last three decades.[75-76] Such processes opened access to well-defined polymers (controlled molecular weights and low dispersities) and complex architectures.[77]

RDRP is based on a dynamic/reversible equilibrium between an active radical species ($P_n^{\bullet}$) and a dormant species (P_n-T), in which the radical is bonded to a moderating/trapping agent, and rests on one of two following strategies: reversible termination (RT,

Figure 3.1, left) and degenerative transfer (DT,

Figure 3.1, right). In RT methods, the propagating radical species ($P_n^{\bullet}$) results from the homolytic P_n-T bond cleavage in the dormant species, with an activation rate constant k_a. At the same time, the moderating agent (T) is also liberated and becomes available for further trapping of the growing radical species, with a deactivation rate constant k_{da}, and regeneration of the dormant species. Radical addition to monomer and bimolecular terminations follow the propagation rate constant k_p and termination rate constant k_t, respectively (

Figure 3.1, left). An appropriate pseudo-equilibrium between active and dormant species ($K = k_a/k_{da}$) will lead to lowering of the concentration of free radical species, therefore favoring radical propagation (chain growth) *versus* bimolecular terminations. This is known as the "persistent radical effect" (PRE).[78] In DT methods, the propagating radical species ($P_n^{\bullet}$) is released from dormant species (P_n-T) by exchange with another growing radical species, in an associative manner. In such method, the dormant species acts as a reversible and degenerate chain transfer agent (like in immortal polymerization processes[79-80]). There is no moderating agent, whose role is to reduce the radical concentration, nor PRE, and the reaction follows the free polymerization kinetics. However, a controlled chain growth is accessible when the associative exchange is much faster than the propagation (k_{exch}[T-P]>>k_p[M],

Figure 3.1, right).

The present chapter will focus on RDRP techniques in which a transition metal complex plays a crucial role for the control of the polymerization, namely atom transfer radical polymerization (ATRP) and organometallic mediated radical polymerization (OMRP).

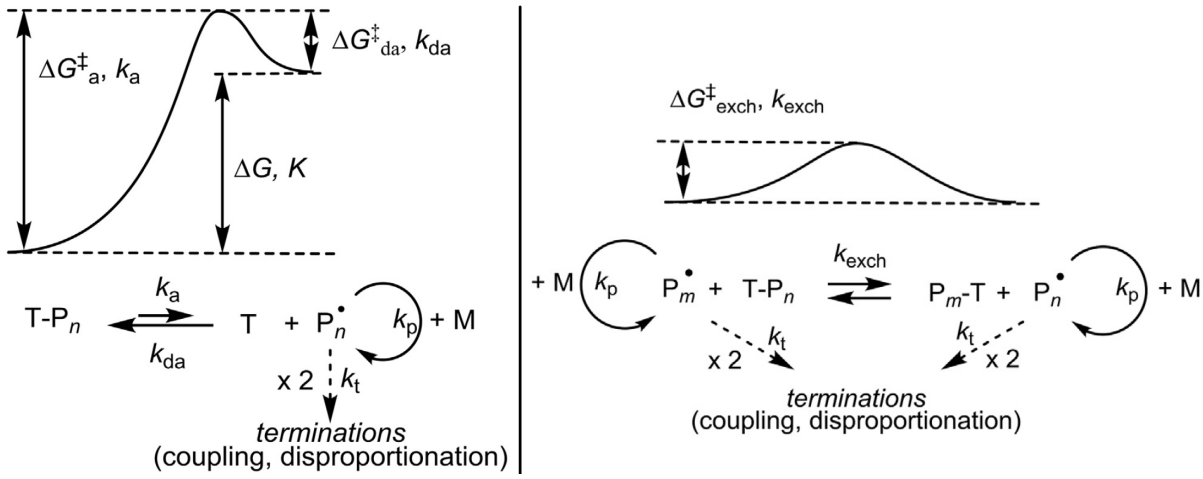

Figure 3.1. Mechanisms and free energy profiles of RDRP based on reversible termination (RT, left) and degenerative transfer (DT, right). $P_{n/m}$: polymer chain with degree of polymerization n or m; T: radical mediating agent; M: monomer. Adapted with permission from [81]. Copyright 2019, Elsevier.

3.2. Monomers

In radical polymerization, monomers are generally classified into two categories: the "more activated monomers" (MAMs) and the "less activated monomers" (LAMs), although the separation is arbitrary because all monomers and their associated radicals are dispersed on a continuous scale of relative activity. The monomer reactivity is inversely proportional to the reactivity of the associated radical. Indeed, while MAMs form stabilized active radical species, because they benefit from π delocalization of the unpaired electron, LAMs lead to very reactive radicals owing to a lack of stabilizing group. Therefore, the deactivation of active radicals generated from LAMs is easy, but they form very strong bonds with the radical mediating agent (T), and reactivation of the dormant species (T-P_n) is often slow or ineffective (see Figure 3.4 and Figure 3.29 for the control equilibria in ATRP and OMRP, respectively). That is the reason why the controlled radical polymerization (CRP) of LAMs is challenging.

Figure 3.2 qualitatively shows a scale of relative reactivity, specific to radical polymerization, of different monomers and of their associated radicals.

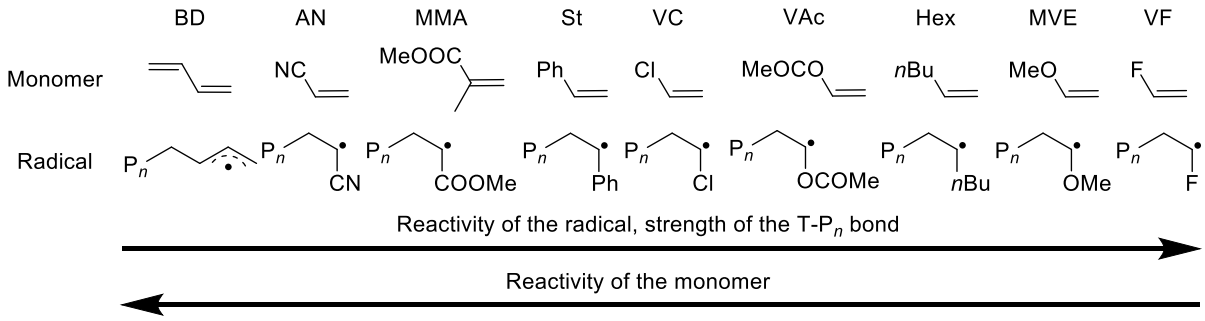

Figure 3.2. Qualitative reactivity order of a few monomers and their corresponding radical chains. BD: 1,3-butadiene; AN: acrylonitrile; MMA: methyl methacrylate; St: styrene; VC: vinyl chloride; VAc: vinyl acetate; Hex: 1-hexene; MVE: methyl vinyl ether; VF: vinyl fluoride.

Several RDRP methods, either working under RT or DT mode, readily achieve the controlled polymerization of MAMs,[75] while reaching a good control and high molecular weight materials for LAMs remains challenging. As stated above, T-P_n bonds are much stronger for LAMs than for MAMs, and therefore the reactivation of the dormant species in RT methods may become difficult (or impossible), leading to a slowdown (or to a complete stop) of the polymerization. Hence, moderating agents that form weak bonds with the propagating radical chains should be favored. However, as for any RDRP method, if the T-P_n bond is too weak, the trapping will not be efficient, and the polymerization will follow a free radical polymerization mechanism.[82] In DT methods, the broken and formed bonds are similar, therefore the T-P_n bond strength is not an issue to control the polymerization of LAMs, as long as the degenerative exchange process (k_{exch}) is very fast (vs. propagation).

Another parameter, the substitution of the monomer itself, affects the control in LAMs polymerization, both in RT and DT modes. When the two alkylidenes forming the monomer are different, they may be referred to as “head” and “tail”. The “head” refers to the more substituted alkylidene and the “tail” refers to the less substituted one (generally CH_2). In the case of MAMs, only regular head-to-tail addition occurs because the head radical, which is located at the chain end, is much more stabilized than the tail radical. This is not true for LAMs, because the difference of stability (head vs. tail radical) is less important, and although the regular head to tail addition dominates, a significant level of inverted head-to-head addition occurs, leading to isomeric tail radicals (Figure 3.3). During a polymerization following the RT mode, the more reactive tail radical will form a stronger bond with the moderator in the dormant species and therefore the latter will be less easily reactivated and will accumulate, slowing down the polymerization and possibly stopping it (see

Figure 3.1).[81]

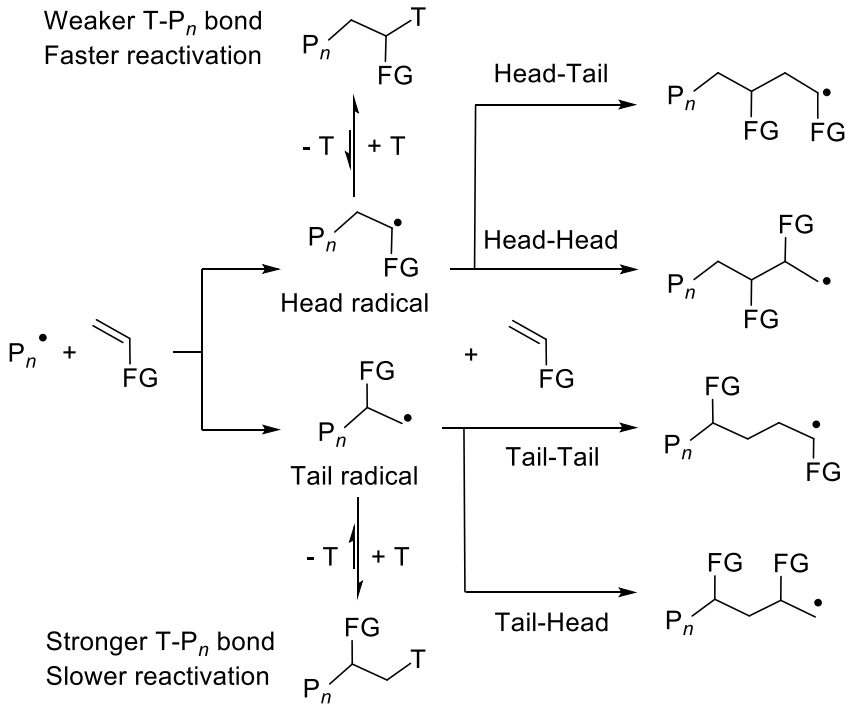

Figure 3.3. Different monomer addition possibilities for asymmetric LAMs. FG: functional group, T: moderating agent.

The inverted monomer addition (for asymmetric monomers) also affects the control during a polymerization following the DT mode. While the exchange between the major head dormant chains with the major head propagating radicals is still degenerative, the isomeric tail radicals generated by inverted monomer addition leads to non-degenerative exchange with formation of a more stable dormant species. The latter, which cannot be easily reactivated by the major head radicals, will accumulate and "consume" the moderating agent (see

Figure 3.1). Only tail radicals can reactivate this more stable dormant species, but these species are in very low concentration.[81] While the inverted monomer addition slows down the polymerization in RT methods (or stops it), it slows down the exchange rate in DT methods, leading to a loss of control.

Coordination chemistry has been shown to be a powerful tool to overcome these limitations, especially by the development of the OMRP (see Section 3.4).[81, 83-84]

3.3. Atom Transfer Radical Polymerization

3.3.1. Introduction

Since its discovery, in 1995, almost at the same time by the groups of Matyjaszewski (copper catalyst)[85] and Sawamoto (ruthenium catalyst),[86] atom transfer radical polymerization (ATRP) has become one of the most used and studied RDRP technique.[87-89] ATRP can be applied to a large variety of monomers (styrenics, (meth)acrylates, (meth)acrylamides…), to form various structures (copolymers, stars, brushes…), and can be performed in solution, in bulk or in heterogeneous media (suspension, emulsion…). These advantages allow the preparation of well-defined nanostructured functional materials for many applications.[90-91]

The control equilibrium in ATRP is based on the reversible/dynamic trapping of the propagating radical ($P_n^{\bullet}$) by the deactivator form of the ATRP catalyst (metal halide (Y) complex at a higher oxidation state: L/Mt^{x+1}-Y), leading to the formation of the dormant species (P_n-Y) and the activator form of the ATRP catalyst (metal complex in a lower oxidation state: L/Mt^{x}, Figure 3.4). For an effective process, i.e. high K_{ATRP} value ($K_{ATRP} = k_{a,\ ATRP}/k_{d,\ ATRP}$), the activator should be capable of mediating the C-Y cleavage in the (macro)initiator ($k_{a,\ ATRP}$) and the radical trapping by the deactivator must be fast ($k_{d,\ ATRP}$). Two ways of initiation of an ATRP process have been explored initially. The "Normal ATRP" initiation occurs by reaction between an alkyl halide (R_0-Y, ATRP initator) and the ATRP activator, leading to the active radical species ($P_n^{\bullet}$) and the ATRP deactivator (Figure 3.4, top right). In the "Reverse ATRP" initiation, a conventional azo initiator decomposes thermally into a primary radical ($R_0^{\bullet}$), and the latter rapidly reacts with the ATRP deactivator to form *in-situ* an alkyl halide and the ATRP activator (Figure 3.4, top left). The advantage of this method is that it does not require the handling of air-sensitive precursors (e.g. Cu^{I} or Fe^{II} complexes or salts).

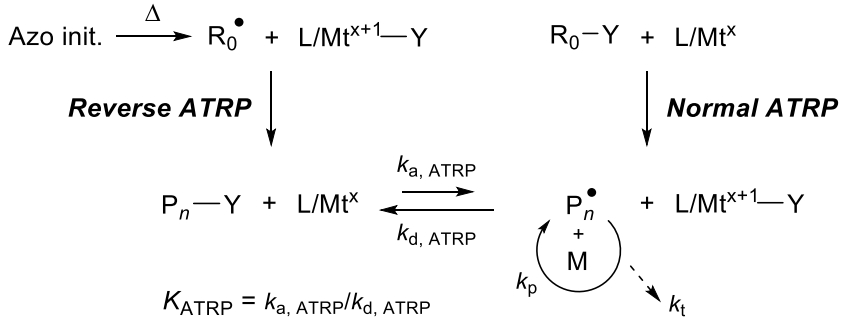

Figure 3.4. Dynamic ATRP equilibrium (bottom), normal (top, right) and reverse (top, left) ATRP initation.

Many transition metals have been applied to ATRP processes (see next sections), however the field is dominated by copper. Concurrently, the development of iron-based ATRP catalysts has gained increasing attention, because this metal has a benign environmental impact, it is abundant, has a low cost and low toxicity.[92-93]

Over the last 25 years, many efforts have been devoted to the development, on one hand, of more active ATRP catalysts, essentially *via* ligand design and, on the other hand, of "greener" processes, *via* activator regeneration methods. These improvements allow a reduction of the catalyst loading, as low as a few ppms, the use of less sensitive precursors and cheap or non-toxic additives (reducing agents, sacrificial electron donor) or the spatial and temporal control of the polymerization *via* an external stimulus.

The following sections will present the evolution of initiation or activator regeneration methods and highlight, with a special emphasis on the most used copper and iron metals, how catalyst/ligand design has improved ATRP processes.

3.3.2. Initiation and/or Activator Regeneration Methods

This section will highlight how ATRP catalysts enter the main ATRP equilibrium (Figure 3.4, bottom) or are regenerated along the process. The evolution of the initiation and/or activator regeneration methods played a crucial role in the development of ATRP, and the catalysts performances may be conditioned by the ATRP method applied. For example, as a result of the kinetics that are governing

ATRP,[94] a given highly active catalyst, used at ppm levels in an appropriate protocol (*e.g*. ICAR ATRP, see below), would give excellent results, while it would lead to fast radical generation and thus rapid bimolecular termination under normal ATRP conditions.

In the early stage of the development of ATRP (1995), two initiation methods, namely normal and reverse (see Section 3.3.1 and Figure 3.4), were reported.[85, 95-96] While in this seminal work, large amounts of (air-sensitive) catalysts were used, the most recent developments allow the use of only few ppm catalysts or a temporal control of the polymerization *via* an external stmuli.

3.3.2.1. RDRP in the Presence of Zero-Valent Metals (SARA ATRP and SET-LRP)

During an ATRP process, the L/Mt^{x+1}-Y deactivator may accumulate due to the PRE. Matyjaszewski and coworkers showed that the addition of a zero-valent metal (Mt^0) to typical ATRP systems (Cu^0 and Fe^0 for Cu- and Fe-mediated ATRP, respectively) resulted in an increased rate of polymerization and the production of well-defined polymers, because it can undergo a comproportionation reaction with the accumulated L/Mt^{x+1}-Y deactivator to gradually regenerate the L/Mt^x activator, thus acting as a reducing agent.[97] Noteworthy, the Mt^0 can also directly react with the alkyl halide initiator and therefore act as a supplemental activator, but most of the initiator remain activated by the L/Mt^x activator that is generated by deactivation or by comproportionation from L/Mt^{x+1}-Y. The name of this method, supplemental activator and reducing agent (SARA) ATRP, originates from the aforementioned two roles of the Mt^0 species.[98-99] Several zero-valent metals, such as copper, iron, zinc, magnesium, silver, in various forms (powders, wires, plates) could be applied to SARA ATRP,[98, 100-101] and when used with very active catalysts, allowed a temporal control of the polymerization.[102]

A second mechanism, called single-electron transfer living radical polymerization (SET-LRP), was proposed by Percec and co-workers for the ATRP of (meth)acrylates and vinyl chloride in the presence of Cu^0 in polar organic solvents.[103] The proposed mechanism assumes 1) the exclusive activation of the alkyl halide initator by Cu^0 *via* an outer-sphere electron transfer to form the corresponding radical and L/Cu^{I}-Y (Y = halogen) species, 2) instantaneous disproportionation of L/Cu^{I}-Y species to Cu^0 and L/Cu^{II}-Y_2 and 3) absence of bimolecular termination.[103-104] The involvement of the SARA ATRP or the SET-LRP mechanism in the presence of zero-valent metal has been the subject of debate for a long time. Recent contributions from Matyjaszewski, Gennaro and co-workers strongly support the SARA ATRP mechanism, while contradicting the SET-LRP mechanism, since they observed that 1) the activation step involves an inner-sphere electron transfer rather than outer-sphere electron transfer, 2) the alkyl halide initiators are mostly activated by L/Cu^{I} species not by Cu^0 and 3) radical terminations occur.[105-109] A comparison between the SARA ATRP and SET-LRP mechanisms is depicted in Figure 3.5.

RDRP in the presence of zero-valent metals could be performed in various organic solvents and aqueous medium and was successfully applied to a large variety of monomers with a good control over molecular weight and chain-end fidelity, therefore allowing the formation of complex architectures and the resulting materials found applications in various fields.[101, 110-111]

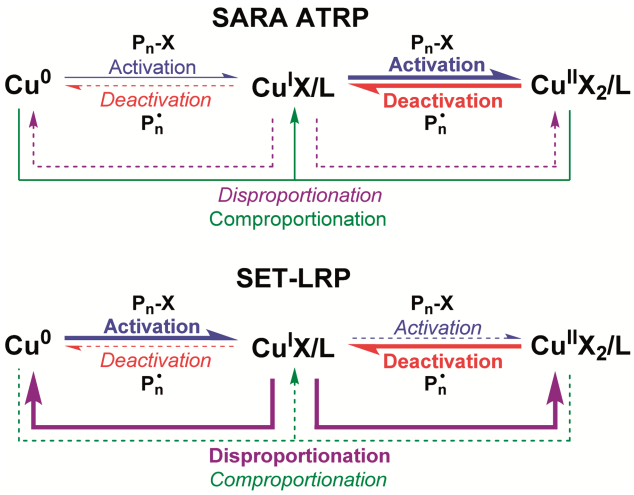

Figure 3.5. The mechanisms of SARA ATRP (top) and SET-LRP (bottom). The major reactions are outlined by bold arrows, whereas supplemental or contributing reactions are indicated by solid arrows and minor reactions that can be neglected from the mechanisms by dashed arrows. [107] – Reproduced by permission of The Royal Society of Chemistry. Copyright 2014, The Royal Society of Chemistry.

3.3.2.2. *Simultaneous Reverse and Normal Initiated (SR&NI) ATRP*

The initially developed normal and reverse ATRP were found to be limited to less active catalysts, because more active catalysts were generating too many radicals, too fast, leading to increased level of radical terminations. Moreover, reverse ATRP does not allow the synthesis of block copolymers. These drawbacks could be bypassed by the development of the simultaneous reverse and normal initiated (SR&NI) ATRP, using a combination of $CuBr_2$ and N-based ligands in a 1:1 molar ratio, and initiated by 2,2'-azobis(isobutyronitrile) (AIBN) and an alkyl halide ($Y\text{-}R_0$), as depicted in a more general way in Figure 3.6.[112-113]

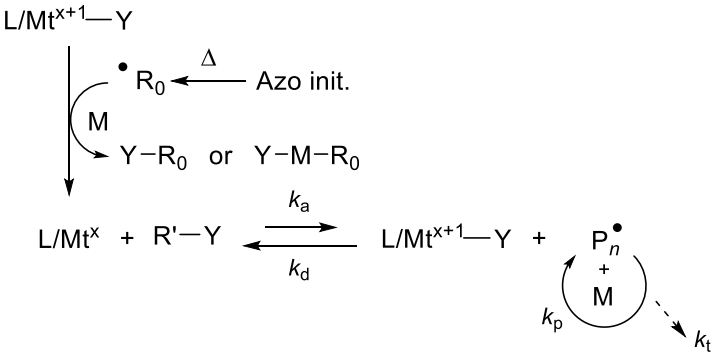

Figure 3.6. Mechanism of simultaneous reverse and normal initiated (SR&NI) ATRP.

3.3.2.3. *Activators Generated by Electron Transfer (AGET) ATRP*

In both the reverse and SR&NI ATRP processes, the catalyst activation (initially present as $L/Mt^{x+1}\text{-}Y$) requires the use of a conventional radical initiator (*e.g.* AIBN). In contrast, activators generated by electron transfer (AGET) ATRP makes use of non-radical generating reducing agents, such as tin(II) 2-ethylhexanoate[114] ($Sn(EH)_2$) or non-toxic ascorbic acid (allowing mini-emulsion polymerization),[115] to generate the L/Mt^x activator, which further activates the alkyl halide initiator ($R_0\text{-}Y$) and the ATRP

process proceeds (Figure 3.7). AGET ATRP still has the advantages of using air-stable L/Mt^{x+1}-Y (*e.g.* Cu^{II}, Fe^{III}) precursors and can be combined with highly active catalysts, which can be used in low amounts.[116] Furthermore, the reducing agent may act as oxygen scavenger, rendering AGET ATRP tolerant to air.

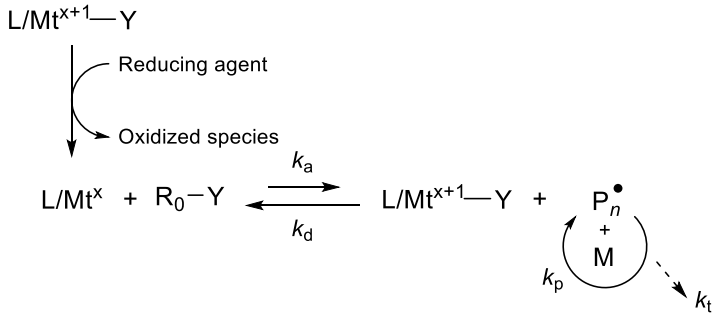

Figure 3.7. Mechanism of activator generated by electron transfer (AGET) ATRP.

3.3.2.4. Activators ReGenerated by Electron Transfer (ARGET) ATRP

Activators regenerated by electron transfer (ARGET) ATRP makes use of reducing agents to continuously regenerate the L/Mt^x activator from L/Mt^{x+1}-Y that accumulates during the process, due to irreversible radical terminations (Figure 3.8).[117-119] Therefore, the catalyst loading in ARGET ATRP can be lowered to only a few ppm in the presence of the appropriate reducing agents. In that sense, ARGET ATRP can be considered as a "greener" way to conduct ATRP, more so because FDA (food and drug administration) approved $Sn(EH)_2$ and natural products can be used as reducing agents.[117-118, 120] It is noteworthy that, despite their similarities (use of reducing agents and air-stable L/Mt^{x+1}-Y precursors, limited tolerance to air), ARGET and AGET ATRP differ by the role of the reducing agent that is not limited to the initiation in the former process. ARGET ATRP was initially applied to St, *n*BA and MMA under various conditions, with the active $CuCl_2$/Me_6TREN or TPMA systems, and produced well-defined polymers and block copolymers.[117-119]

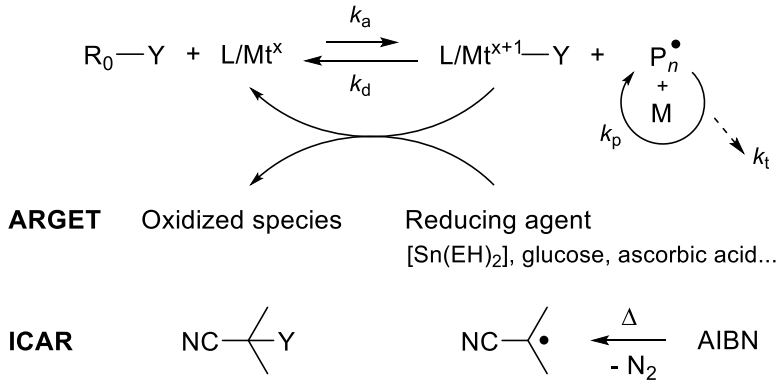

Figure 3.8. General mechanism of activator regenerated by electron transfer (ARGET) and initiators for continuous activator regeneration (ICAR) ATRP.

3.3.2.5. Initiators for Continuous Activator Regeneration (ICAR) ATRP

The principle of initiators for continuous activator regeneration (ICAR) ATRP is very similar to that of ARGET ATRP, which consists in the slow and continuous regeneration of the L/Mt^x activator. The

reduction of the latent L/Mt^{x+1}-Y in ICAR ATRP is accomplished by an organic radical that is produced by decomposition of a conventional radical initiator (vs. chemical reducing agent in ARGET ATRP), such as AIBN (Figure 3.8).[119] The successful implementation of an ICAR ATRP requires slow decomposition of the radical initiator, which can be tuned by its nature, concentration and the reaction temperature. This method is usually applied with low loading of active catalysts. In their pioneering work, Matyjaszewski and coworkers successfully applied the ICAR ATRP protocol to St, MMA and *n*BA under various conditions. The active Me_6TREN- and TPMA-$CuCl_2$ systems (50 ppm cat. loading) afforded well-defined polymeric materials ($Đ \leq 1.12$), while the less active dNbpy- and PMDETA-$CuCl_2$ systems led to broader dispersities ($Đ > 1.6$).[119] Very recently, a bio-inspired and fully oxygen-tolerant aqueous ICAR ATRP protocol was reported, allowing a temporal control of the polymerization by the temperature ("on" at 45°C and "off" at 0°C) and based on the continuous conversion of O_2 to CO_2 catalyzed by glucose oxidase (glucose and sodium pyruvate as sequential sacrificial substrates).[121]

3.3.2.6. Electrochemically Mediated (eATRP) ATRP

Thorough efforts have been devoted over the last decades to the development of polymerization techniques controlled by external stimuli, such as temperature, light, electricity, ultrasound, microvawes, etc.[122] The use of physical regulators, allows the preparation of precise and complex architectures as well as a spatiotemporal-control of the polymerization and may avoid contamination with "chemical regulators" and side-reactions. Beyond thermal activation (decomposition of a radical initiator), which is the basics of radical polymerization, temporal control of the process has been achieved by temperature variations (see previous sections). Many regulation methods were successfully applied to ATRP, as detailed in the following sections.[100]

As an alternative to the use of chemical reducing agents as in the ARGET ATRP protocol, Matyjaszewski, Gennaro and coworkers developed the electrochemically-mediated ATRP (*e*ATRP) that make use of an electrical current to toggle between the L/Mt^x (activator) and L/Mt^{x+1}-Y (deactivator) states of the catalyst, as depicted in Figure 3.9 (left).[123-124] The work required a complex three-electrode setup, with working (Pt), reference (Ag^+/Ag) and counter (Pt) electrodes, the two later being separated from the reaction medium. This method was applied to the controlled polymerization of MA with an excellent temporal control of the process, using $CuBr_2$/Me_6TREN as catalyst (50 ppm vs monomer).[123]

The use of an aluminum wire as sacrificial counter electrode, directly immersed into the reaction mixture, led to the so-called simplified electrochemically mediated ATRP (*se*ATRP) method, which could be conducted under either potentiostatic or galvanostatic conditions.[125]

A recent review discusses the fundamental aspects, advantages, limitations and applications of (*s*)*e*ATRP.[126]

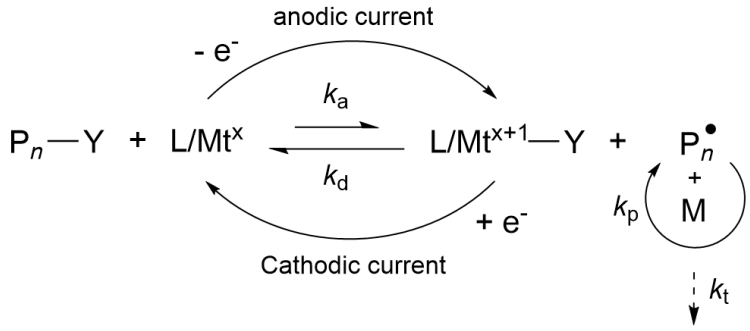

Figure 3.9. Left. Proposed mechanism of *e*ATRP under a cathodic current to (re)generate the L/Mt^{x} activator and optional anodic current to switch to the L/Mt^{x+1}-Y deactivator for stopping the polymerization.

3.3.2.7. Photochemically Mediated (photoATRP) ATRP

The use of light to mediate ATRP, known as *photo*ATRP, has been recognized as a powerful tool for the synthesis of well-defined polymeric materials, and many review articles are dealing with this topic.[100, 122, 127-131] Different mechanisms may operate in *photo*ATRP, depending on the strategy or conditions applied, however most of them rest on the photochemical (re)generation of the L/Mt^{x} activators by reduction of the L/Mt^{x+1}-Y deactivators. This process can be induced by the use of additional photoinitiators, photosensitizers or photocatalysts (Figure 3.10, A and B3), or by the use of photosensitive complexes that undergo excitation on irradiation and further redox reactions with the ligands or other components leads to the formation of free radicals, which finally induce reduction of the deactivators to (re)form the activators (Figure 3.10, B2). Another approach is based on the photoexcitation of (photosensitive) L/Mt^{x} activators that are quenched by alkyl halide initiators or dormant chains to (re)generate the oxidized L/Mt^{x+1}-Y deactivators and propagating radical chains (Figure 3.10, B1). All these mechanistic aspects were well summarized and discussed in different reviews.[129, 131] It has been shown that *photo*ATRP allows excellent spatial-, temporal-, and sequence-controlled processes.[100, 122, 132] Moreover, *photo*ATRP can be mediated by various transition metals (Cu, Fe, Ir, Ru…) and applied to many monomers, such as simple and functional acrylates and methacrylates, for the precise preparation of advanced materials.[127-128]

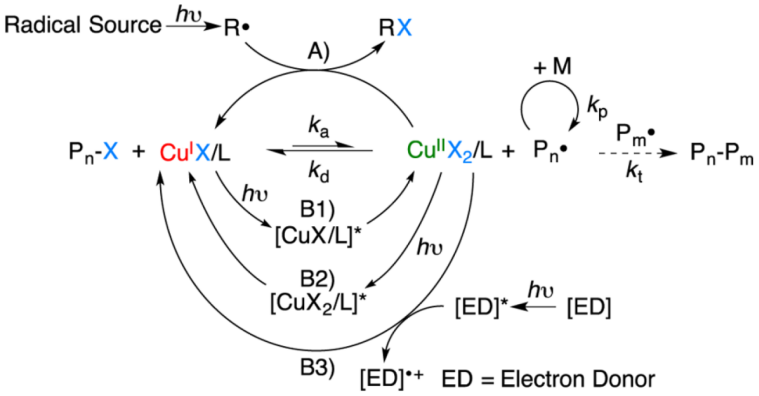

Figure 3.10. Simplified mechanisms that can operate in *photo*ATRP (depicted here for a copper catalyst). A) Photoinitiation by reduction of Cu^{II}X$_2$ dormant species with a photogenerated radical; B1) Cu^{I}X/L is used as a photocatalyst; B2) reduction of Cu^{II}X$_2$/L *via* photoexcitation; B3) reduction of Cu^{II}X$_2$/L with an added photocatalyst. Reproduced with permission from [131]. Copyright 2016, American Chemical Society.

3.3.2.8. Mechanically/Ultrasonically Induced (mechano-/sonoATRP) ATRP

Ultrasound-induced ATRP, named *mechano*ATRP, was only very recently discovered and solely applied to copper-based ATRP catalysts, however it already experienced several developments.[122] Initially, piezoelectric nanoparticles ($BaTiO_3$, ZnO) were used to induce, upon sonication, an electron transfer from their surface to the ATRP deactivator ($Cu^{II}X_2/L$), allowing its reduction and (re)generation of the ATRP activator ($Cu^{I}X/L$), further promoting the polymerization of acrylate monomers (Figure 3.11, left).[133-135] The use of low amounts of an active catalyst allowed an excellent temporal control of the process.[133] Mechanistic investigations confirmed that the major contribution to the activator generation resides in the reduction of the Cu^{II} to Cu^{I} species *via* electron transfer from piezoelectric nanoparticles.[134] In more recent protocols, called *sono*ATRP, the use of piezoelectric materials was avoided. An aqueous *sono*ATRP of water-soluble (meth)acrylate monomers was reported, and in this case, the ATRP activator (re)generation was made possible by the formation of hydroxyl radicals (from water) upon sonication.[136] *sono*ATRP could also be performed using (bi)carbonate salts in DMSO, *via* the ultrasound-mediated decomposition of the *in-situ* formed $(CO_3)Cu^{II}/L$ species, from the $[Cu^{II}X/L]^+$ deactivator, which generates the $[Cu^{I}/L]^+$ activator and carbonate radical anion ($CO_3^{\bullet -}$), thereafter quenched by DMSO to form dimethylsulfone and CO_2.[137]

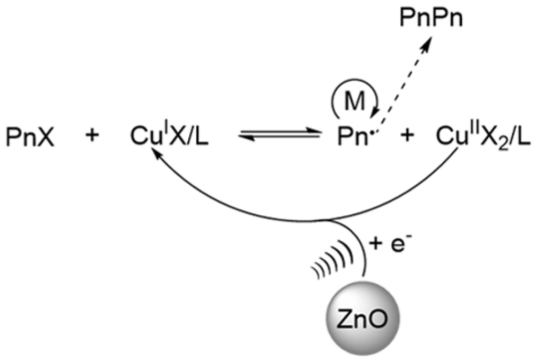

Figure 3.11. Proposed mechanism of *mechano*ATRP. Reprinted with permission from [134]. Copyright 2017 American Chemical Society.

3.3.2.9. ATRP Initiated with High-valent Metal Complex without Reducing Agent and Radical Initiator

Noh and coworkers introduced the concept of generation of activators by monomer addition (GAMA) ATRP in the late 2000's after reporting that iron(III) complexes of phosphine-containing ligands could initiate the ATRP of (meth)acrylate and St monomers in the absence of reducing agent (AGET) or radical initiator (ICAR).[93, 138] Various combinations of phosphine-based ligands and iron(III) precursors ($FeBr_3$, $FeCl_3$) were then evaluated, and will be discussed in Section 3.3.4. The terminology GAMA ATRP arised from the mechanism proposed by the authors, which rests on the generation of the phosphine-$FeBr_2$ activator by reaction between MMA and the phosphine-$FeBr_3$ precursor, and the concomitantly formed methyl 1,2-dibromoisobutyrate would supposedly serve as an initiator.[139] However, Matyjaszewski and coworkers showed that phosphines were also able to reduce Fe^{III} species to Fe^{II}, in the absence of monomer, and activate a Br-capped polySt sample.[140]

Furthermore, it was recently shown that isolated methyl 1,2-dibromoisobutyrate does not initiate the MMA polymerisation in the presence of the $FeBr_2/PPh_3$ activating system.[141] In a very recent contribution, Xue, Poli and coworkers reported the $FeBr_2$-catalyzed ATRP of MMA under solvent-, ligand- and radical initiator-free conditions, starting from $FeBr_3$, ethyl 2-bromophenylacetate (EBrPA) and simple inorganic salts.[142] Mechanistic investigations allowed the authors to show that $FeBr_3$ reduction do not occur by the direct action of the monomer under thermal conditions (as suggested for GAMA ATRP). Rather, the inorganic salt (MtX) activates EBrPA to yield the oxidizing $Mt^{+}(BrX^{\bullet})^{-}$ species, which is removed by MMA, and the carbon-based ($EPA^{\bullet}$) radical that further reduce $FeBr_3$ by atom transfer and subsequently, regular ATRP.[142-143] Although the early work by Noh and coworkers mentions the applicability of this method to iron and copper catalysts, its was later essentially applied to iron.

3.3.3. Copper Catalysts

As stated in Section 3.3.1, catalyst/ligand design has contributed to render ATRP more effective (e.g. cat. loading, reaction temp., polymerization rate and control)[87-88, 93] and more popular for the synthesis of advanced materials.[90-91, 110] This section will recount the evolution of the copper-based ATRP catalysts, especially those containing nitrogen-based ligands, the most effective.

Various parameters affect the ATRP thermodynamic constant, K_{ATRP} ($K_{ATRP} = k_{a,\,ATRP}/k_{d,\,ATRP}$), such as the nature of the (macro)alkyl halide (R_0-Y/P_n-Y) that has to be (re)activated,[144-145] the solvent,[146] and of course the copper catalyst.[87] Indeed, the catalyst activity (more active = larger K_{ATRP}) was shown to be directly correlated to the $Cu^{I/II}$ redox potential (Figure 3.12), the latter being dependent on the ligand nature.[145, 147] K_{ATRP} increases by approximatively one order of magnitude for each 60 mV shift of the redox potential toward more negative values. In addition to the $Cu^{I/II}$ redox potential, the stability of the Cu^{II}-Y bond (also referred as halidophilicity),[73] and the structural rearrangements that may occur upon oxidation/reduction also affect the ATRP equilibrium.[148]

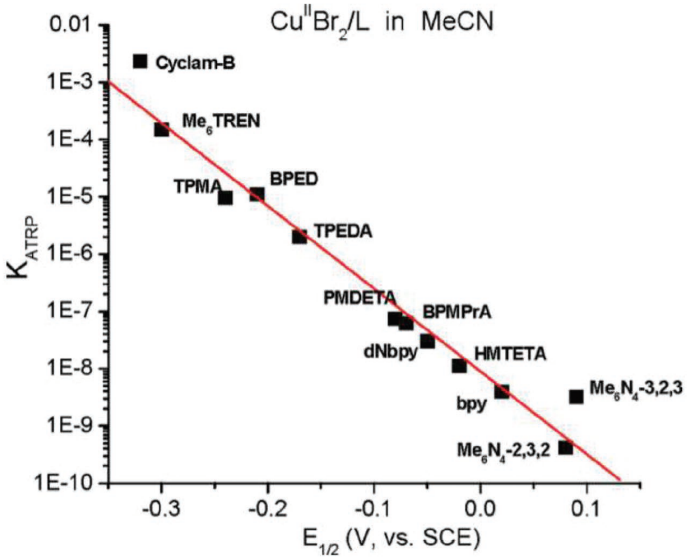

Figure 3.12. Correlation between K_{ATRP} and redox potential ($E_{1/2}$) for various ATRP catalysts supported by polydentate nitrogen-based ligands. Reproduced and adapted with permission from [87] and [145], repsectively. Copyright 2008, American Chemical Society and Copyright 2019, Wiley-VCH.

3.3.3.1. Bipyridine, Terpyridine and Derivatives and Other Diimines

2,2'-Bipyridine (Bipy, **3.1**) was the first ligand used in copper-catalyzed ATRP.[85, 95-96] However, the resulting [$Cu^{I/II}$(Bipy)$_2$] system was not fully soluble in bulk monomer, the use of Bipy derivatives substituted at the 4,4'-positions with aliphatic solubilizing groups markedly improved the solubility of the resulting catalysts and the control of the polymerization of St and MA, with dispersity values ($Đ$) ≤ 1.05 (**3.2**-**3.4**, Figure 3.13).[149] The introduction of electron-withdrawing (EWGs: Cl) or electron-donating groups (EDGs: NMe_2, OMe, 5-nonyl, Me) on the 4,4'-positions of Bipy (**3.4**-**3.8**, Figure 3.13) greatly influenced the performances of the resulting copper catalysts in the normal ATRP of MA and MMA.[150] Under the studied conditions, the fastest polymerization rate was obtained with the [Cu^{I}(**3.5**)$_2$]$^+$ catalyst, functionalized with the most electron-donating NMe_2 group, while the Bipy and Cl-functionalized Bipy (**3.8**) derivatives were inactive. However, the high activity of [Cu^{I}(**3.5**)$_2$]$^+$ led to a lower initiation efficiency, resulting in higher M_n values than expected, because too many radicals are produced and terminate in the early stage of the polymerization. As a result, the most successful catalyst was found to be [Cu^{I}(**3.6**)$_2$]$^+$, bearing the intermediate OMe electron-donating group, which exhibited an intermediate rate of polymerization but an excellent match between experimental and theoretical M_n values assorted with dispersities lower than 1.1. The observed trend of polymerization rate in this series of copper-Bipy derivatives could be well correlated with their redox potential ($E_{1/2}$), the more reducing it is, faster the polymerization and higher the K_{ATRP} are.

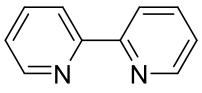

Bipy (**3.1**)

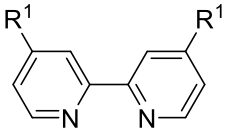

R^1 = ^{t}Bu (**3.2**), ^{n}Hept (**3.3**), 5-nonyl (**3.4**)

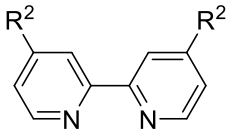

R^2 = NMe_2 (**3.5**), OMe (**3.6**), Me (**3.7**), Cl (**3.8**)

Figure 3.13. 2,2'-Bipyridine (Bipy) and 4,4'-disubstituted derivatives used in ATRP.

2,2':6',2''-Terpyridine (Terpy, **3.9**, Figure 3.14) copper(I) chloride or bromide complexes were also evaluated in the bulk ATRP of St and MA, however these systems exhibited poor control which was attributed to the low solubility of the [$Cu^{II}Y_2$(Terpy)] (Y = Cl or Br) species.[151] This obstacle could be overcome by the introduction of solubilizing *tert*-butyl or 5-nonyl-substituents on the 4,4',4''-positions of terpy (**3.10** and **3.11**, respectively).[151-152] The CuBr or CuCl/Terpy system was reported to be an efficient catalyst for the ATRP of VAc in bulk at 70°C (up to 80% conv. in 10 h, 1.57 < $Đ$ < 1.74), and the living character was assessed by a self-chain extension reaction.[153]

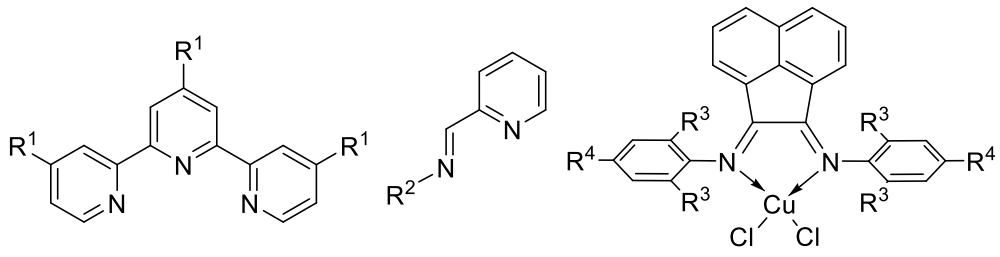

Figure 3.14. 2,2':6',2''-terpyridine (Terpy) ligand and 4,4',4''-trisubsituted derivatives, and other ligands or complexes incorporating a N=C-C=N backbone.

Cu-ATRP catalysts of pyridineimine (**3.12**-**3.13**)[154-155] and bis(aryl-imino)acenaphthene (**3.14**-**3.15**)[156] derivatives (Figure 3.14), N,N'-bidentate ligands with a similar N=C-C=N backbone as bipy, were evaluated in normal ATRP of MMA (90°C, 33% v/v in xylene) and reverse ATRP of St (80°C, 50% v/v in toluene), respectively. In both cases a linear increase of MW with conversion was observed, but also broader dispersities.

3.3.3.2. Polydentate Alkyl Amines

A series of simple bi-, tri- and tetra-dentate alkyl amine ligands, tetramethylethylenediamine (TMEDA, **3.16**), *N*,*N*,*N*',*N*'',*N*''-pentamethyldiethylenetriamine (PMDETA, **3.17**) and 1,1,4,7,10,10-hexamethyltriethylenetetramine (HMTETA, **3.18**, Figure 3.15), respectively, were initially evaluated in the normal ATRP reaction of MA, MMA and St, using copper(I) bromide as metal precursor and an appropriate alkyl halide initiator.[157] In the case of bidentate **3.16**, for which a 2:1 ligand/Cu^{I} ratio is used (as for Bipy and derivatives), the ATRP of both MA and MMA monomers exhibited linear first-order kinetics, linear increase of MW with conversion and dispersities lower than 1.5. In contrast, the ATRP of St showed a significant deviation from first-order kinetics with respect to the monomer and relatively high *Đ* values (>2) at higher conversions, which were attributed to a lower concentration of the copper(II) halide deactivator due to solubility issues. The tridentate **3.17** and tetradentate **3.18** ligands, which could be used in a 1:1 ligand to [Cu^{I}Br] ratio, both exhibited higher polymerization rates than Bipy (**3.1**) and **3.16** for MA and St, and a linear increase of M_n vs conv was observed for MA, St and MMA monomers. However, while *Đ* values remained low for **3.18** even at conversion >75%, they rapidly increased for **3.17** above 70% conversion. Noteworthy, the cyclic voltammetry (CV) studies of the $[Cu^{II}Br(L)]^+$ (for L = **3.17** and **3.18**) or $[Cu^{II}Br(\mathbf{3.8})_2]^+$ complexes, which gave $E_{1/2}$ = -0.02, -0.05, -0.08 V vs SCE for **3.17**, Bipy derivative **3.8**, and **3.18**, respectively, were in agreement with the observed polymeration rates trend and with model studies that gave the following K_{ATRP} = 7.5 x 10^{-8}, 3.0 x 10^{-8}, 1.1 x 10^{-8} for **3.17**, **3.8**, and **3.18**.[145]

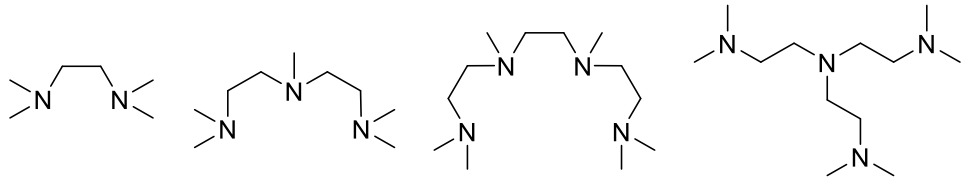

Figure 3.15. Alkyl amine ligands used in Cu-catalyzed ATRP.

The use of the tetradentate, tripodal tris(2-(dimethylamino)-ethyl)amine (Me_6TREN, **3.19**, Figure 3.15) ligand in place of linear amine ligands such as **3.16**-**3.18**, drastically affected the ATRP activity of the resulting copper catalyst. While linear amine ligands required elevated polymerization temperature, the CuBr/**3.19** (1:1 molar ratio) system readily mediated the bulk ATRP of MA and BA at room temperature with an excellent control.[158] In a comparative study, the rate of MA polymerization (in bulk at 50°C) achieved with CuBr/**3.19** was much faster than those observed with CuBr/**3.17** or CuBr/(**3.4**)$_2$, and again this fact is in correlation with a much lower redox potential ($E_{1/2}$ = -0.30 V vs. SCE) and greater K_{ATRP} (1.5 x 10^{-4}) for the CuBr/**3.19** catalyst.[145]

Moreover, from structural investigations on copper(I)/copper(II) complexes relevant to Cu-catalyzed ATRP,[159] it was shown that in the case of Me_6TREN (**3.19**) the resulting copper(I) and copper(II) halide complexes are structurally very similar. The tetradentate tripodal nature of the ligand leads to an encapsulation of the copper center from one face and an ideal pre-organisation to coordinate the incoming halide atom during ATRP activation, on the other face, with only very little structural rearrangement. It is known that minimizing inner sphere reorganizational energy would accelerate electron transfer and therefore lead to faster rates of ATRP activation. This fact greatly contributes to the exceptional performances of tetradentate tripodal ligands such as Me_6TREN (**3.19**) and TPMA (**3.23**, see section 3.3.3.3) in Cu-catalyzed ATRP.[148]

Monoanionic ligands related to Me_6TREN (**3.19**), in which one -$(CH_2)_2NMe_2$ arm was replaced by a phenoxy donor, were developed with the aim of a stronger coordination of the ligand to the copper center, and therefore a greater K_{ATRP}.[160-161] However, the introduction of an anionic donor slowdown the deactivation and reduces the polymerization control.

3.3.3.3. Picolylamine-Based Ligands

Copper complexes of picolylamine-based ligands represent an important class of ATRP catalysts. The tridentate *N*,*N*-bis(2-pyridylmethyl)octylamine ligand (**3.20**, Figure 3.16), in combination with CuBr and the appropriate bromoalkylinitiator (1:1:1 molar ratio) was applied to the normal Cu-ATRP of St (PEBr, bulk, 110°C), MA (EBP, bulk, 50°C) and MMA (50 vol% in anisole, 50°C).[162] For both St and MA, the process was well-controlled, however for MMA, M_n values significantly higher than expected were obtained. This was attributed to a poor initiation efficiency and therefore fast radical termination at the beginning of the polymerization. Under identical conditions, similar trends were observed with related tridentate N-based ligand.[163] Similarly to the trend observed with the Bipy derivatives (see Section 3.3.3.1), introduction of electron-donating groups on the pyridyl rings, to form ligand **3.21** (Figure 3.16), led to a more active (more reducing) and highly hydrophobic ATRP Cu catalyst that was successfully applied to the controlled polymerization of *n*BA under miniemulsion conditions.[164]

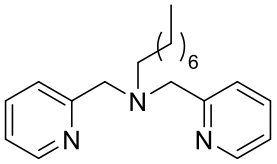

3.20

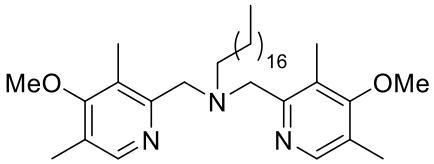

3.21

Figure 3.16. Tridentate picolylamine-based ligands used in Cu-catalyzed ATRP.

The tetradentate tris(2-pyridylmethyl)amine (TPMA, **3.22**,

Figure 3.17) ligand is one of the most important ligands in Cu-catalyzed ATRP, and many studies (electrochemical, structural…) were dedicated to the $Cu^{I/II}$/TPMA couple to rationalize its exceptional performances.[145, 165] The CuBr/**3.22** (1:1 molar ratio) catalyst mediated the bulk polymerization of St (PEBr init., 110°C) and MA (EBP init., 50°C) under "normal ATRP" conditions with an excellent level of control and reached 80% conversion after 1 and 4 h, respectively.[162] For MMA, the high activity of both the catalyst and the PMMA-Br chain-end led to a significant degree of termination at the beginning of the process and therefore lower control. The high activity of this Cu-ATRP catalyst is well explained by 1) its relatively low redox potential ($E_{1/2}$ = -0.24 V vs SCE) and great K_{ATRP} (9.6 x 10^{-6}) and 2) the very small structural changes between the Cu^{I}(**3.22**)$^{+}$ activator and $Cu^{II}Br$(**3.22**)$^{+}$ deactivator, as for the Me_6TREN (**3.19**, see section 3.3.3.2) system.[148]

Regarding the increased activity obtained by the introduction of EDGs in Bipy-based ligands, the same strategy was applied to the TPMA skeleton. The series TPMA*^{1}-TPMA*^{3} (**3.23**-**3.25**,

Figure 3.17), with 1-3 corresponding to the number of pyridyl rings functionalized with two methyl and one methoxy groups, were synthesized and the performances of the resulting Cu-ATRP catalysts compared.[166-167] The Cu/**3.25** (TPMA*^{3}) system was applied to the ATRP of *n*BA and MA under various initiation/regeneration methods (see section 3.3.2).[167] The high reactivity of this ATRP catalyst was not compatible with normal ATRP conditions, leading to a significant amount of terminated chains at the early stage of the reaction. In contrast, a well-controlled polymerization of acrylates was observed by applying SARA ATRP (MA monomer), eATRP (*n*BA monomer) and ARGET ATRP (*n*BA, $Sn(EH)_2$ as reducing agent) with low catalyst loadings, and in all cases the control was slightly improved compared to the Cu/**3.22** (TPMA) system. The improved performances of the ATRP catalyst by going from TPMA (**3.22**) to TPMA*^{3} (**3.25**) was much more evident under ICAR ATRP conditions ($CuCl_2$, AIBN), the latter affording faster polymerization rates, better correlation between experimental and theoretical M_n values and lower dispersities, with catalyst loadings as low as 10 ppm. Cyclic voltammograms of the [Cu^{II}(TPMA*$^{1\text{-}3}$)Br][Br] complexes afforded $E_{1/2}$ values of -0.31 (TPMA*^{1}, **3.23**), -0.36 (TPMA*^{2}, **3.24**) and -0.42 (TPMA*^{3}, **3.25**) V vs SCE, clearly indicating that the presence of EDGs on the TPMA skeleton increases the reducing ability of the resulting copper complexes.[166] The higher ATRP activity observed for the Cu/TPMA*^{3} system can be explained by its lower reduction potential compared to TPMA (-0.42 vs -0.24 V vs SCE) that is correlated to a higher K_{ATRP} for the former (4.2 x 10^{-4} vs 9.6 x 10^{-6}).

Further modifications of the TPMA scaffold were realized over the recent years.[168-170] Notably, a series TPMA-based ligands functionalized on the 4-position with cyclic or acyclic amino groups (**3.26**-**3.29**,

Figure 3.17) were reported and their related copper complexes were studied. Electrochemical studies revealed $E_{1/2}$ values for the [Cu^{II}Br(**3.26**-**3.29**)][Br] complexes between -0.433 and -0.503 V vs SCE, which are much lower than the previously reported very active [Cu^{II}(**3.25**)Br][Br] complex, and these values follow the order **3.29** ≈ **3.26** < **3.28** < **3.27** (< **3.25** (TPMA*^{3}) << **3.22** (TPMA)). As expected, complexes with the lower redox potential exhibited the higher ATRP activity (K_{ATRP} = 1.6 x 10^{-1} (**3.29**) and 3.1 x 10^{-1} (**3.26**)). These systems were evaluated in Cu-catalyzed ICAR ATRP of *n*BA using very low catalyst loadings (10-25 ppm), EBiB as initiator and AIBN as conventional radical initiator. High conversions (70-80%) were reached after 4 h reaction time, and the recovered polymer samples had MW close to the expected values. However, with 10 ppm catalysts the *Đ* values obtained remained high (≈ 1.5) and the evolution of MW with conversion was not linear. Using 25 ppm catalysts allowed a substantial decrease in the dispersity values and the M_n evolution (vs conv.) became nearly linear.

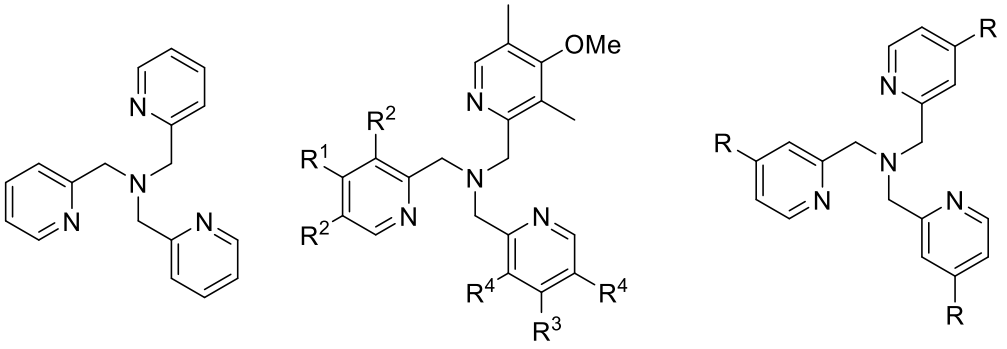

Figure 3.17. Tetradentate tris(2-pyridylmethyl)amine (TPMA, **3.22**) and related ligands functionalized with EDGs used in Cu-catalyzed ATRP.

Similarly to what was done with Me_6TREN (**3.19**, see section 3.3.3.2), monoanionic derivatives of TPMA, in which one picolyl arm was replaced by a pyrrolide or phenoxy donor, were developed with the aim of a stronger coordination of the ligand to the copper center, and therefore a greater K_{ATRP}.[160, 171] The resulting copper catalysts exhibited high polymerization rates but poor control that were attributed to an inefficient deactivation.

Inspired by the successful TPMA scaffold in Cu-catalyzed ATRP, the hexadentate *N*,*N*,*N'*,*N'*-tetrakis(2-pyridylmethyl)ethylenediamine ligand (TPEN, **3.30**), in combination with CuBr, was applied to the normal ATRP of MA, MMA and St, and exhibited very fast polymerization rates with well-controlled molecular weights and low polydispersities with catalyst/initiator molar ratio as low as 0.005.[172] Compared to the active catalysts based on TPMA (**3.22**) or Me_6TREN (**3.19**), the Cu^{II}Br(TPEN)$^+$ complex exhibited a higher redox potential ($E_{1/2}$ = -0.17 V vs SCE) and smaller K_{ATRP} (2.0 x 10^{-6}),[145] however under normal ATRP conditions the latter performed better because it is less prone to extensive radical termination than the former.

3.3.3.4. Macrocyclic Ligands

A series of macrocyclic poly-alkylamine ligands were tested in Cu-catalyzed ATRP. Normal ATRP of *n*BA, using a combination of the ligand 4,11-dimethyl-1,4,8,11-tetraazabicyclo[6.6.2]hexadecane (CyClam-B, **3.31**, Figure 3.18) and CuBr was fast and moderately controlled at room temperature.[173] Interestingly, cyclic voltammetry studies of $[Cu^{II}Br(\mathbf{3.31})]^+$ afforded a value of $E_{1/2}$ = -0.32 V vs SCE and model studies determined a K_{ATRP} = 4.3 x 10^{-3}, which indicate that the Cu/**3.31** ATRP catalytic system is much more active than the active Cu/Me_6TREN or Cu/TPMA (see above).[145, 173] However, the Cu/**3.31** catalyst exhibits a lower control over the polymerization (match between experimental and theoretical M_n values and *Đ*) than the latter systems, which was attributed to a poor deactivation efficiency due to the high stability of the $[Cu^{II}Br(\mathbf{3.31})]^+$ species. Moreover, *a contrario* to the Me_6TREN and TPMA systems, Cu-catalysts of Cyclam-derivatives suffer from large structural rearrangement during atom transfer, slowing down the deactivation process.[148]

The very active ligand 5,5,7,12,12,14-hexamethyl-1,4,8,11-tetraazacyclotetradecane (Me_6CyClam, **3.32**, Figure 3.18) was successfully applied to the Cu-catalyzed ATRP of less activated monomers (LAMs).[174-175] The CuCl/**3.32** catalyst, with initial addition of $CuCl_2$ to promote deactivation, readily mediated the relatively fast and controlled ATRP of *N*-vinylpyrrolidone (NVP) and vinyl acetate (VAc), and the resulting halogen-capped macroinitiators could be further chain extended to produce block copolymers.

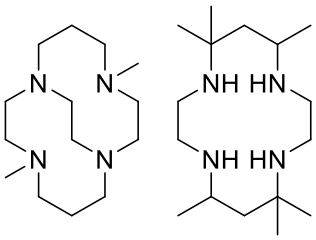

3.31 **3.32**

Figure 3.18. Macrocyclic poly-alkylamine ligands used in Cu-catalyzed ATRP.

3.3.3.5. Bis(oxazoline) Ligands

Tang and co-workers thoroughly investigated, in Cu-catalyzed SARA ATRP of MMA, the potential of bis(oxazoline) ligands (**3.33**-**3.41**, Figure 3.19), with various substituents on the oxazoline ring, and side armed bis(oxazoline) ligands (**3.42**-**3.52**, Figure 3.19), based on the indane-bis(oxazoline) (**3.41**) and with different substitution pattern on the bridge carbon.[176-180] The authors could highlight that the nature of the substituents on the bis(oxazoline) skeleton significantly affect the polymerization rate, MW, *Đ* and stereoselectivity. Under the studied conditions ($CuCl_2$ cat., Cu^0 act., BPN init., THF 50%v, 25°C, 12 h), the side armed bis(oxazoline) **3.45** was found the most active, producing well-defined PMMA with high tacticity (72% rr).[180] The $CuBr_2$/**3.45** ATRP catalyst was found to be very efficient towards a large scope of monomers, i.e. various methacrylates, acrylates, styrenic monomers, *N*,*N*-dimethylacrylamide and methacrylic acid, and the side arm functionalization was crucial to reach these performances (compared to ligand **3.41**).[177]

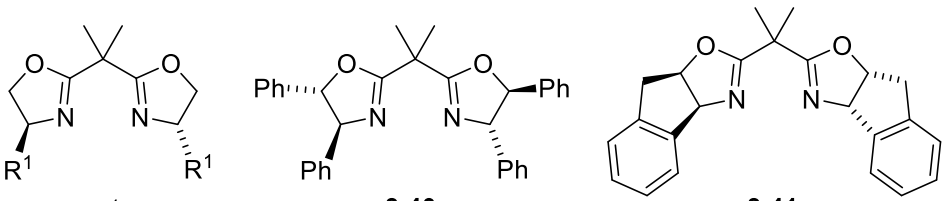

3.33: R^1 = H
3.34: R^1 = ^{t}Bu
3.35: R^1 = Cy
3.36: R^1 = ^{i}Pr
3.37: R^1 = ^{s}Bu
3.38: R^1 = Ph
3.39: R^1 = Bn

3.40

3.41

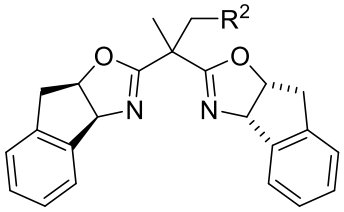

3.42: R^2 = Cy
3.43: R^2 = Ph
3.44: R^2 = 4-^{t}BuC$_6$H$_4$

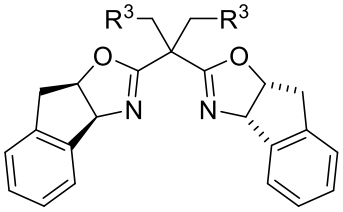

3.45: R^3 = Cy
3.46: R^3 = Ph
3.47: R^3 = 4-^{t}BuC$_6$H$_4$
3.48: R^3 = 3,5-(CF$_3$)$_2$C$_6$H$_3$
3.49: R^3 = 4-(OMe)C$_6$H$_4$
3.50: R^3 = (CH$_2$)$_2$CH$_3$
3.51: R^3 = (CH$_2$)$_6$CH$_3$
3.52: R^3 = (CH$_2$)$_{10}$CH$_3$

Figure 3.19. Bis(oxazoline) (**3.33**-**3.41**) and side armed bis(oxazoline) (**3.42**-**3.52**) ligands used in Cu-catalyzed ATRP.

3.3.3.6. Other Ligands

As stated above, nitrogen-based ligands have been found to be the best suited to form efficient copper ATRP catalysts. Copper complexes of softer ligands such as diphosphines[181] or *N*-heterocyclic carbenes[182] were, however, evaluated in ATRP of MMA, but in all cases only poor control was observed (discrepancy between theoretical and experimental M_n values, high *Đ*).

3.3.4. Iron Catalysts

3.3.4.1. Phosphorous-Based Ligands

The first reports about iron-catalyzed ATRP dates back to 1997, with the use of the well-defined [$FeCl_2(PPh_3)_2$] complex **3.53** (Figure 3.20),[183] or a mixture of $FeBr_2$ and PPh_3 (1:3 molar ratio) (or N-based ligands, see section 3.3.4.2),[184] which afforded a controlled polymerization of MMA and St, respectively. Following these early works, several studies focused on the use of binary systems composed of phosphine ligands and iron(II) or iron(III) salts in ATRP. In particular, considerable attention was given to the latter systems and reverse initiation protocols (Reverse, AGET, ARGET, ICAR and GAMA ATRP), because Fe^{III} precursors are air-stable and easier to handle than their Fe^{II} analogues.[93] Some debates arose about the activation mechanism of Fe^{III} ATRP catalytic systems (reduction of Fe^{III} to Fe^{II}) working in the absence of any organic halide, radical sources or reducing agents, which was proposed to be promoted by the phosphine or the monomer itself.[139-140, 185-186]

Sawamoto and co-workers extended the library of [$FeX_2(PR_3)_2$] complexes (**3.54**-**3.57**, Figure 3.20), by varying both the halogen atom and the phosphine ligand, and studied the influence of theses parameters on the ATRP performances of the catalysts.[187] Complex **3.57** exhibited the best

results in terms of activity and control for the ATRP of MMA, with 90% conversion (1000 eq. vs **3.57**) after 36 h at 60°C in toluene and a *Đ* value of 1.2. It was successfully applied to the block copolymerization of MMA and *n*-butyl methacrylate.

Matyjaszewski and coworkers showed that, similarly to the trend observed in Cu-catalyzed ATRP with Bipy- and TPMA-derived ligands, functionalization of the PPh_3 ligand with EDGs, leading to ligands **3.58** and **3.59** (Figure 3.20), strongly enhanced the activity of the resulting (*in situ* generated) iron catalyst.[140] The activity increased with the number of EDG; the $FeBr_3$/**3.59** system reached 91% conversion of St in 21 h (St:Fe:**3.59** = 200:1:2, 100°C, 50% v/v in anisole, *Đ* = 1.25), while under the same conditions, $FeBr_3$/**3.58** and $FeBr_3/PPh_3$ systems reahed 19% and 9% conversion, respectively. Under the appropriate conditions, these systems also mediated well-controlled polymerizations of *n*BA and MMA.

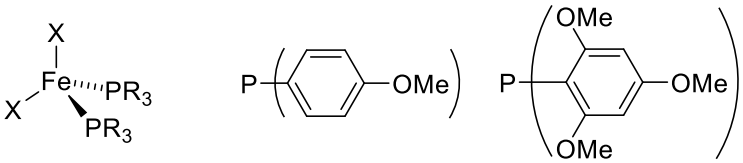

3.53: X = Cl, PR_3 = PPh_3 **3.58** **3.59**
3.54: X = Br, PR_3 = PPh_3
3.55: X = Cl, PR_3 = $PMePh_2$
3.56: X = Br, PR_3 = $PMePh_2$
3.57: X = Br, PR_3 = P^nBu_3

Figure 3.20. Phosphine ligands and phosphine iron complexes applied to Fe-catalyzed ATRP.

Several bidentate P-based ligands, such as diphosphine,[186, 188-189] pyridylphosphine (**3.61**-**3.62**) [138, 189-191] and aminophosphine (**3.63**-**3.65**) [188] ligands (Figure 3.21) were also successfully applied to Fe^{II}- or Fe^{III}-catalyzed ATRP since the late 2000's. Combination of Fe^{II} or Fe^{III} salts with these ligands resulted in very active ATRP catalysts that exhibited a very good controllability of the ATRP of MMA and St. Importantly, Noh and coworkers showed that *in-situ* generated iron(III) complexes of ligands **3.61** and **3.62** (and other P-based mixed ligands) catalysed ATRP in the absence of reducing agent and conventional radical initiator (GAMA ATRP, see section 3.3.2.9).[138] The improvement in Fe^{II}-catalyzed ATRP of MMA provided by such bidentate P-based ligands was nicely illustrated by the use of the isolated [$FeBr_2$(**3.65**)] complex **3.60** (Figure 3.21), which exhibited higher activity and better controllability than [$FeBr_2(P^nBu)_2$] (**3.57**, Figure 3.20).

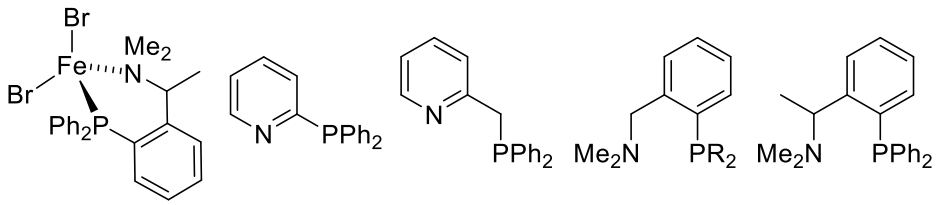

3.60 **3.61** **3.62** **3.63**: R = Ph **3.65**
3.64: R = Cy

Figure 3.21. Isolated P,N-iron complex and amino- and pyridyl-phosphine ligands applied to Fe-catalyzed ATRP.

A series of isolated half metallocene (Cp or Cp*) iron(II) bromide complexes (**3.66**-**3.67**, Figure 3.22) with a mixed carbonyl/phosphine coordination sphere were prepared by reaction between their dicarbonyl precursors and the desired phosphine ligand under UV irradiation, and were found to be efficient catalysts for the ATRP of MMA.[192-193] Model studies have shown that the really active catalysts are unsaturated $16e^-$ species resulting from the *in-situ* elimination of a CO ligand from coordinatively saturated $18e^-$ precursors under polymerization conditions, allowing radical generation (or regeneration) from haloalkyl initiator (or dormant species). The Cp* derivatives exhibited higher catalytic activities than the Cp ones in the ATRP of MMA and could be successfully applied to MA and functional methacrylate monomers.[192]

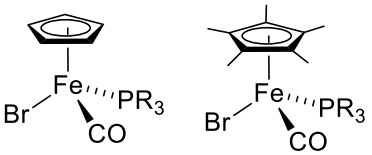

3.66 **3.67**

PR_3 = PPh_3, $PMePh_2$, PMe_2Ph, $P(m\text{-tol})_3$, $P(p\text{-tol})_3$]

Figure 3.22. Half metallocene iron(II) complexes applied to Fe-catalyzed ATRP.

3.3.4.2. Nitrogen-Based Ligands

Gibson and coworkers developed a library of *α*-diimine iron(II) complexes (**3.68**,
Figure 3.23) that were applied to the ATRP of St and MMA.[194-199] For both St and MMA polymerization, catalysts bearing alkyl substituents on the R^1 positions (or electron-donating groups on R^1 and R^2) were very efficient, affording well-defined and narrowly dispersed polymeric material with predictable MW. In contrast, the catalysts substituted on the R^1 positions with aryl groups (or electron-withdrawing groups on R^1 and R^2) suffered from interfering catalytic chain transfer (CCT) process, leading to polymer chains with MW much lower than expected.
The same group showed that tridentate salicylaldiminato iron(II) chloride complexes (**3.69**,

Figure 3.23) were very effective catalysts for the ATRP of St, exhibiting high polymerization rates, linear increase of MWs with conversion, excellent fitting between theoretical and experimental MW values and low dispersities.[200] Related bidentate salicylaldiminato iron(III) complexes of general formula [(*N*,*O*)$FeCl_2$] exhibited a poor control in the ATRP of St and MMA.

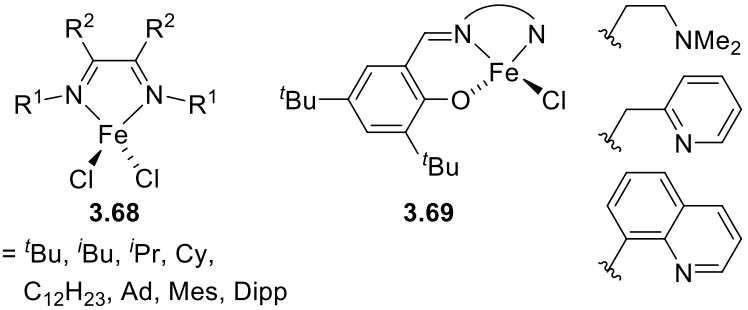

3.68 **3.69**

R^1 = ^{t}Bu, ^{i}Bu, ^{i}Pr, Cy, $C_{12}H_{23}$, Ad, Mes, Dipp

R^2 = H, Me, Ph, *p*-MeC_6H_4, *p*-FC_6H_4, *p*-$OMeC_6H_4$, *p*-$NMe_2C_6H_4$

Figure 3.23. *α*-Diimine and salicylaldiminato iron(II) complexes applied to Fe-catalyzed ATRP.

Nagashima and coworkers reported the synthesis of various iron(II) complexes of *N*,*N*,*N*-trialkylated-1,4,9-triazacyclononane (R_3TACN) ligands (**3.70**-**3.71**, Figure 3.24) and their application in ATRP of St, MMA and BA.[201] All complexes reached high conversions in the ATRP of St and exhibited a very good level of controllability, with an excellent match between theoretical and experimental MW values and dispersities lower than 1.35. Concerning the ATRP of MMA, apart from the complexes bearing the smallest R = Me group, all other catalysts were found to be very active and afforded polymeric materials with predictable chain lentghs and low MWDs (<1.35). In contrast, good control in the polymerization of BA was only achived for mononuclear iron bromide (vs. iron chloride) complexes, i.e. those substituted with the more bulky R groups, reaching high conversions and exhibiting a very good match between theoretical and experimental MW values and *Đ* values between 1.21 and 1.25. The iron catalysts that are formed as ion pairs (structure **3.70**) could be removed, up to 99.3%, from the produced materials by precipitation from methanol and recycled up to three times without loss of efficiency.

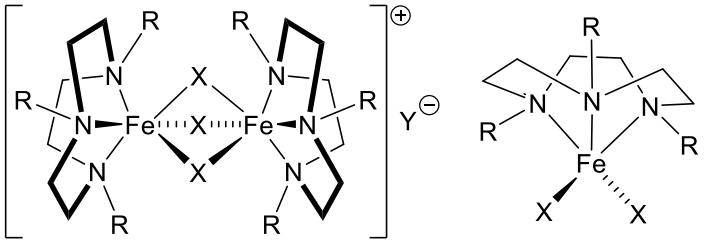

3.70 For small R groups

3.71 For bulky R groups

X = Cl, Br

Y = Cl, Br, [(R_3TACN)$FeCl_3$]

R = Me, *p*-$OMeC_6H_4CH_2$, cyclopentyl, cycloheptyl, ^{i}Bu, ^{i}Pr

Figure 3.24. *N*,*N*,*N*-trialkylated-1,4,9-triazacyclononane (R_3TACN) iron(II) complexes applied to Fe-catalyzed ATRP.

Among a series of iron(III) complexes of tetradentate amine-bis(phenolate) ligands (**3.72**, Figure 3.25), these substituted in the R^1 and R^2 positions with Cl were shown, by Shaver and coworkers, to be extremily efficient catalysts for the ATRP of St and MMA, affording polymeric materials with MWs in good agreement with theoretical values and narrow dispersities.[202-203] Mechanistic studies revealed an interplay between ATRP and OMRP mechanisms.

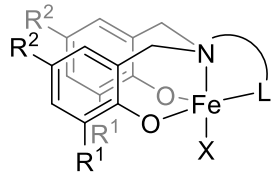

3.72

X = Cl, Br

R^1, R^2 = Me, ^{t}Bu, Cl

L = $(CH_2)_2OMe$, $(CH_2)_2NMe_2$,
CH_2(tetrahydro-2-furanyl),
CH_2(2-pyridinyl)

Figure 3.25. Amine-bis(phenolate) iron(III) complexes applied to Fe-catalyzed ATRP.

Besides well-defined iron complexes (see above), several efficient *in-situ* generated iron catalysts of N-based ligands were reported (Figure 3.26). A combination of $FeCl_3$ and monodentate mono-, di- or tributylamine (**3.73**) mediated the ATRP of St and MMA, in the absence of reducing agent, with an excellent level of control, but required longer reaction times than their phosphine analogues (see section 3.3.4.1) to achieve similar conversions.[186] Also, while the phophine/$FeCl_3$ systems were able to achieve the ATRP of MA with moderate control, the amine/$FeCl_3$ systems were inactive. The water-soluble amine **3.74** was successfully applied to the Fe^{II}-catalyzed bulk (normal) ATRP of St[204] and to Fe^{III}-catalyzed AGET ATRP[205] and ICAR ATRP[206] processes, and offered the advantage that the corresponding iron catalyst could be easily extracted from the polymeric material by washing with water.

Over the last 25 years, the ATRP efficiencies of iron catalysts of several other N-based ligands (bi-, tri- or tetradentate alkylamines, aromatic amines…) were studied, they were often lower than those discussed above and cannot be detailed here. Interested readers are encouraged to consult dedicated reviews.[92-93, 207-208]

3.73 **3.74**

n = 1, 2, 3

Figure 3.26. Simple alkylamines used as ligands in Fe-catalyzed ATRP.

3.3.4.3. Organic Salts as Ligands

The commercially available tetra-*n*-butylammonium (**3.75**) and tetra-*n*-butylphosphonium (**3.76**) bromide salts were widely studied as ligands in Fe-catalyzed ATRP (Figure 3.27). Zhu and coworkers successfully applied these ligands to the iron(III)-catalyzed AGET ATRP of St[209] and MMA[210-211] and the authors observed that both polymerization rate and controllability could be improved by the addition of catalytic amounts of inorganic bases. Matyjaszewski and coworkers reported the $FeBr_2$- and $Fe(OTf)_2$-catalyzed ATRP of MMA in non-polar solvents using the ammonium triflate salt (**3.75**),[212] and the $FeBr_3$-catalyzed SARA ATRP and/or ICAR ATRP of St and MMA using ppm amounts of catalysts and the ammonium bromide salt (**3.75**), with a good control over MW and MWDs.[213-214] The use of the bulky phosphazenium salts (**3.77**) also led to efficient iron(II) catalysts for the ATRP of MMA (and PEGMA), affording polymeric materials with controlled MWs, narrow dispersities, and presented the advantage of easy catalyst removal by washing with water.[215] The imidazolium salts / ionic liquids (**3.78**) combined to $FeCl_3 \cdot 6H_2O$ mediated the AGET ATRP of MMA, using ascorbic acid as reducing agent, and afforded polyMMA samples with predictable MWs and relatively narrow *Đ*.[216]

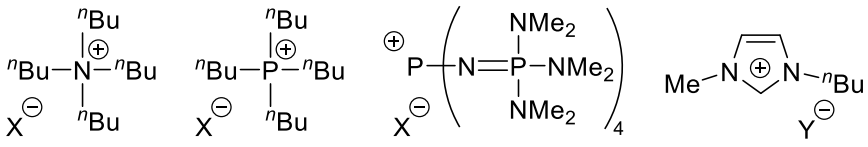

3.75 **3.76** **3.77** **3.78**

X = Cl, Br, CF_3SO_3 ; Y = OH, PO_4, CO_3, HCO_3

Figure 3.27. Organic salts used as ligands in Fe-catalyzed ATRP.

3.3.4.4. Other Systems

Iron(III) complexes of *N*-heterocyclic carbene ligands (**3.79**, Figure 3.28) readily mediated the ICAR ATRP of St and MMA with a very good match between theoretical and experimental MW values and dispersities below 1.5, even at catalyst loading as low as 50 ppm.[217]

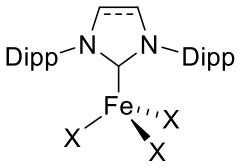

3.79

X = Cl, Br

Figure 3.28. NHC-iron(III) complexes used in Fe-catalyzed ATRP.

It was demonstrated by the group of Matyjaszewski that Fe-catalyzed ATRP of MMA could be performed without conventional ligands, only using the coordination and solubilization abilities of polar solvents such as *N*-methyl-2-pyrrolidone (NMP), DMF or MeCN.[218] This specificity was further exploited by Xue and coworkers to mediate the AGET ATRP of MMA using $Sn(EH)_2$, Zn^0, Fe^0 or alcohols as reducing agents.[219-220] Polyethylene glycol, which has low cost and toxicity, can also be used as an alternative to classical polar solvent in the AGET ATRP of MMA, using $FeCl_3{\cdot}6H_2O$ as metal precursor and sodium ascorbate as reducing agent to exhibit all features of a well-controlled process.[221]

Very recently, Xue, Poli and coworkers reported the ligand- and solvent-free ATRP of MMA promoted by a combination of $FeBr_2$ or $FeBr_3$ and inorganic salts. These systems exhibited all the features of well-controlled processes.[142-143]

3.3.5. Other Catalysts

Several other metals were used to prepare ATRP catalysts, such as Ru, Ni, Re, Mo, Mn, Os, however they generally exhibit lower performances or are less attractive in terms of synthesis, price, toxicity etc. Therefore, they will not be detailed in the present chapter, and interested readers are encouraged to refer to the following reviews.[89, 207-208, 222-223]

3.4. Organometallic Mediated Radical Polymerization

3.4.1. Introduction

Organometallic mediated radical polymerization (OMRP) is another RDRP technique that makes use of a coordination compound as moderator, and differs from ATRP by the role of the later in the moderating equilibrium. In ORMP, the complex directly interacts with the active/propagating radical species to form an organometallic dormant species (Figure 3.29).[82, 84, 224] OMRP can function in reversible termination mode (OMRP-RT), if the number of active radical species do not exceed this of metal centers and the Mt-C/P_n bond dissociation energy (BDE) is low, or in degenerative transfer mode (OMRP-DT) if i) the number of radicals exceeds this of metals, ii) the metal coordination geometry allows it and iii) the exchange is fast relative to chain propagation ($k_{ech} >> k_p$). The initiation of an OMRP can be achieved using either a unimolecular $L/Mt^{x+1}\text{-}R_0$' initiator (direct initiation) or a dual initiating system composed of L/Mt^x and a conventional radical initiator that

generates *in situ* the primary R_0 radical (indirect initiation, Figure 3.29). Several mechanisms may interplay with OMRP, such as ATRP (in the presence of halogen atom(s)), catalytic chain transfer (CCT) or catalytic radical termination (CRT), and this particularity has been well reviewed.[81, 84, 225] While complexes of several transition metals, such as Ti, V, Cr, Mo, Fe were applied to OMRP,[226-228] the field is clearly dominated by cobalt complexes,[226-227, 229-230] which are particularly performant for the controlled polymerization of LAMs.[81, 83] It should be noted that in OMRP the metal complex is used in a stoichiometric amount vs. polymer chain, while in ATRP it can used in catalytic amounts (see section 3.3.2).

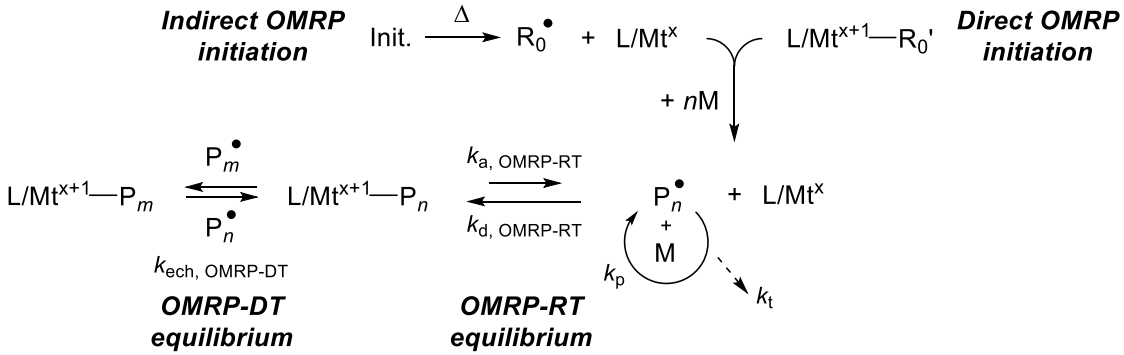

Figure 3.29. Initiation paths and moderating equilibria possibly involved in organometallic-mediated radical polymerization.

3.4.2. Cobalt Moderators

Cobalt is the most studied metal for OMRP and led to the controlled polymerization of the widest range of monomers. After the initial report dealing with the use of a tetramesitylporphyrin (TMP) oragnocobalt(III) as initiator for OMRP,[231] Wayland and coworkers showed that both the dual initiating system Co^{II}(TMP)/V-70 (**3.80**) and the unimolecular initiator Co^{III}(TMP)(CH(CO_2CH_3)CH_3) (**3.81**) efficiently promoted the OMRP of acrylate monomers (Figure 3.30), leading to well-defined PMA and PMA-*b*-PBA (co)polymers. Noteworthy, the polymerization rate was found much faster under OMRP-DT conditions than under OMRP-RT conditions.

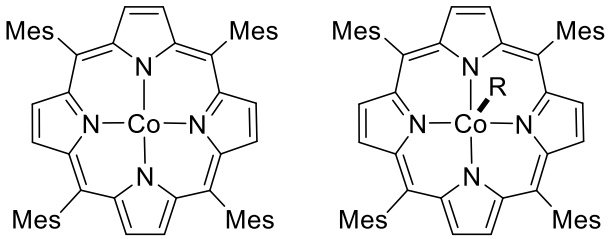

Figure 3.30. Tetramesitylporphyrin Co^{II} and Co^{III} complexes applied to the OMRP of acrylate monomers.

The five-coordinate cobalt(II) acetylacetonate complexes (**3.82**, Figure 3.31) of 1,3-bis(2-pyridylimino)isoindolate-type ligands exhibited excellent performances in the OMRP of MA and *n*BA, with a linear increase of M_n values with conversion, which were close from the theoretical values, and very low dispersities ($Đ$ < 1.13) using V-70 as radical initiator (monomer:Co:V-70 =

600:1:1) in benzene at 60°C.[232] For one example, a well-defined PMA-*b*-P*n*BA block copolymer could be produced. The six-coordinate methanol adducts and the acetato (vs. acetylacetonato) analogues of this series of complexes were less efficient due to the prerequisite of MeOH dissociation for effective radical trapping and low solubility under these conditions, respectively.

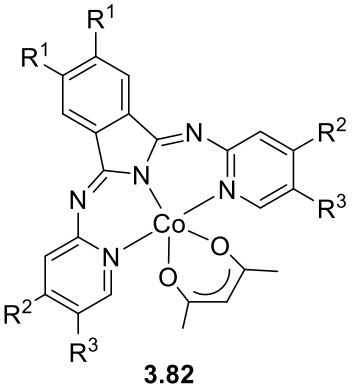

3.82

R^1 = H, Me, Hex, Cl, NO_2
R^2 = H, ^{t}Bu, OMe, Cl
R^3 = H, Cl

Figure 3.31. Five-coordinate cobalt(II) acetylacetonate complexes of 1,3-bis(2-pyridylimino)isoindolate-type ligands applied to the OMRP of MA and *n*BA.

In 2005, Debuigne *et al*. reported the use of commercially available $Co^{II}(acac)_2$ (acac = acetylacetonate) (**3.83**, Figure 3.32), in combination with V-70 (V-70/Co = 6.5), to efficiently mediate the bulk OMRP of VAc at 30°C (M_n up to 10^5 and $Đ$ as low as 1.11).[233] Following this pionneering work, the authors reported several improvements of the system, such as the isolation of a [(R_0-(CH_2-CHOAc)$_{<4}$-$Co^{III}(acac)_2$] complex that could be used as unimolecular macroinitiator,[234] the use of peroxides instead of the thermal sensitive azo initiator V-70 (redox initiation),[235-236] and its application to the controlled polymerization of a large variety of monomers.[83, 229] The mechanism operating in the $Co^{II}(acac)_2$–mediated OMRP of VAc and the remarkable performances of this moderator in the OMRP of LAMs in general were subjected to some investigations and the results were well summarized and discussed in a recent publication.[237] A couple studies have shown that the presence of bulky (^{t}Bu) or electron-withdrawing (CF_3) groups on the ligand scaffold affected the OMRP performances of the resulting moderator (**3.84**, Figure 3.32), by affecting the Co-C bond strength in the organometallic dormant species.[238-239]

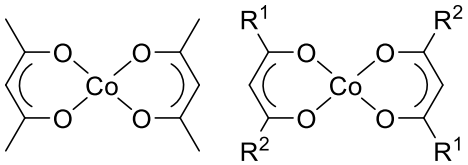

3.83 **3.84**

R^1 = ^{t}Bu, Me, CF_3
R^2 = ^{t}Bu, CF_3

Figure 3.32. Cobalt(II) bis(acetylacetonate) (**3.83**) and derivatives applied to OMRP.

Cobalt(II) complexes of *β*-diketoiminato ligands (**3.85**, Figure 3.33), which are at the same time bulkier (effect of weakening the Co-C bond) and electronically more donating (antagonist effect of

stabilization of Co^{III}) than the isoelectronic $Co^{II}(acac)_2$ system, exhibited a poorer control than the latter in the OMRP of VAc.[240] More recently, a cobalt(II) complex of a salen-type ligand (**3.86**, Figure 3.33) has succeeded in the controlled polymerization of VAc and MA, exhibiting a linear increase in MW with conversion and low dispersities (1.13–1.30).[241]

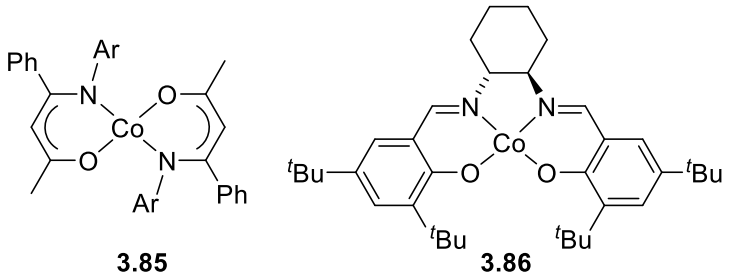

3.85 **3.86**

Ar =Ph, Xyl, *p*-$CF_3C_6H_4$

Figure 3.33. Cobalt(II) complexes of *β*-diketoiminato and salen ligands applied to the OMRP.

3.4.3. Other OMRP Moderators

Asandei and coworkers reported the use of $[Ti^{III}Cp_2Cl]$ (**3.87**/**3.87'**, Figure 3.34), *in situ* generated by reduction of titanocene dichloride with Zn, as moderator for the OMRP of St, which was initiated by radical ring opening of oxiranes (Figure 3.34).[242] While the use of other Ti precursors did not improve the system, further studies have shown that aldehydes, peroxides and alkyl halides were also efficient initiators and that $[Ti^{III}Cp_2Cl]$ also readily mediated the OMRP of IP and copolymerization IP/St.[237]

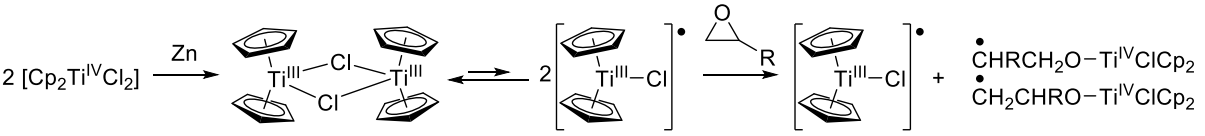

3.87 **3.87'**

Figure 3.34. Initiation of OMRP by the $[Ti^{III}Cp_2Cl]$/epoxide system.

Shaver and coworkers reported a well-controlled OMRP of VAc and other vinyl esters (vinyl propionate, vinyl pivalate, vinyl benzoate) in the presence of bis(imino)pyridine vanadium(III) complexes (**3.88**, Figure 3.35), with a linear increase of M_n values with conversion and narrow MWDs (≈ 1.3).[243-245] While the experimental MWs agree well with theoretical values at low conversions (up to ca. 30%), a discrepancy is observed at higher conversions, and was attributed to complex decomposition. Experimental and computational investigations were in agreement with an OMRP mechanism involving the V^{II}/V^{III}-R couple.

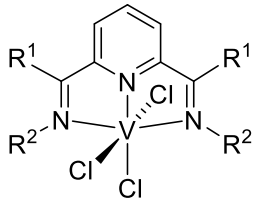

3.88

R^1 = Me, H, Ph, Et, ^{i}Pr

R^2 = Cy, Ph, Mes, Dipp, 4-MeC_6H_4, 4-FC_6H_4, 2,6-$Me_2C_6H_3$, 2,6-$Et_2C_6H_3$

Figure 3.35. Bis(imino)pyridine vanadium(III) complexes used in the OMRP of vinyl esters.

Poli, Smith and coworkers have shown that Cr^{II}/Cr^{III} systems (**3.89**/**3.90**, Figure 3.36) can be used in the OMRP of VAc, however the level of control remained modest.[246] More interesting is the fact that the authors could experimentally evidence a strong weakening of the Cr-polyVAc bond (lower Cr-C BDE) upon increasing the size of the *ortho* substituents of the N-Ar rings. This observation was supported by computational studies on model compounds, which revealed higher Cr-R BDEs for Ar = Ph than Xyl, and within each family the values increased in the order R = CH(Me)Ph < CH_2Ph < CH(Me)OOCMe (from bigger to smaller R group). The same trend is observed for the calculated Cr^{III}-C bond lengths.

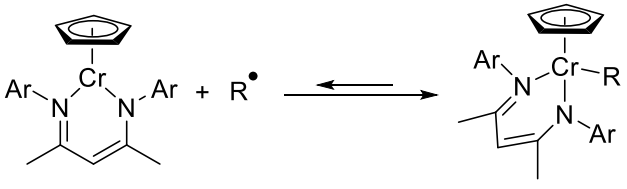

3.89 **3.90**

Ar = Dipp, 2,6-$Me_2C_6H_3$, Ph
R = CH(Me)Ph, CH_2Ph, CH(Me)OOCMe
Cr-C BDE: ⟶

Figure 3.36. Chromium complexes applied to the OMRP of VAc.

As stated in section 3.3.4, iron complexes were found to be successful ATRP catalysts.[93, 228] However, for application in "pure" OMRP, without interference of ATRP, the complexes used should not contain halogen atoms, and such examples are quite rare.[237] An interesting report by Poli and coworkers highlighted that; compared to the very efficient $Co^{II}(acac)_2$ moderator (**3.83**, Figure 3.32, section 3.4.2) and despite their similarity, the ability of $Fe^{II}(acac)_2$ (**3.91**) to control the radical polymerization of VAc was quite poor (MW higher then expected, $Đ > 1.2$).[247]

4. Lactide and Related Cyclic Esters Polymerization

4.1. Introduction

The ring-opening polymerization (ROP) of cyclic esters, catalyzed by metal coordination complexes has attracted tremendous interest over the past fifteen years. In particular, polylactide (PLA), a bio-sourced and biodegradable polymer arising from the ROP of lactide (LA, a dimer of lactic acid) has already found numerous applications as commodity materials and in the biomedical area.[248-252] Commercial PLA, PLLA, is industrially produced by ROP of L-LA using a Sn-based catalyst,[253-254] but a large number of various well-defined ligand-supported metal alkoxides may efficiently polymerize lactide in a controlled manner.[255] Besides control and activity, the stereoselective ROP of *rac*-lactide may also be performed with metal complexes with appropriate metal-ligand design, which has certainly stimulated research on more advanced meatl catalyst over the past years. In this regard, the production of PLLA-*b*-PDLA isotactic stereoblocks, possible through the *iso*-selective ROP of rac-lactide, is of interest since such materials may exhibit significant enhanced thermal and mechanical properties vs. commercial PLA. The metal-mediated ROP of related cyclic lactones such as ε-caprolactone and β-butyrolactone was also studied along with the biodegradability of the derived polymers and their applications in biomedicine.

Though other mechanisms are known for cyclic esters ROP, such monomers are typically polymerized *via* a coordination-insertion mechanism using a metal-alkoxide catalyst, as depicted in Figure 4.1.[256] While the Lewis acidity appears central for monomer activation, alkoxide nucleophilicity is also crucial for initiation and chain growth, thereby favoring the use of electropositive and oxophilic metal centers for effective catalysts. Ideally, the ROP thus proceeds in a living manner with chain length control. Stereocontrol may be achieved either *via enantiomorphic site* control, where the metal-ligand chiral pocket induces stereocontrol, or through a *chain-end* stereocontrol mechanism, in which the last inserted monomer of the growing polymer chain dictates the stereochemistry of the incoming monomer.

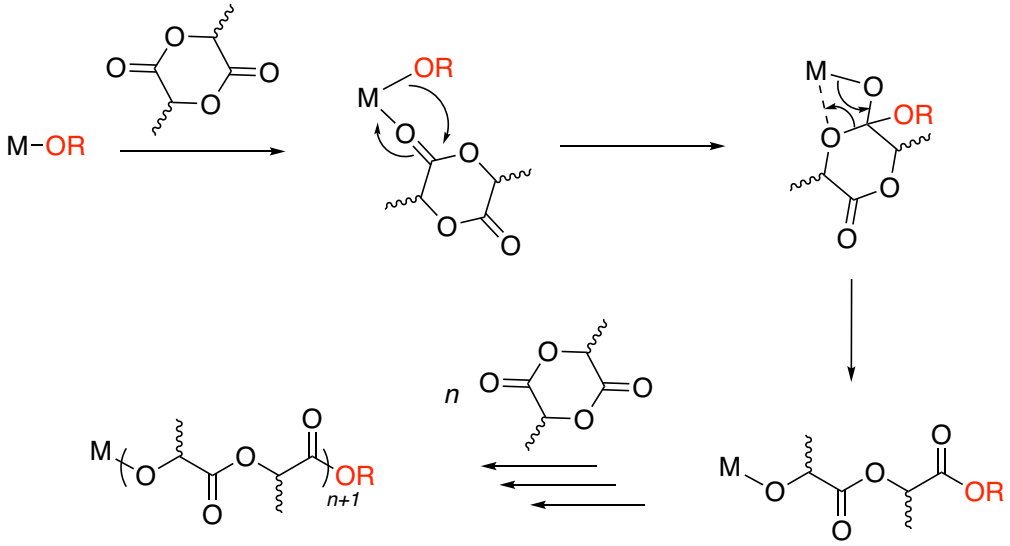

Figure 4.1. General coordination/insertion mechanism for the ROP of cyclic esters initiated (taking the example of lactide) by metal alkoxide complexes.

The field of metal-based cyclic esters ROP has been extensively reviewed over the past years, including with recent reviews cited herein. The present part will highlight key representative coordination metal complexes for the ROP of lactide that have contributed to the major progress of the field since 2003.

4.2. Group 1-2 Metal Catalysts

4.2.1. Alkali Metals

Numerous alkali metal aryloxide species (ArOM) were shown to efficiently polymerize lactide under mild conditions.[257-260] The steric and electronic properties of the supported aryloxide ligand play a crucial role in ROP activity and stereoselectivity, with the preferred use of multidentate aryloxide ligands, such as **4.1**-**4.3** (Figure 4.2),[261-265] to control and limit catalyst aggregation. Remarkably, salts **4.3**, in which the Na^+ or K^+ metal ion is supported by an ancillary crown ether and a sterically demanding phenoxide, are highly active catalysts for the *iso*-selective ROP of *rac*-lactide, producing chain-length-controlled isotactic PLA (complete conversion of 500 equiv LA, 10 min, RT, 10 equiv BnOH, P_m = 0.82).[266-267]

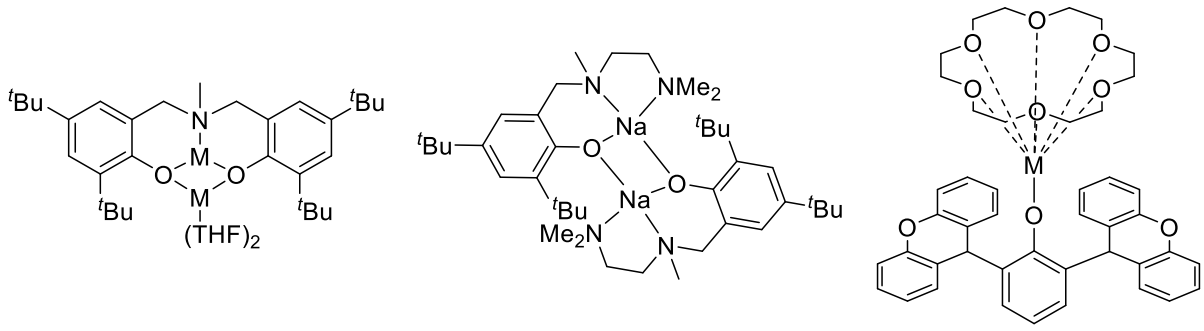

4.1
M = Li, Na

4.2

4.3
M = Na, K

Figure 4.2. Representative examples of Group 1 metal initiators for cyclic esters ROP.

4.2.2. Group 2 Metals

Well-defined magnesium(II) complexes bearing various N-/O-based multidentate ligands are well-established cyclic esters ROP initiators and typically exhibit high catalytic activity.[268] For most systems, the catalytically active Mg-alkoxide is generated *in situ via* alcohol protonolysis of the corresponding Mg-amido/alkyl precursor.[269] Supporting ligands that have thus far been developed most notably include *β*-diketiminates,[270] Schiff bases,[271-272] trispyrazolylborates,[258] heteroscorpionate[273] and aminophenolates.[274-275] Despite their limited hydrolytic stability, such ROP catalysts are particularly attractive since magnesium is an earth-abundant and benign metal source. Representative classes of single-site Mg^{II} and Ca^{II} complexes (**4.4**-**4.8**) for use in the ROP of cyclic esters are depicted in Figure 4.3. The vast majority of Mg-based catalysis for *rac*-lactide ROP lead to atactic and hetero-enriched PLA. However, recent studies showed that chiral oxazolyl aminophenolate Mg^{II} species, such as **4.6**, are highly active catalysts for the *iso*-selective ROP of *rac*-lactide to isotactic stereoblock PLA *via* an enantiomorphic site control mechanism thanks to the chirality of the system and the dinuclearity of the catalytically active Mg^{II} species (P_m = 0.80, TOF up 54,000 h^{-1} at RT).[276] The bis-pyrrolidine aminophenolate Mg^{II} complex **4.7** was also found to be an extremely active lactide ROP catalyst allowing precise production of PLLA-*b*-PDLA multiblock copolymers with up to 500 repeating units per block, allowing access to novel high melting PLA materials.[277] Though studied to a lesser extent, calcium(II) complexes were also shown to be extremely active cyclic esters ROP catalysts, with Ca > Mg. Single-site Ca-OR species typically require severe steric protection, such as for **4.8**, and are much less developed than Mg^{II} analogues.[258, 278-279]

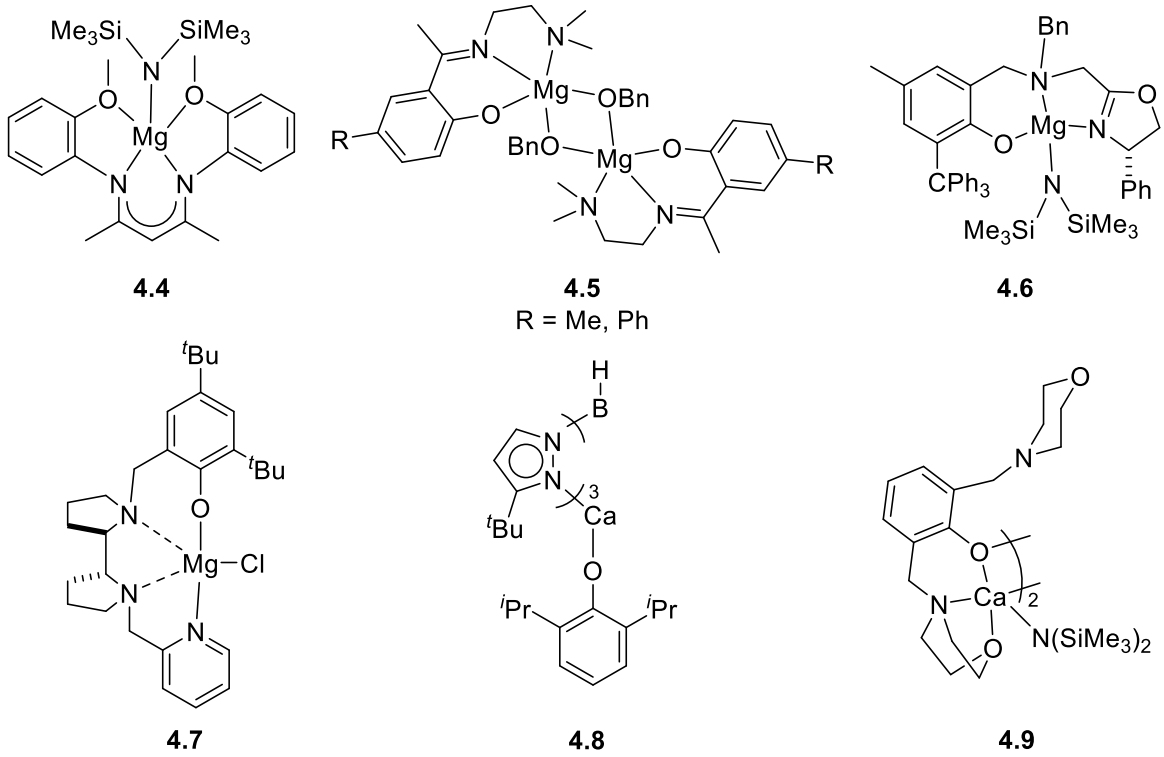

Figure 4.3. Representative examples of Group 2 metal initiators for cyclic esters ROP.

4.3. Group 4 Metal Catalysts

Group 4 metal (Ti, Zr and Hf) alkoxides supported by various aryloxide-based multidentate ligand platforms have widely been used in the ROP of lactide and related cyclic esters.[280-281] A number of thorough studies indicated that catalytic activity increases upon going down from titanium(IV), to zirconium(IV) and then hafnium(IV) derivatives, which was primarily ascribed to the smaller size of Ti(IV) *vs.* Zr(IV) and Hf(IV).[282] Representative Group 4 metal cyclic esters catalysts **4.10**-**4.12** are depicted in Figure 4.4. Despite the frequent use of chelating ligands with fine-tuned stereo-electronic properties, ROP stereoselectivity and control follow no clear trend in these systems. However, highly *hetero*-selective Group 4 metal catalysts, such as compound **4.12**, were reported in *rac*-lactide ROP.[283]

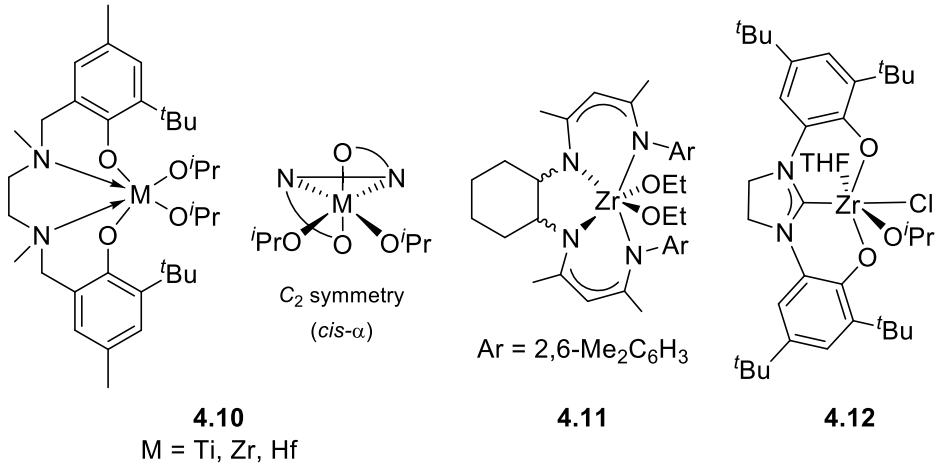

Figure 4.4. Representative examples of Group 4 metal initiators for cyclic esters ROP.

4.4. Group 12 Metal Catalysts

Zinc(II) alkoxides have been widely studied over the past twenty years as ROP initiators of cyclic lactones, primarily lactide, since Zn is a cheap and low toxicity metal source.[284-289] Early studies in the late 90's by the groups of Coates and Tolman showed that single-site discrete Zn^{II} alkoxides bearing *N*-/*N*- or *N*-/*O*-based ligands, such as **4.13** and **4.14** (Figure 4.5), were highly effective and well-behaved catalysts for the controlled ROP of lactide.[290-291]

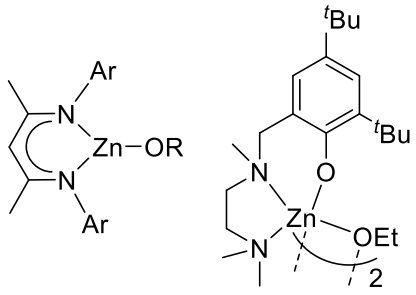

4.13 **4.14**

Figure 4.5. Early examples of highly effective single-site Zn-based catalysts in lactide ROP.

In particular, catalyst **4.14** was found to be a remarkably active ROP catalyst with the quantitative polymerization of 500 equiv of lactide within 5 min at RT to well-defined and chain-length-controlled PLA. Since then, various Zn–OR species supported by diverse ligand platforms have been reported for use in cyclic lactones ROP, as compiled in a number of reviews.[284-289] Representative examples of structurally diverse Zn^{II} ROP initiators (**4.15**-**4.18**) are depicted in Figure 4.6.[284, 292-294]

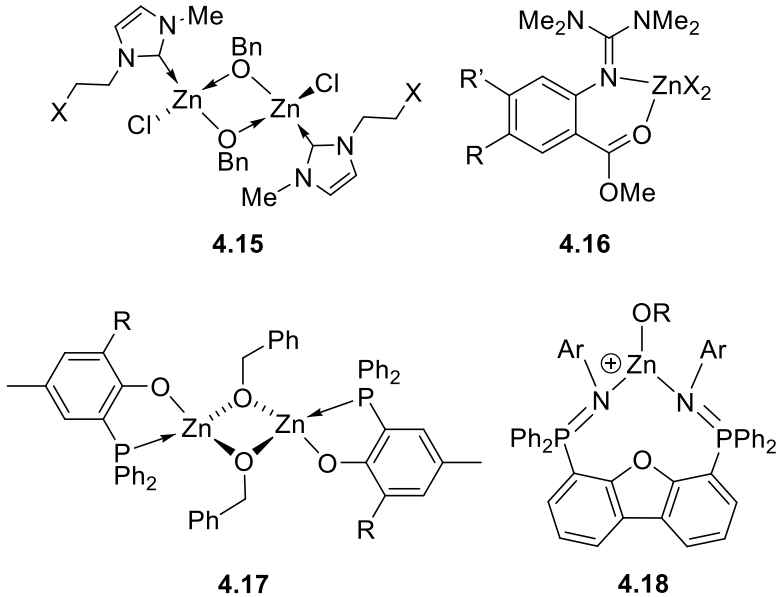

4.15 **4.16**

4.17 **4.18**

Figure 4.6. Structurally diverse Zn^{II} initiators for the ROP of cyclic lactones.

As a general tendency, Zn^{II} species display a ROP activity between those of Al^{III} and Mg^{II} derivatives, but are typically less sensitive towards hydrolysis than the latter due to a less polar M–OR bond. On the other hand, when compared to Al^{III} catalysts (*vide infra*), Zn^{II}-based systems able to *iso*-selectively polymerize *rac*-lactide remain much less developed and efficient catalysts in the area,

such as species **4.19**-**4.21** (Figure 4.7), were only recently reported.[295-297] In particular, the aminophenolate-supported Zn^{II} species **4.19** efficiently mediates the *iso*-selective ROP of *rac*-lactide at room temperature to afford stereoblock isotactic PLA (P_m up to 0.87, TOF up to 3312 h^{-1}). Further broadening the scope of Zn-based systems for stereoselective ROP of cyclic lactones, chiral Zn^{II} complex **4.21** was also recently demonstrated to promote the *syndio*-selective ROP of *β*-butyrolactone allowing access to melt processable syndio-enriched PHB material.

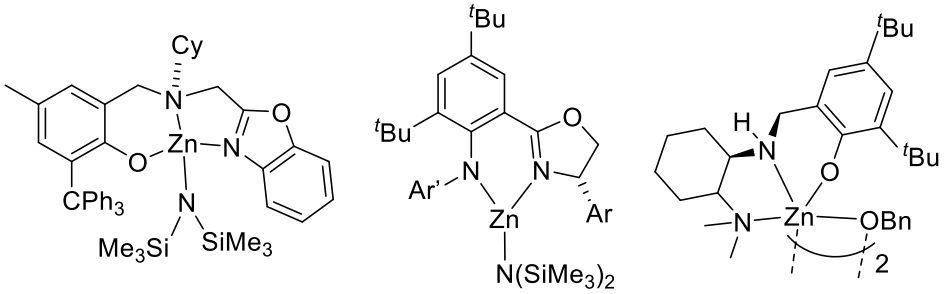

4.19 **4.20** **4.21**

Figure 4.7. Selected zinc(II) complexes mediating the stereoselective ROP of cyclic lactones.

4.5. Group 13 Metal Catalysts

Ligand-supported aluminum alkoxide species, such as (salen*)AlOR derivatives of type **4.22** (Figure 4.8), are of historical importance since they are the first metal-based initiators reported to mediate the stereoselective (*iso*-selective) rac-lactide ROP.[298] These investigations, as well as those with (Porph)AlX-type complexes as cyclic ROP catalysts,[299] triggered numerous studies on Al species. The synthesis of Al alkoxides bearing various chelating ligands has thus received great attention for the ROP of cyclic esters, primarily LA, ε-CL and β-lactones, over the past fifteen years. This has allowed the efficient and controlled production of well-defined and/or stereoregular polyesters using Al catalysts. For the most part, the ROP of cyclic esters mediated by Al alkoxide species typically occurs through a well-established coordination/insertion mechanism. Several comprehensive reviews thoroughly covering the area have recently been published in the literature.[260, 300-307] While Al derivatives are typically less active catalysts than Group 1 and Group 2 metal species, they frequently exhibit superior performances in stereoselective ROP of *rac*-lactide, often with the production of *iso*-enriched PLA such as PLLA-PDLA isotactic stereoblocks. Recent progress on the use of "chiral-at-metal" Al species such as complex **4.23** (Figure 4.8), which bears two configurationally stable Al-bonded chiral nitrogens, showed a significant improvement of stereocontrol in *rac*-lactide ROP.[308] Such systems were proposed to stereoselectively polymerize *rac*-lactide *via* a dual-stereocontrol mechanism, differing from the classical enantiomorphic site and chain-end control mechanisms.[309]

Several indium(III) and, to a lesser extent, gallium(III) complexes were successfully investigated as ROP initiators of cyclic esters.[310] Though typically less catalytically active in lactide ROP compared to their Al^{III} counterparts, dinuclear In^{III} species **4.24** (Figure 4.8) promotes the highly controlled ROP of *rac*-lactide and retains its dinuclear structure as the ROP proceeds with a In-O-In bridging polymeryl chain.[311] Salen-supported Ga^{III} species **4.25** (Figure 4.8) were shown to be effective catalysts for the controlled and moderately *iso*-selective ROP of *rac*-lactide.[312]

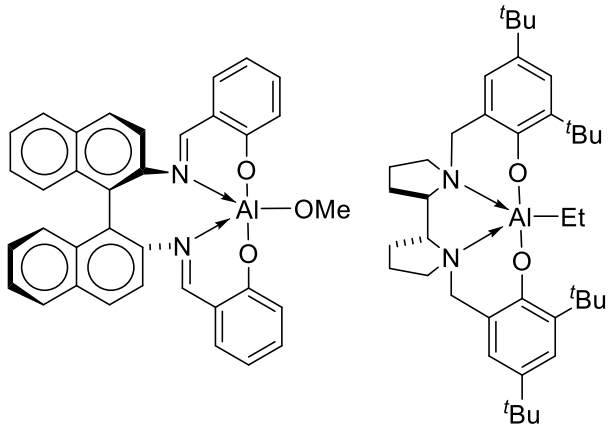

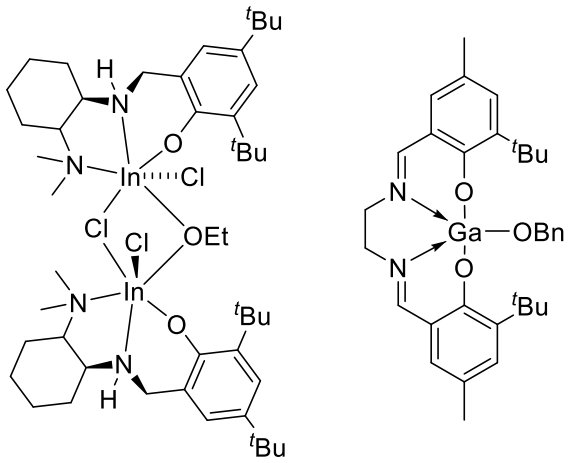

Figure 4.8. Representative examples of Group 13 metal initiators for cyclic esters ROP.

5. CO_2/Epoxides Copolymerization

5.1. Introduction

The copolymerization epoxides with CO_2 is a straightforward synthetic method for producing a range of aliphatic polycarbonates. The reaction was discovered in 1969 and has since continued of being attractive by means of manufacturing biodegradable CO_2-based polymers for switching our current polymer productions away from the intensively used petroleum-based resources. The copolymerization of epoxides with CO_2 activity and selectivity mostly relies on the selection of the catalyst, and initially based on low performances of ill-defined heterogeneous catalysts, the discovery quickly extended to more well-defined homogeneous catalyst systems.

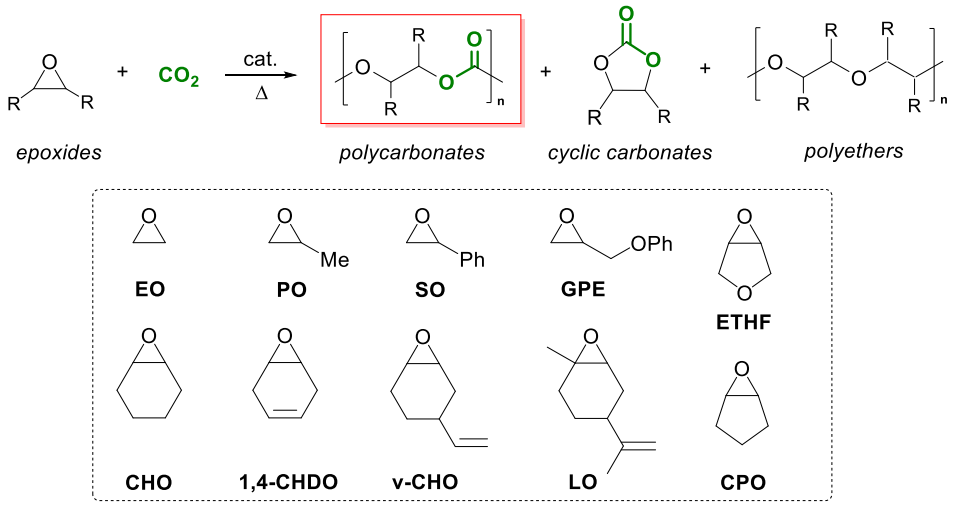

Figure 5.1. Typical epoxide/CO_2 copolymerization reaction for producing polycarbonates and concomitant side products (cyclic carbonates and polyethers). Principal structures and abbreviations of monomers discussed in this section: EO: ethylene oxide, PO: propylene oxide, SO: styrene oxide, GPE: glycidyl phenyl ether, ETHF: 3,4-epoxytetrahydrofuran, CHO: cyclohexene oxide, 1,4-CHDO: 1,4-cyclohexadiene oxide, v-CHO: 4-vinyl-cyclohexene oxide, LO: limonene oxide and CPO: cyclopentene oxide.

During the last 20 years, most of the investigations were founded on well-defined homogeneous catalysts and largely stimulated and dedicated toward catalysts based on chromium and cobalt salen-type ligands, zinc β-diketiminate (BDI), and aluminum porphyrin complexes,[313-320] due to their exceptional activity and selectivity toward polycarbonates affording often no concomitant formation of side products (cyclic carbonates or polyethers). However, in recent years, attention has turned towards other metals and type of ligands for getting around the minefield of patents and to harness the potential of other metals that could be less toxic, more accessible and abundant elements reducing the factor of future supply risk.[321] Over the last 15 years, several excellent reviews have outlined the key development of those seminal examples of metals catalyzing the copolymerization of epoxides with CO_2 (i.e. with Cr, Co, Zn and Al) and therefore, we include here only a brief outline of their key features. The majority of this book chapter section, however, is devoted to the recent advances using other metals. For comparing catalyst activities and selectivities among other different catalytic systems, these key parameters have been used and defined as following: catalyst activity reported as TOF in h^{-1} ($mol_{epoxide}/mol_{catalyst}$*(%conv./100)/time in hour), the selectivity for polycarbonates over cyclic carbonates formation, and the degree of carbonate linkage defining the amount of CO_2 coupled with the epoxides against ether linkages (homopolymerization) in the produced polymers. Activities are classified as very high (> 1000 h^{-1}), high (1000-200 h^{-1}), moderate (5-200 h^{-1}), low (1-5 h^{-1}) and very low (< 1 h^{-1}).

5.2. Catalysts Survey

5.2.1. Group 2 Metal Catalysts

In contrast to the Lewis acidic main group zinc and aluminum catalysts, the magnesium-based catalysts have received much less consideration, despite their productivity in the ring-opening polymerization (ROP) of *rac*-lactide.[322-323] Among the early studies, the use of homoleptic $Mg(OAc)_2$

and $MgEt_2$-H_2O for the copolymerization of PO/CO_2 were first reported, and both showed very poor activity (TOF < 0.1 h^{-1}).[324-325] More recently, Ding and co-workers reported bimetallic Mg complexes generated *in situ* from the reaction of multidentate bis(α,α-diarylprolinol)phenolate ligands (**a**-**o**, Figure 5.2) with Mg(^{n}Bu)$_2$, and subsequently treated with alcoholic or phenolic additives were found moderately active (TOFs < 43 h^{-1}) and selective in CHO/CO_2 copolymerization.[326] Although the active species were not isolated, the putative structure **5.2a** was proposed. It is derived from the alcoholysis of di-Mg(^{n}Bu) species (**5.1a**), and exhibited the best activity (TOF = 9 h^{-1}) in affording the completely alternating PCHC (carbonate linkages >99%) under mild conditions (P_{CO2} = 1 bar, T = 60 °C, albeit with a high catalyst loading (molar ratio of CHO:**a**:Mg(^{n}Bu)$_2$:^{n}BuOH = 20:1:2:0.4).

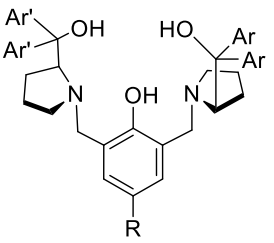

Ar/Ar' = Ph, R = Me (**a**); Ar/Ar' = 4-MeC_6H_4, R = Me (**b**);
Ar/Ar' = 3-MeC_6H_4, R = Me (**c**); Ar/Ar' = 4-$(OMe)C_6H_4$, R = Me (**d**);
Ar/Ar' = 4-PhC_6H_4, R = Me (**e**); Ar/Ar' = 4-$(CF_3)C_6H_4$, R = Me (**f**);
Ar/Ar' = 3,5-$(CF_3)_2C_6H_3$, R = Me (**g**); Ar/Ar' = 3,5-$Me_2C_6H_3$, R = Me (**h**);
Ar/Ar' = 4-ClC_6H_4, R = Me (**i**); Ar/Ar' = Ph, R = NO_2 (**j**);
Ar/Ar' = Ph, R = ^{t}Bu (**k**); Ar/Ar' = Ph, R = H (**l**);
Ar = Ph, Ar' = 4-ClC_6H_4, R = Me (**m**);
Ar = Ph, Ar' = 3,5-$(CF_3)_2C_6H_3$, R = Me (**n**);
Ar = 3,5-$(CF_3)_2C_6H_3$, Ar' = 3,5-$Me_2C_6H_3$, R = Me (**o**)

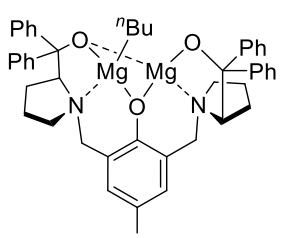

5.1a

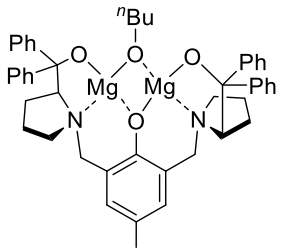

5.2a

Figure 5.2. Bis(α,α-diarylprolinol)phenolate magnesium catalysts.

In 2012, Williams and co-workers reported a series of more active bimetallic magnesium catalysts (**5.3**-**5.5**, Figure 5.3) containing a bis(phenolate)tetraamine macrocyclic ligand.[327] All catalysts copolymerize efficiently CHO in presence of 1 bar of CO_2 at 100 °C (TOF up to 750 h^{-1} especially for **5.4** and **5.5**) and produced PCHCs with >99% selectivity and carbonate linkages. The copolymerization of CHO/CO_2 using **5.3**-**5.5** afford a linear relationship between M_n and CHO conversion, coupled with a narrow polydispersity ($Đ$ < 1.2). More importantly, catalyst **5.4** exhibited high tolerance to most common impurities found in the captured CO_2 gas feed, such as amines ($HNEt_2$, H_2NMe, $H_2N(CH_2)_2OH$), thiols (H_2S, $HS(C_8H_{17})$), SO_2, O_2 and water, without compromising the activity or selectivity.[328] The di-Mg complex (**5.4**) also catalyzes the copolymerization of 1,4-cyclohexadiene oxide (1,4-CHDO) and the terpolymerization of 1,4-CHDO/CHO (4:1) with CO_2 under low pressure (1 bar), yielding completely alternated polycarbonates with low molecular weights (M_n = 2-4 kg mol^{-1}) and narrow polydispersities ($Đ$ < 1.2), albeit the activity for both reactions are considerably reduced (TOFs = 6 and 21 h^{-1}, respectively).[329]

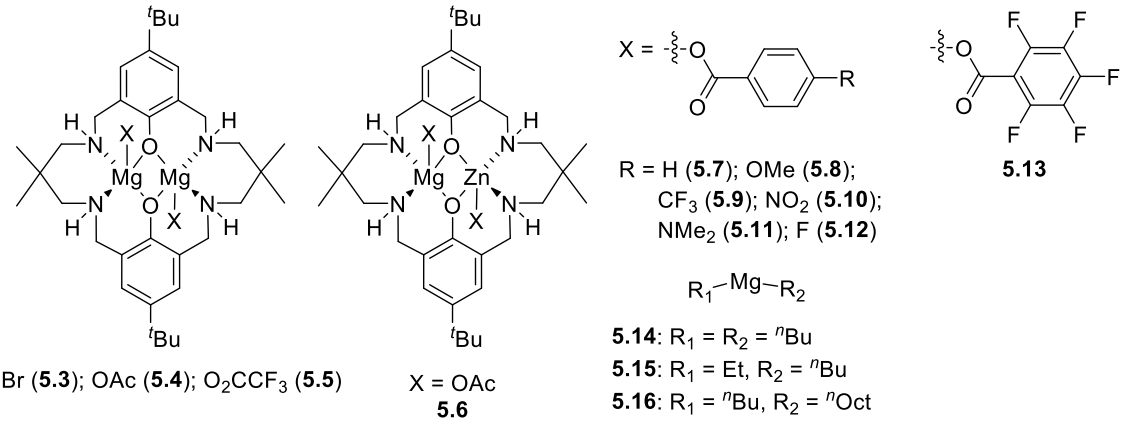

Figure 5.3. Bimetallic magnesium (**5.3**-**5.5**) and magnesium/zinc (**5.6**-**5.13**) catalysts of a bis(phenolate)tetraamine macrocyclic ligand and simple dialkylmagnesium catalysts (**5.14**-**5.16**).

In a recent study, a series of heterobimetallic Mg-Zn compounds (**5.6**-**5.13**, Figure 5.3), wrapped by a bis(phenolate)tetraamine macrocyclic ligand and bearing various carboxylate as co-ligands, were examined for the CHO/CO_2 alternating copolymerization under atmospheric pressure.[330-331] The mixed dinuclear catalysts exhibited very high catalytic performances, independently of the co-ligands used, with TOFs reaching 8800 h^{-1} for **5.9** especially under high temperature and pressure regime (120 °C, 20 bar), which are superior to the homodinuclear catalysts (Mg-Mg or Zn-Zn) when tested alone or mixed together. Complex **5.8** was also tested for the copolymerization of various epoxides with CO_2 (under 1 bar at 80 °C). The latter catalyzes in a selective manner the formation of polycarbonate with high content in carbonate linkages (>99%) and with several epoxides, such as CPO (TOF up to 76 h^{-1}, Sel_{PCPC} = >99%), v-CHO (TOF = 71 h^{-1}, Sel_{PvCHC} = >99%), 1,4-CHDO (TOF = 1 h^{-1}, Sel_{PCHDC} = 74%) and 3,4-epoxytetrahydrofuran (TOF = 14 h^{-1}, Sel_{PTHFC} = 98%), except for PO (TOF = 8 h^{-1}, carbonate linkages = 98%, Sel_{PPC} = 26%).[331]

Further studies based on Mg have shown that simple achiral dialkylmagnesium compounds (**5.14**-**5.16**, Figure 5.3) work effectively as catalysts at 100 °C under low CO_2 pressures (1-10 bar) without additives or co-catalysts for the isoselective copolymerization of neat CHO with CO_2, affording isotactic polycarbonate (P_m = *m*-centered tetrads: 79-80%) in high yields, in a controlled manner ($Đ$ < 2.8 and M_n up to 32 kg mol^{-1}) and with relatively high carbonate linkages (80-92%).

5.2.2. Rare-Earth Metal Catalysts

Initially triggered by the report of ternary lanthanide (including Group 3) species as efficient catalysts for the ROP of epoxides, similar catalysts such as Ln-based tertiary systems composed of $Y(P_{204})_3/Al(^iBu)_3$/glycerol (with P_{204} = $-O(O)P(O\text{-}CH_2(C_2H_5)CH(CH_2)_3CH_3)_2$)[332] and $Nd(O_2CCCl_3)_3/ZnEt_2$/glycerol[333] were found to be the most active to produce PPC (30-40% carbonate unit content and >95% carbonate linkages, respectively).[334-335]

Following up on these preliminary studies revealing the potential of lanthanide species for activating epoxides, even though the role of Al or Zn/alcohols combined with lanthanides were still unclear, further single-component lanthanide complexes were studied in the copolymerization of epoxides with CO_2. In general, all single-component catalysts required CO_2 pressure and reaction temperatures superior to 10 bar and 60 °C, respectively, and moderate activities and selectivity toward the formation of polycarbonates were observed. As prominent examples of single-

component Ln catalysts, Hou and co-workers demonstrated that rare-earth metal half-sandwich bis(alkyl) complexes $(C_5Me_4SiMe_3)Ln(CH_2SiMe_3)_2(THF)$ (**5.17**-**5.20**) and polyhydride complexes $[(C_5Me_4SiMe_3)Ln(\mu\text{-}H)_2]_4(THF)_x$ (**5.21**-**5.23**) exhibit a moderate activity in copolymerizing CHO with CO_2 to produce nearly selectively PCHC (carbonate linkages: >90%) with high molecular weights (M_n = 14-39 kg mol^{-1}), and often with wide-ranging molecular distributions ($Đ$ = 4-10) (Figure 5.4).[336] While the most efficient catalyst is based on Lu(III) complex (**5.19**) for the selective production of PCHC, in contrast its Sc(III) analogue (**5.20**) exhibits low activity and high content of ether linkages (carbonate linkages: 23%) under similar reaction conditions (12 bar, 70 °C). Both isolated bis(carboxylate) complexes (**5.24**-**5.25**) resulting from the reaction of (**5.17** and **5.19**) with CO_2 were also found moderately active in the copolymerization suggesting carboxylate-bridged bimetallic species as possible catalytic intermediates.[336] A variety of other cyclopentadienyl-ligated lanthanides such as bimetallic hydrides (**5.26**-**5.28**), bis(silylamido) yttrium (**5.29**), silylamido ytrocene (**5.30**) complexes and silylamido yttrium complex bearing one BDI ligand (**5.31**) were successfully tested in the copolymerization CHO/CO_2.[337-338] Among the reported series of cyclopentadienyl Ln catalysts, complex (**5.29**) showed the highest activity (TOF = 33 h^{-1}, at 75 °C, 8.5 bar CO_2), producing a polymer with carbonate linkages exceeding >85% and a relatively broad polydispersity ($Đ$ = 1.9).[337]

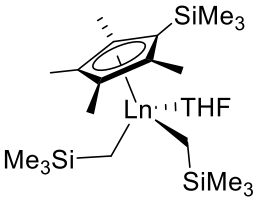

5.17: Ln = Y
5.18: Ln = Dy
5.19: Ln = Lu
5.20: Ln = Sc

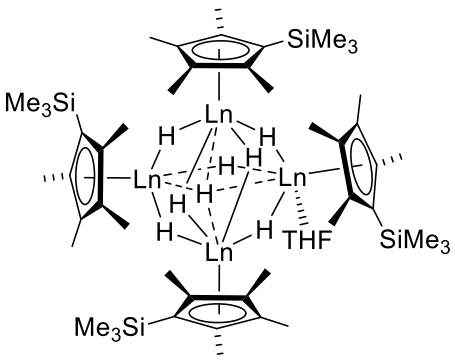

5.21: Ln = Y
5.22: Ln = Lu

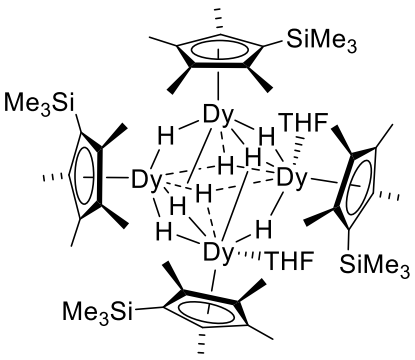

5.23

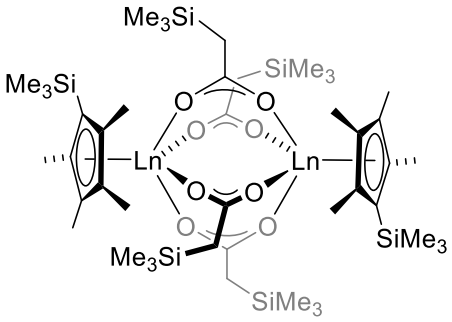

5.24: Ln = Y
5.25: Ln = Lu

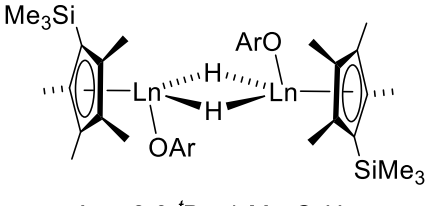

Ar = 2,6-^{t}Bu-4-Me-C_6H_2

5.26: Ln = Y
5.27: Ln = Dy
5.28: Ln = Lu

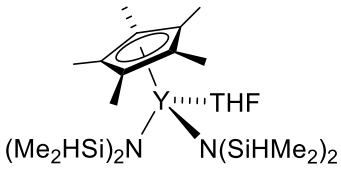

5.29

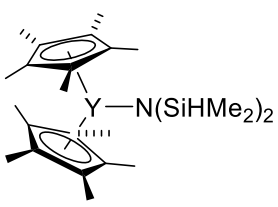

5.30

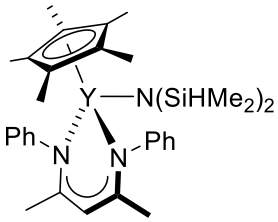

5.31

Figure 5.4. Representative half-sandwich and β-diketiminate rare-earth metal catalysts.

Inspired by the high activity and selectivity of (BDI)-zinc catalysts (*vide infra*) in the copolymerization of CHO with CO_2, a range of mono- and bis-(BDI) complexes (**5.32**-**5.47**) of rare-earth metals were also investigated (Figure 5.5).[339-340] Initial experiments indicated that the mono(BDI) rare-earth bis(alkyl) complexes (**5.34**-**5.39**) were more active and selective toward the formation of PCHCs without formation of cyclic carbonates (TOF =12-39 h^{-1} with carbonate linkage up to 93%) compared to the bis(silylamido) complexes (**5.32**-**5.33**) showing 5-10% of CHC byproduct (TOF up to 2.3 h^{-1} with carbonate linkages up to 82%) under nearly similar catalytic conditions in toluene. Catalysts such as yttrium bis(alkyl) bearing an *O*-anisol-substituted BDI ligand (**5.34**) exhibits so far the best recorded activity (TOF = 47 h^{-1}) with high carbonate linkages (99%) and narrow polydispersity (*Đ* = 1.7), unfortunately under harsh conditions (130 °C, 15 bar) and using 1,4-dioxane as solvent.[340]

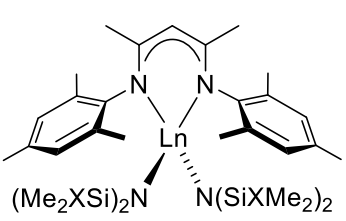

5.32: Ln = La, X = Me
5.33: Ln = Y, X = H

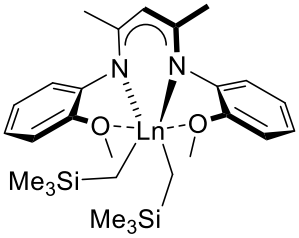

5.34: Ln = Y
5.35: Ln = Lu
5.36: Ln = Sc

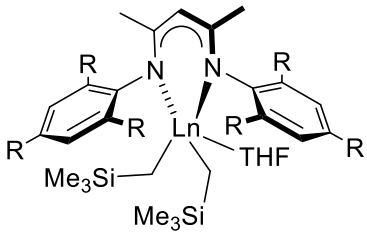

5.37: Ln = Y, R = Me
5.38: Ln = Lu, R = Me
5.39: Ln = Lu, R = H

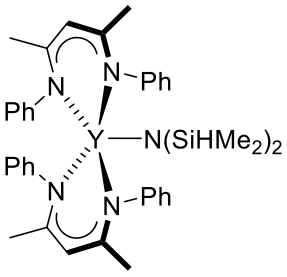

5.40

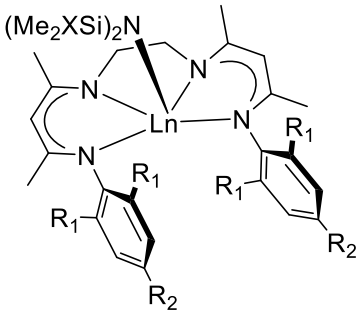

5.41: Ln = La, X = Me, R_1 = R_2 = Me
5.42: Ln = Y, X = Me, R_1 = R_2 = Me
5.43: Ln = La, X = H, R_1 = R_2 = Me
5.44: Ln = La, X = Me, R_1 = ^{i}Pr, R_2 = H

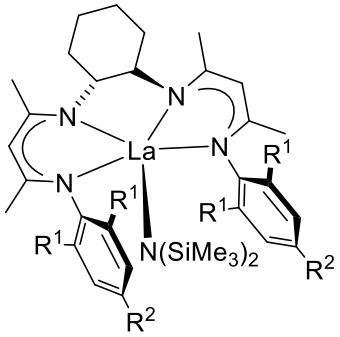

5.45: R^1 = R_2 = Me
5.46: R^1 = Et, R_2 = H
5.47: R^1 = ^{i}Pr, R_2 = H

Figure 5.5. Representative β-diketiminate rare-earth metal catalysts.

Following the seminal works on salen-chromium and cobalt copolymerization catalysts,[315] Kleij and co-workers recently reported the copolymerization of CHO/CO_2 catalyzed by a combination of homoleptic and heteroleptic lanthanide(salen)-based complexes (**5.48**-**5.55**) in the presence of various nucleophilic additives ([PPN]X with X= Cl, Br, I, OAc, N_3, [$^{n}Bu_4N$]Cl and DMAP) at 20 bar CO_2, which afforded PCHCs in moderate yields (Figure 5.6).[341] Among this series of Ln(salen) catalysts, the best results were obtained with complex (**5.48**) (TOF= 31 h^{-1}, CHO:Yb:[$^{n}Bu_4N$]Cl = 1000:1:0.5, at 90 °C, 20 bar) leading to PCHC with 99% linkage carbonates (M_n = 10.2 kg mol^{-1}, *Đ* = 1.54).

Comparatively, Yb(salen)-based catalysts (**5.48**-**5.51**) showed to some extent lesser reactivity in relation to Sc and Y(salen) complexes (**5.52**-**5.55**), but with much better copolymerization control combining high molecular weight, narrow polydispersities, and very little formation of the CHC by-product.[341]

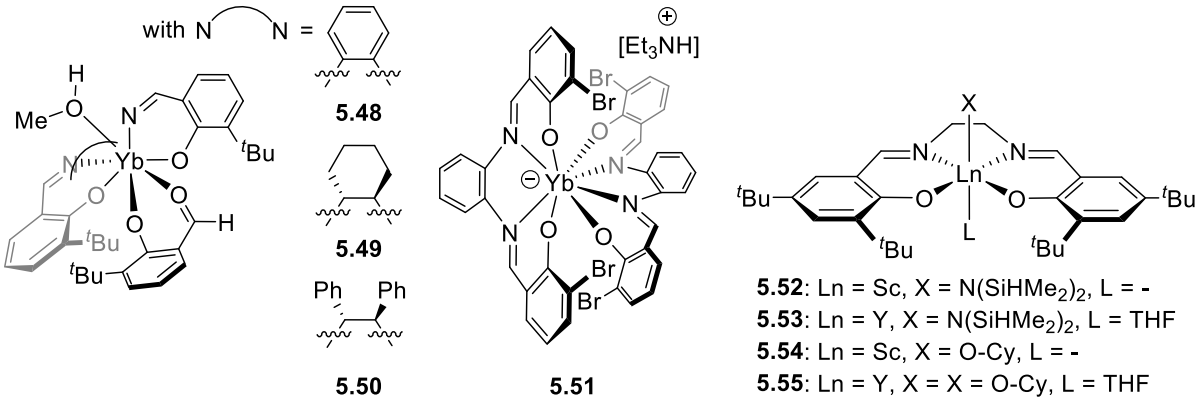

Figure 5.6. Representative salen-type rare-earth metal catalysts.

Based on the previous work on ternary Ln catalytic systems, a series of bimetallic dysprosium(III) acetate complexes bearing three different hydrazine-functionalized Schiff-base ligands (**5.56**-**5.58**) were conveniently synthesized in a one-pot reaction from $Dy(OAc)_3{\cdot}4H_2O$ as precursor and all complexes (**5.56**-**5.58**, Figure 5.7) were moderately active as catalysts for copolymerization of CHO/CO_2 without co-catalysts (TOF = 7-18 h^{-1}, carbonate linkages = 79-99%).[342] One of the most interesting features for these Dy-based catalysts is their relative stability under air, particularly for catalyst (**5.57**), which produced a perfectly alternating PCHC under these conditions with a high molecular weight (17 kg mol^{-1}) albeit with broad polydispersity ($Đ$ = 2.72). In line with the earlier examples showing a cooperation between lanthanide and zinc centers for ill-defined ternary heterogeneous systems,[332-333, 343-347] various well-defined Ln-Zn multinuclear catalysts, bearing phenylenediamine-bridged tris(phenolato) (**5.59**-**5.60**, Figure 5.7),[348] macrocyclic tris(salen) (**5.63**-**5.70**, Figure 5.7)[349-350] and ethanolamine-bridged bis(phenolato) (**5.61**-**5.62** and **5.71**, Figure 5.7)[351] ligands, were synthesized and reported to be active in the CHO/CO_2 copolymerization. While heterobimetallic Ln-Zn catalysts with acetate-bridged co-ligands (**5.59**-**5.60**) showed very close activity and lower selectivity in PCHCs compared to the homoleptic $Zn(OAc)_2$ under similar reaction conditions (70 °C, 24 h at 30 bar CO_2),[351] the other heterobimetallic Ln-Zn catalysts (**5.59**-**5.60** and **5.63**-**5.70**) exhibited high efficiency and selectivity in initiating the copolymerization of CHO with CO_2 under quite mild conditions (T = 25-100 °C, P_{CO2} = 3-10 bar). For example, the di-Nd-Zn complex (**5.59**) copolymerized CHO/CO_2 with high polycarbonate content (> 99%) as well as high-molecular weight (up to 296 kg mol^{-1}) under relatively mild conditions (T = 25 °C, P_{CO2} = 7 bar).[348] Among all the heterobimetallic Ln-Zn catalysts, the Ce-Zn_3 system (**5.64**) exhibited the highest activity with TOFs ranging from 300 to 370 h^{-1} and steadily increasing with CO_2 pressure (from 3 to 10 bar) with high selectivity in completely alternated PCHC while maintaining narrow polydispersities ($Đ$ < 1.3).[349-350]

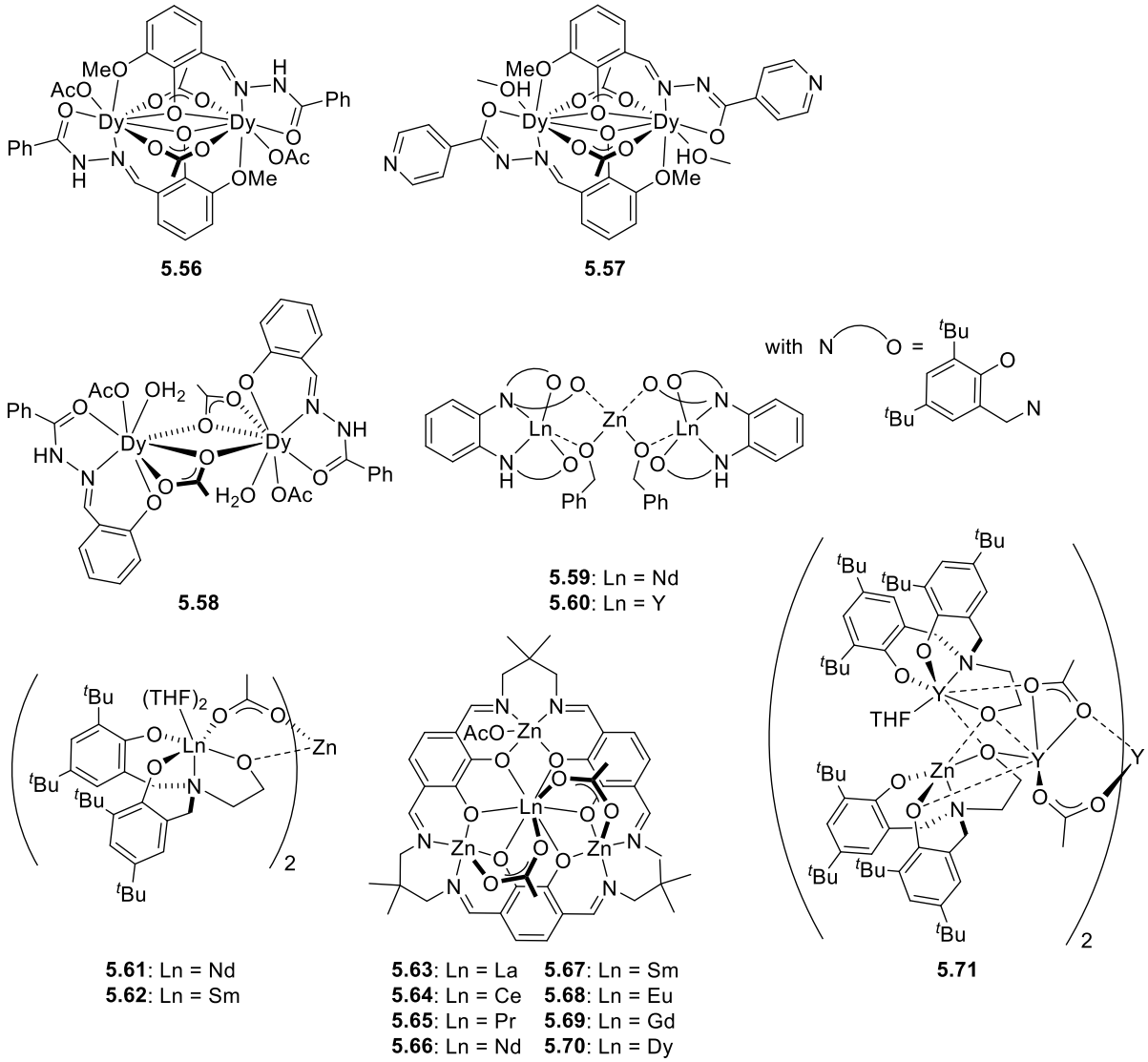

Figure 5.7. Rare-earth metal catalysts of Schiff-base and other phenolato-based ligands.

5.2.3. Group 4 Metal Catalysts

Although Group 4 metals are well-known to efficiently catalyze the ring-opening polymerization (ROP) of cyclic ethers,[352-354] their use in the copolymerization of epoxides with CO_2 has only appeared lately in comparison with other oxophilic metals.[355-356] Nozaki and co-workers were the first to report tetravalent Ti and Zr complexes supported by a tetradentate 1,9-bis(2-oxidophenyl)dipyrrinate (boxdipy) ligand (**5.72**-**5.73**, Figure 5.8) as active catalysts when combined with [PPN]X salts (X = Cl, N_3, $OCOC_6F_5$) as co-catalyst for the copolymerization of bulk PO or CHO with CO_2.[357] While (**5.72**)/[PPN]Cl binary catalytic system showed decent activity in forming PCHC (TOF = 76 h^{-1}) with a high selectivity and carbonate linkages (99%), (**5.73**)/[PPN]Cl showed a reduced catalytic activity (TOF = 8 h^{-1}) and a low selectivity in PCHC (carbonate linkage = 54%) under 20 bar of CO_2 at 60 °C. Complex (**5.72**) once activated with 1 equiv. of [PPN]Cl was found moderately active for copolymerizing PO with CO_2 (TOFs up to 33 h^{-1}) albeit with a low selectivity in PPCs (37-73% with carbonate linkages = 96-99%). However, using a substoichiometric amount of [PPN]Cl (1/2 equiv.) with complex (**5.72**) allowed a considerable increase in the selectivity in PPC to 82% even though the

amount of carbonate linkages (96%) was reduced. In contrast, (**5.73**)/[PPN]Cl is ineffective in the PO/CO_2 copolymerization and produces exclusively 100% of CPC without formation of PCC under same reaction conditions.

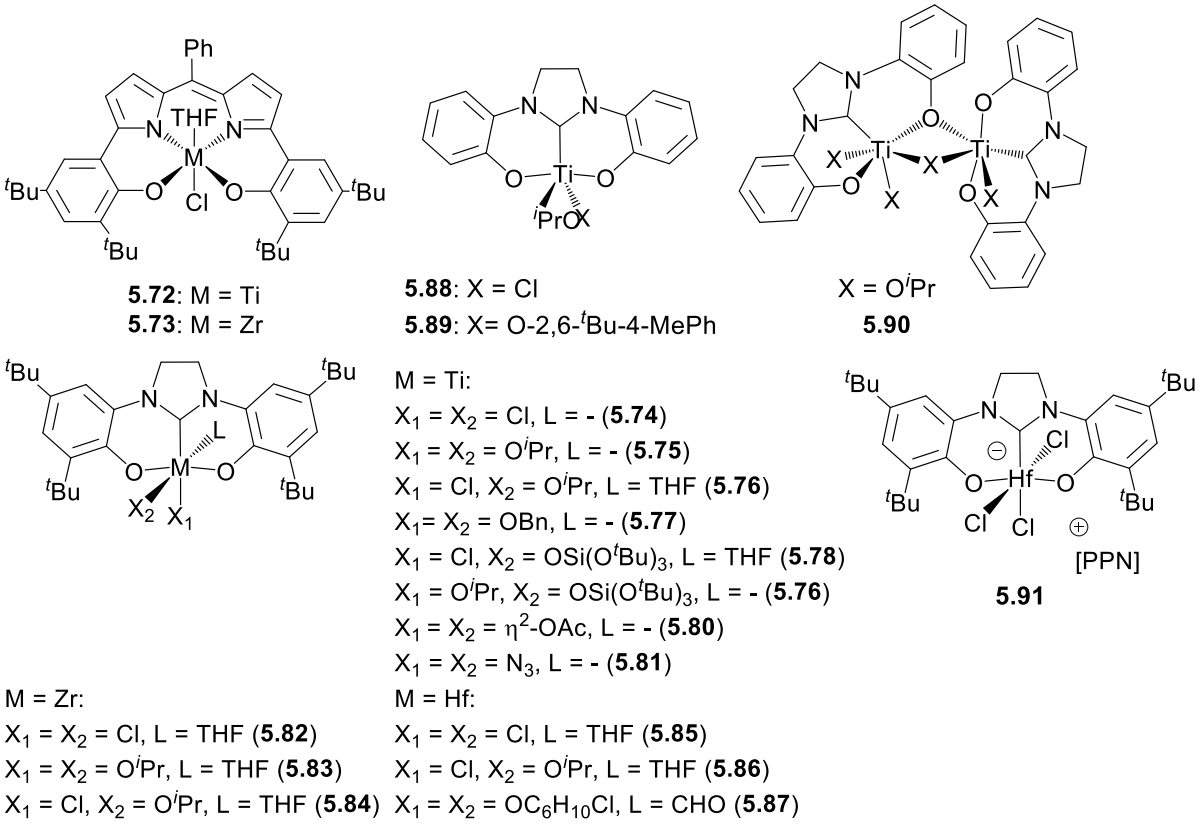

5.72: M = Ti
5.73: M = Zr

5.88: X = Cl
5.89: X= O-2,6-^{t}Bu-4-MePh

X = O^{i}Pr
5.90

M = Ti:
$X_1 = X_2$ = Cl, L = **-** (**5.74**)
$X_1 = X_2 = O^iPr$, L = **-** (**5.75**)
X_1 = Cl, $X_2 = O^iPr$, L = THF (**5.76**)
$X_1 = X_2$ = OBn, L = **-** (**5.77**)
X_1 = Cl, $X_2 = OSi(O^tBu)_3$, L = THF (**5.78**)
$X_1 = O^iPr$, $X_2 = OSi(O^tBu)_3$, L = **-** (**5.76**)
$X_1 = X_2 = \eta^2$-OAc, L = **-** (**5.80**)
$X_1 = X_2 = N_3$, L = **-** (**5.81**)

5.91

M = Zr:
$X_1 = X_2$ = Cl, L = THF (**5.82**)
$X_1 = X_2 = O^iPr$, L = THF (**5.83**)
X_1 = Cl, $X_2 = O^iPr$, L = THF (**5.84**)

M = Hf:
$X_1 = X_2$ = Cl, L = THF (**5.85**)
X_1 = Cl, $X_2 = O^iPr$, L = THF (**5.86**)
$X_1 = X_2 = OC_6H_{10}Cl$, L = CHO (**5.87**)

Figure 5.8. Group 4 metal catalysts of bis-phenolato-dipyrrinate and bis-phenolato-NHC-based ligands.

Shortly afterwards, a new class of tridentate bis(phenolate) NHC complexes of Group 4 (**5.74**-**5.90**, Figure 5.8) was also shown to catalyze efficiently the copolymerization of CO_2 in neat CHO.[358-362] All catalytic systems after activation by 1 equiv. of [PPN]X salts (with X = Cl, NO_2, N_3), exhibited high selectivity in polycarbonates (≥99% in PCHC) along with a good activity (TOFs up to 46 h^{-1} with CHO:Ti = 2500, at 60°C) under low pressure of CO_2. Although most of these titanium catalytic systems are more effective in the PCHC production when activated with [PPN]X co-catalysts, the zirconium-based catalytic systems can be activated by phosphorus-free co-catalysts such as DMAP and [^{n}BuN]Cl with the later showing nearly identical activity (TOF: 28 h^{-1}) to binary catalytic systems NHC-M/[PPN]X (M = Ti, Zr, Hf).[360] Changing the nature of co-ligands likewise affected, to some extent, the activity, and the initiation step is slightly accelerated with good nucleophiles and sterically less-hindered co-ligands, and follows this trend: N_3 > OAc ≈ O^{i}Pr > Cl > OBn ≈ OSi(O^{t}Bu)$_3$.[361] The modification of bulky substituents (tBu → H) on the NHC-phenolate rings has been reported to substantially influence the activity favoring the formation of low solubility and unstable species (**5.88**-**5.90**), and thus reducing considerably the activity.[359] Much higher activities have recently been reported for the isolated anionic NHC-hafnium species (**5.91**), which resulted from the reaction between complex (**5.85**) and 1 equiv. of [PPN]Cl, copolymerizing efficiently CHO/CO_2 (TOFs up to 500 h^{-1}, Sel_{PCHC} = >99%) and CPO/CO_2 (TOF = 14 h^{-1}, Sel_{PCPC} = 54% along with 46% of cyclopentene carbonate).[362]

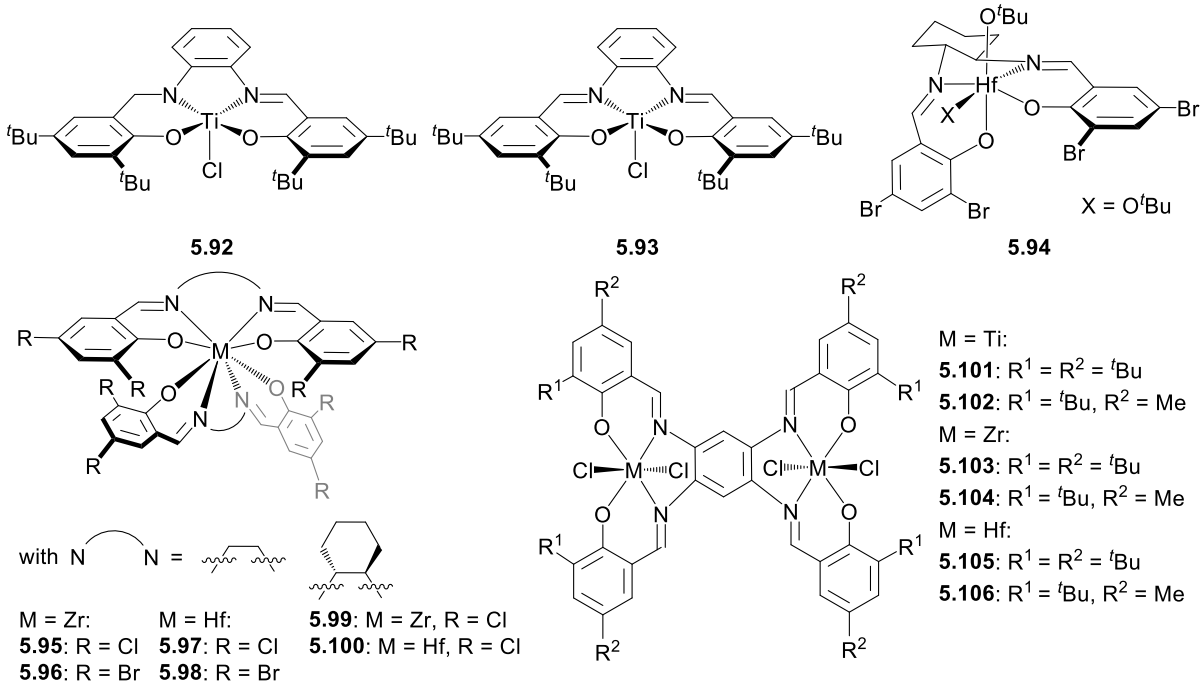

Figure 5.9. Group 4 metal catalysts of salen and salalen ligands.

Base on previous results obtained with trivalent (salen)MX (M = Co, Cr, Al, Mn),[313-317, 319] Wang *et al.* investigated the potential of salen-based titanium complexes as catalysts for the copolymerization of CHO and CO_2. In contrast to other (salen)MX catalytic systems, the *trans*-(salen)$TiCl_2$ complex upon addition of [PPN]Cl as co-catalyst, proved to be inefficient for producing PCHC and only *cis*-cyclic carbonate was obtained. In contrast, the half saturated form of salen ligand, *i.e.* tetravalent (salalen)TiCl (**5.92**, Figure 5.9) complex, when activated with [PPN]Cl allows the formation of completely alternating PCHCs (CHO:Ti = 1000:1, 60 ºC, 40 bar, TOF = 12 h^{-1}, carbonate linkages = 99%, PCHC/CHC = 98/2).[363] Following this work, the same group developed a trivalent salen titanium complex (**5.93**, Figure 5.9) which with the use of [PPN]Cl showed high activity (TOF = 577 h^{-1}) and high selectivity toward the formation of PCHCs (CHO:Ti = 1000:1, 120 °C, 40 bar, with carbonate linkages = 99%, PCHC:CHC = 99:1).[364] Other salen-type complexes, such as heteroleptic β-*cis*-(salen)Hf(O*t*Bu)$_2$ (**5.94**) and homoleptic Zr or Hf(salen)$_2$ (**5.95**-**5.100**) and dinuclear bis(salphen) (**5.101**-**5.106**) were reported by Chakrabourty *et al*. to be active for the coupling of CHO and CO_2 (Figure 5.9).[365-366] Unlike the inactive *trans*-binary catalytic systems (salen)$TiCl_2$/[PPN]Cl, all salen/salphen-based Group 4 precursors (**5.93**-**5.106**) upon activation with [^{n}Bu$_4$N]Br showed high activity (with CHO:M = 1000:1, TOFs ranging from 115 to 145 h^{-1}) at low temperature (50 °C) under high CO_2 pressure (35 bar), but relatively moderate selectivity in PCHCs (≈ 80-85%) were observed along with the persistent formation of side-products (CHC and PCHO). Following these leads, several bis-O^{i}Pr-bridged dinuclear zirconium complexes of salen and salen-based ligands (**5.107**-**5.111**, Figure 5.10) were successfully used for catalyzing the copolymerization of CHO with CO_2 in presence of [^{n}Bu$_4$N]Br (CHO:Zr = 1000:1, 6 h at 50 °C under 35 bar of CO_2).[366-367] Although not many details were provided about the active species, all activated complexes (**5.107**-**5.111**) showed rather similar catalytic performances (TOFs ranging from 118 to 158 h^{-1}) than the aforementioned catalysts (**5.94**-**5.106**). In term of selectivity, a mixture of PCHCs (56-93%), PCHOs (5-29%) and CHC (2-15%) were consistently observed with however M_w/M_n values as low as 1.3 and high molecular weights (up to

16 kg mol^{-1}).[366] Other homoleptic half-salen of titanium (**5.112**-**5.114**), dinuclear half-salen of titanium (**5.115**) and dinuclear homoleptic half-salen of zirconium (**5.116**-**5.118**) complexes were also investigated and showed slightly inferior catalytic performances and selectivities compared with the di-Zr salen complex (**5.109**) (Figure 5.10

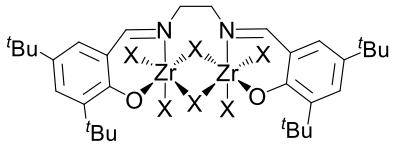

X = O^{i}Pr
5.107

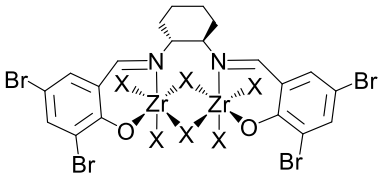

X = O^{i}Pr
5.108

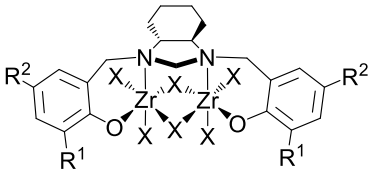

X = O^{i}Pr
5.109: $R^1 = R^2$ = Me
5.110: R^1 = ^{t}Bu, R^2 = Me
5.111: $R^1 = R^2$ = ^{t}Bu

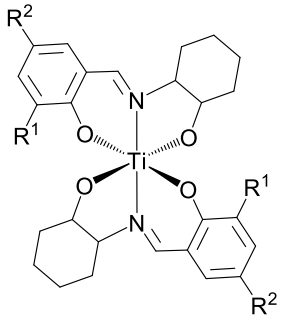

5.112: R^1 = ^{t}Bu, R^2 = Me
5.113: $R^1 = R^2$ = ^{t}Bu
5.114: $R^1 = R^2$ = Cl

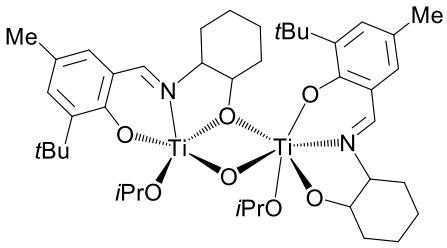

5.115

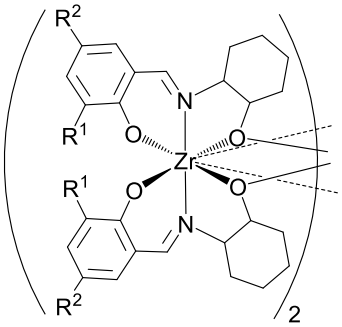

5.116: R^1 = ^{t}Bu, R^2 = Me
5.117: $R^1 = R^2$ = ^{t}Bu
5.118: $R^1 = R^2$ = Cl

Figure 5.10).[368]

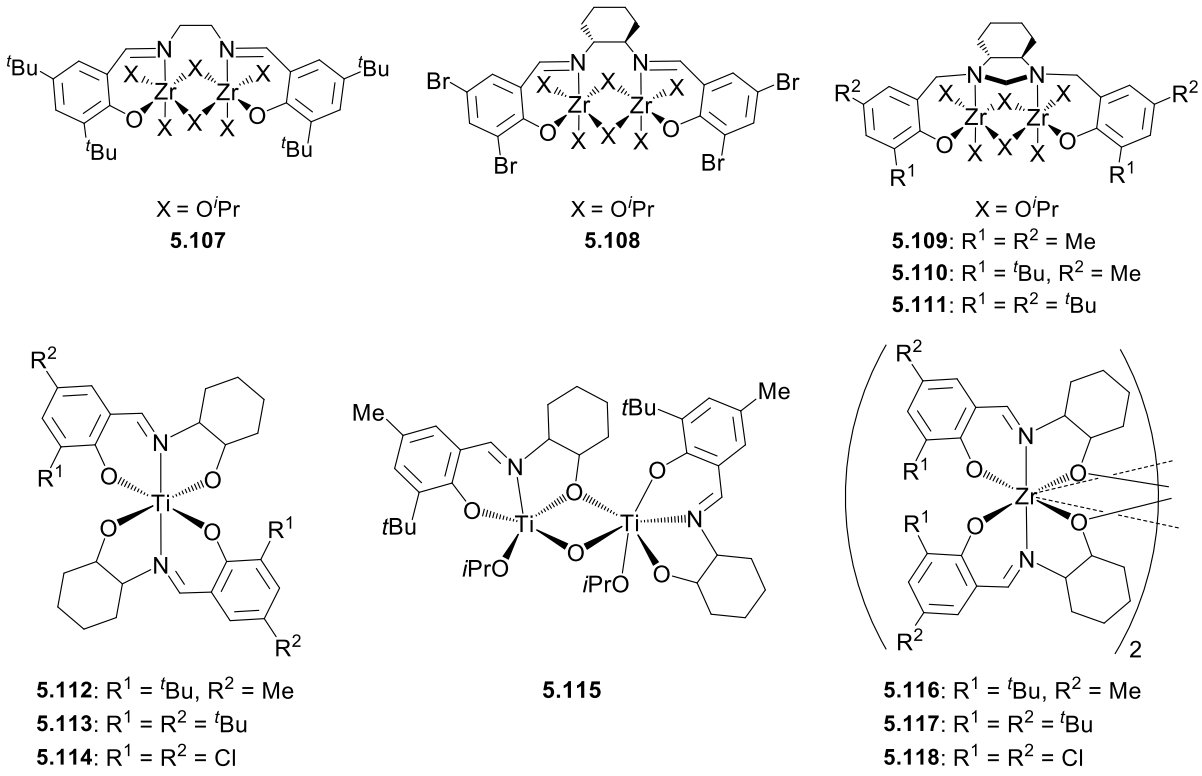

Figure 5.10. Mono- and dinuclear Group 4 metal catalysts of salen, salan and half-salen ligands.

Several benzotriazole phenolate (BTP) and amine-bis(benzotriazole phenolate) complexes of zirconium and hafnium (**5.119**-**5.123**, Figure 5.11) have also been identified to be active in the copolymerization of CHO and CO_2 without co-catalysts.[369-370] These catalysts (**5.119**-**5.123**) were shown to have a moderate activity and selectivity for affording completely alternating PCHCs along with CHC and PCHO under identical conditions (T = 100 °C, P_{CO2} = 20 bar), with the best results being obtained with the Zr homoleptic complex **5.121** (CHO:Zr = 500:1, TOF = 7.6 h^{-1}, Sel_{PCHC} = 93%).[369]

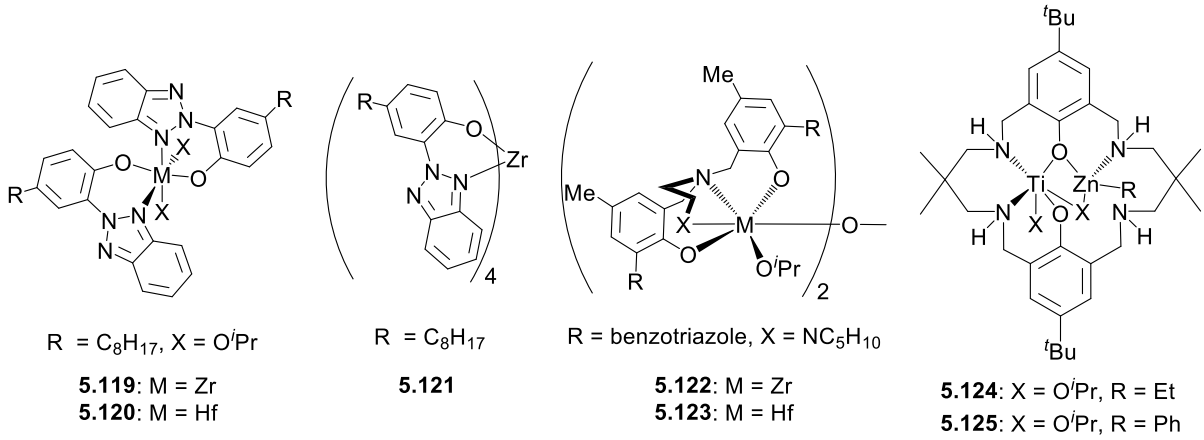

Figure 5.11. Group 4 metal catalysts of other phenolato-based ligands.

Based on the early establishment of high achievements with heterobimetallic Mg-Zn complexes of bis(phenolate)tetraamine macrocyclic ligands as catalysts, two heterobimetallic Ti-Zn complexes (**5.124**-**5.125**, Figure 5.11) were prepared and tested in CHO/CO_2 copolymerization (80 °C, P_{CO2} = 1

bar).[371] Both catalysts are considerably less active that the heterobimetallic Mg-Zn catalysts (TOFs ≈ 2 h^{-1}) affording modest selectivity in PCHCs (94-98%) together with PCHO and CHC as side products.

5.2.4. Group 6 Metal Catalysts

Over the last 20 years, due to their high activity, stereoselectivity and stability, chromium catalysts (together with cobalt and zinc, *vide infra*) have been predominantly used for the copolymerization of CO_2 with a wide range of epoxides, and have been largely well-covered by several reviews from 2004 to 2018.[313-317, 319, 372] In this section, therefore, only a brief overview of Cr-based catalysts is presented.

Although the first chromium catalysts, showing good activity and selectivity toward polycarbonates (for **5.127**: TOFs up to 173 h^{-1}, Sel_{PCHC} < 97%), were based on porphyrin-type ligands (**5.126**-**5.127**, Figure 5.12),[373-377] the most remarkable advances were made by using salen-type ligands and their derivatives, upon addition of various type of neutral and anionic co-catalysts, as embodied in these selected examples: salcy (**5.128**-**5.132**),[378-384] salophen (**5.133**-**5.136**),[380, 382-383, 385] salen (**5.137**-**5.143**),[381-383, 386] salalen (**5.144**),[387] salan (**5.145**-**5.149**),[386, 388-389] and thioether-modified salan\salalen-like (**5.150**-**5.157**)[390-391] ligands (Figure 5.12). Among the diversity of salen-type chromium catalysts, binary catalytic systems such as (**5.132**)/[PPN]N_3 and (**5.134**)/[PPN]Cl were found to be highly active and selective in PCHC (TOF= 1153 h^{-1}, sel_{PCHC} > 99% with CHO:Cr:[PPN]N_3 = 2330:1:1, at 80 °C, 34.5 bar) and PPC (TOF= 192 h^{-1}, sel_{PCC} = 93%, carbonate linkages = 99% with PO:Cr:[PPN]Cl = 2000:1:1, at 60 °C, 34 bar), respectively, leading to polycarbonates with narrow M_w/M_n values (≈1.1) and high molecular weights (up to 50 and 26 kg mol^{-1}, respectively).[381-382] An increase in regioselectivity up to 93% head-to-tail connectivity was seen in the coupling of *rac*-PO with CO_2 by complexes (**5.130**, **5.135**, **5.139** and **5.142** *vs*. 64% for **5.128**) when activated by bulky nucleophiles such as 1,5,7-triazabicyclo-[4,4,0]-dec-5-enes.[383] It was also found that the activities for the binary salan-Cr\DMAP system were up to 30 times higher compared to salen-Cr, and correlated to the reduced electrophilicity of the chromium center bearing salan ligands, and thus favoring a fast reversible exchange between epoxide\DMAP essential for improving the activity.[386]

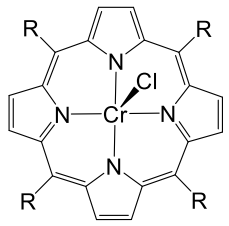

5.126: R = 4-Me-C_6H_4
5.127: R = C_6F_5

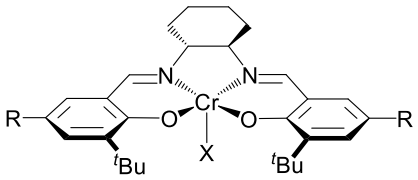

R = ^{t}Bu: X = Cl (**5.128**); N_3 (**5.129**); NO_3 (**5.130**)
R = H; X = N_3 (**5.131**); R = OMe; X = N_3 (**5.132**)

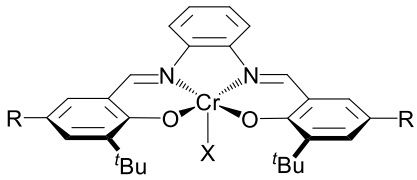

R = ^{t}Bu:
X = Cl (**5.133**); N_3 (**5.134**); NO_3, (**5.135**)
R = H: X = N_3 (**5.136**)

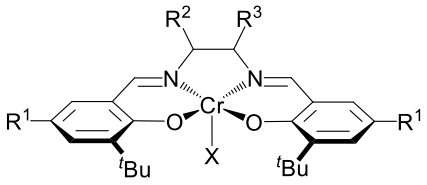

5.143: R_1 = H: R_2 = R_3 = H, X = N_3

R^1 = ^{t}Bu:	R^2	R^3	X
5.137	H	H	Cl
5.138	H	H	N_3
5.139	H	H	NO_3
5.140	Me	H	Cl
5.141	Me	H	NO_3
5.142	Ph	Ph	NO_3

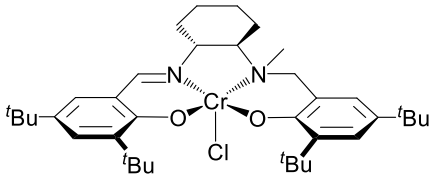

5.144
(see ref. 387 - 10 examples)

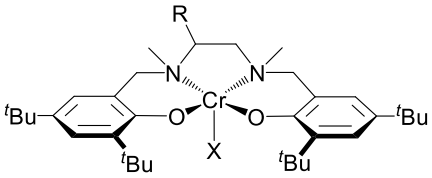

5.145: R = Me, X = NO_3
5.146: R = H, X = NO_3
5.147: R = Me, X = Cl
5.148: R = H, X = Cl
5.149: R = H, X = N_3

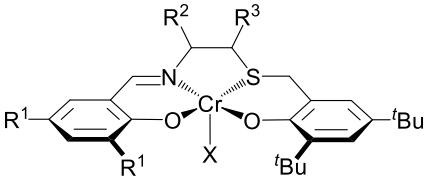

	R^1	R^2	X
5.154	-$(CH_2)_4$-		Cl
5.155	-$(CH_2)_4$-		N_3
5.156	H	H	Cl
5.157	-$(CH)_4$-		Cl

	R^1	R^2	R^3	X
5.150	^{t}Bu	H	H	Cl
5.151	Cl	H	H	Cl
5.152	^{t}Bu	-$(CH)_4$-		Cl
5.153	^{t}Bu	-$(CH)_4$-		N_3

Figure 5.12. Chromium catalysts of porphyrin-type, salcy, salophen, salen, salalen, salan and thioether-modified salan\salalen-like ligands.

In order to increase the activity of the salen-type catalysts, which are all rate dependent of an associative mechanism involving either binary or dinuclear catalytic species, novel strategies were developed for overcoming diffusion limitation at high conversion and low catalyst loading and enhancing selectivity in polycarbonates.[313-317, 319, 372] As a result, strategies evolved towards the design of single-component catalysts, such as compounds tethering a quaternary ammonium salts as co-catalyst to the salcy ligand framework (**5.158**-**5.159**),[392-394] or dinuclear salcy\salophen-Cr species (**5.160**-**5.163**)[395-397] (Figure 5.13). In the absence of a co-catalyst, systems **5.158** and **5.159** were used to catalyze the coupling of CO_2 and CPO, 1,4-CHDO, isobutene oxide, 2,3-epoxy-2-methylbutane, *cis*- and *trans*-2-butene oxide.[392-394] With these single-component catalysts, only monomers such as CPO, 1,4-CHDO and *cis*-2-butene oxide were found selective in the coupling to CO_2 to produce polycarbonates. In contrast, the binary catalytic system **5.128**\[PPN]N_3 only afforded cyclic carbonates for instance. As anticipated, the dinuclear (salcy)CrCl (**5.160**) catalyst, in presence of 2 equiv. of [PPN]Cl, was found to be efficient with TOFs up to 390 h^{-1} at extremely low loadings (CHO:**5.160** = 50000:1) for the copolymerization of CO_2 with CHO without sacrificing polymer selectivity (sel_{PCHC} >99%).[397] High activity and selectivity (TOF = 82 h^{-1}, sel_{PCC} >98%) were similarly obtained with the dinuclear (salophen)CrCl species (**5.163**) at low catalyst loadings for the

copolymerization of PO with CO_2 (PO:**5.163** = 20000:1) without co-catalyst, demonstrating their superior catalytic performances when compared to the mononuclear (salophen)CrCl species (**5.164**, Figure 5.13) under the same conditions (TOF = 7 h^{-1}, sel_{PCC} = 80%, PO:**5.164** = 20000:1).[395] Additionally, the dinuclear species (**5.160**-**5.162**) in the presence of [PPN]X (X = F, Cl, NO_3) were reported to polymerize a degradable polycarbonate made from CO_2 and 1-benzyloxycarbonyl-3,4-epoxy pyrrolidine ($sel_{polym.}$ up to 99%) at low temperatures (≤80 °C), which could be depolymerized in quantitative yield into the starting epoxide monomer at high temperature (≥100 °C).[396]

In attempts to improve the Cr-based catalyst\polycarbonate separation, a liquid-liquid phase separation with a soluble polyisobutylene-bound (salen)CrCl catalyst (**5.165**, Figure 5.13) and a liquid-solid phase separation by immobilizing complex (**5.128**) on a modified poly(aniline-co-*o*-aminophenol) were synthesized and evaluated.[398-399] Both catalysts showed very similar activity and were very selective in the formation of PCHC compared to the corresponding unsupported complexes (**5.137**) and (**5.128**), and only (**5.165**) was reported to be recyclable with a loss of only ca. 4% of the starting Cr accompanied by a drop in 20-30% in polymerization rate.[398]

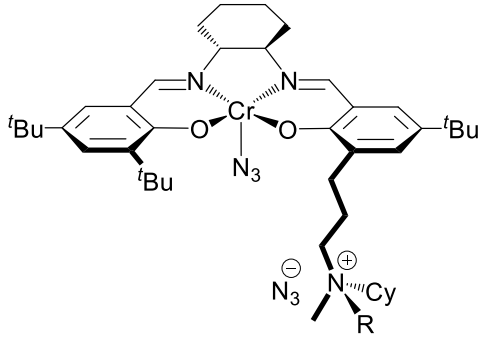

5.158: R = Cy
5.159: R = Me

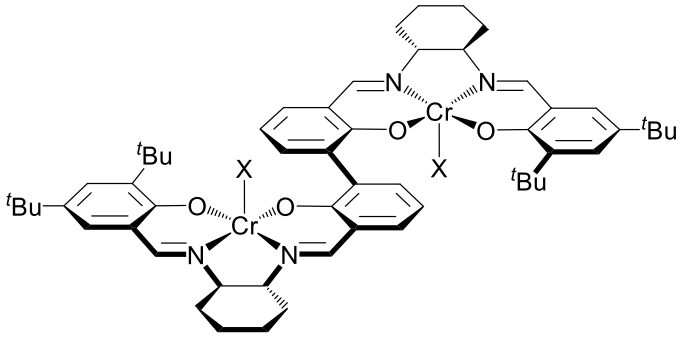

5.160: X = Cl
5.161: X = N_3
5.162: X = NO_3

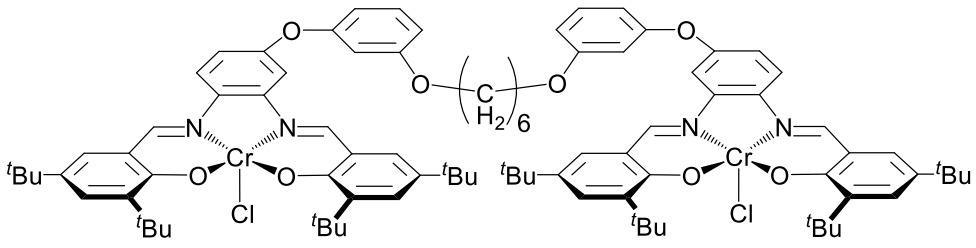

5.163

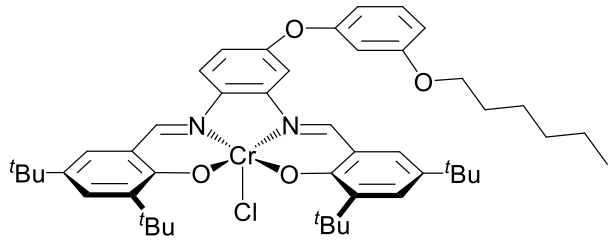

5.164

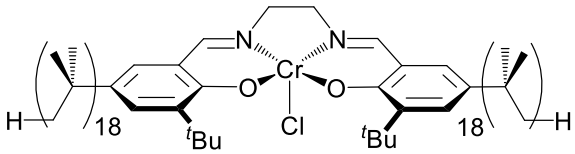

5.165

Figure 5.13. Mono- and di-nuclear chromium catalysts of modified salen-type ligands.

Following these leads, a range of tetradentate N_4-type ligands such as tetraazaannulene (taa) (**5.166**-**5.170**),[400-402] tetraza Schiff base (**5.171**-**5.174**),[403] and N_4-pyridine-carboxamide (**5.175**-**5.177**)[404] have also been employed to prepare discrete chromium(III) chloride complexes (Figure

5.14). Only (taa)CrCl complexes (**5.166**-**5.170**), especially the ones bearing more electron-donor substituents were shown to be highly active and selective toward the copolymerization of CHO and CO_2 affording PCHC in the presence 2 equiv. of $[PPN]N_3$ as a co-catalyst (TOF= 1482 h^{-1}, CHO:**168**:$[PPN]N_3$ = 1700:1:2, at 80 °C, 0.5 h, 35 bar).[401] Another advantage of these (taa)CrCl (**5.166**-**5.170**) catalyts over the less-active (salen)CrX systems is that they have a much lower selectivity towards the formation of CHC byproduct during the copolymerization.

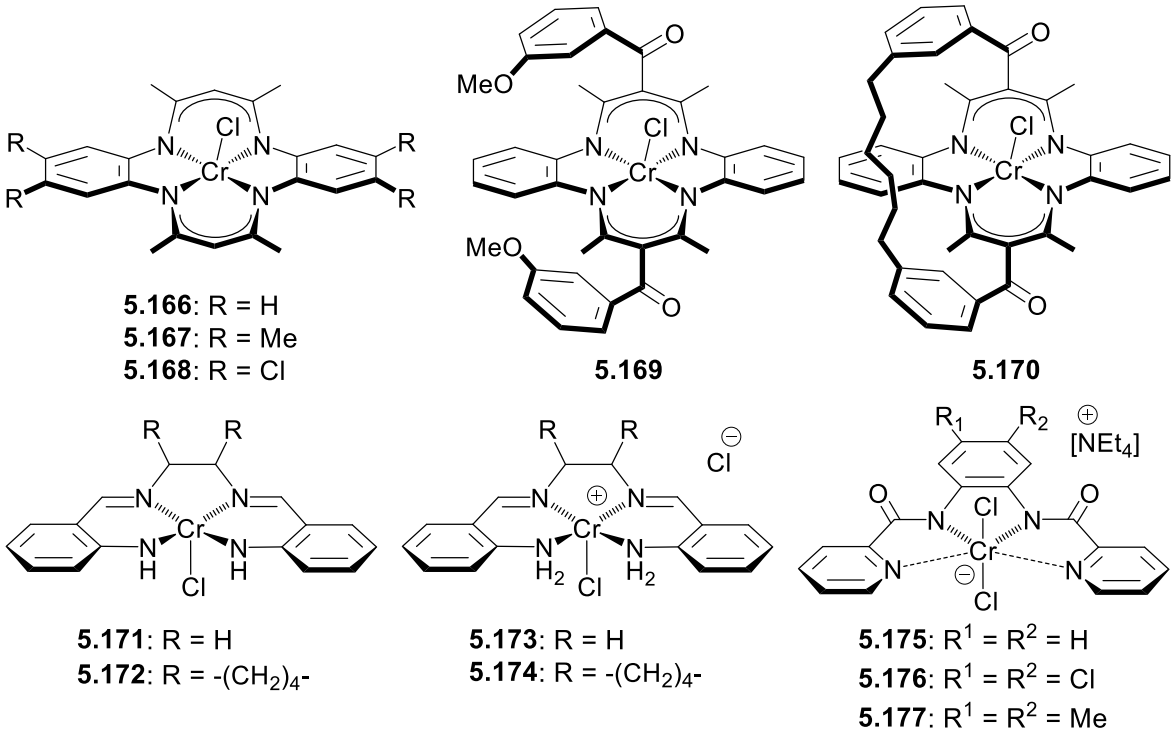

Figure 5.14. Chromium catalysts of tetradentate N_4-type ligands.

Several other chromium catalysts bearing bis-ligated bi- and tri-dentate NN'O Schiff base ligands (**5.178**-**5.181**),[405] bidentate pyridine-aminophosphine, amino-pyridine, amino-\imino-pyrrole ligands (**5.182**-**5.188**),[406] tridentate pyridine-amino-pyrrole ligand (**5.189**),[406] and bis(hydroxyquinoline)butylamine ligands possessing an ONNO chelating pattern (**5.190**-**5.193**)[407-408] have also been reported for this CHO\CO_2 copolymerization reaction, but activities and selectivities are significantly lower than for (salen)CrX catalysts (Figure 5.15). Only the series of complexes (**5.191**-**5.193**) were more active (with TOFs up to 2165 h^{-1} within the first 30 min. after observing an induction period of at least 30 min) with an excess of $[PPN]N_3$ as a co-catalyst for allowing high selectivity in PCHC (TOF = 886 h^{-1}, CHO:**193**:$[PPN]N_3$ = 4168:3.6, at 100 °C, 4 h, 25 bar).[408]

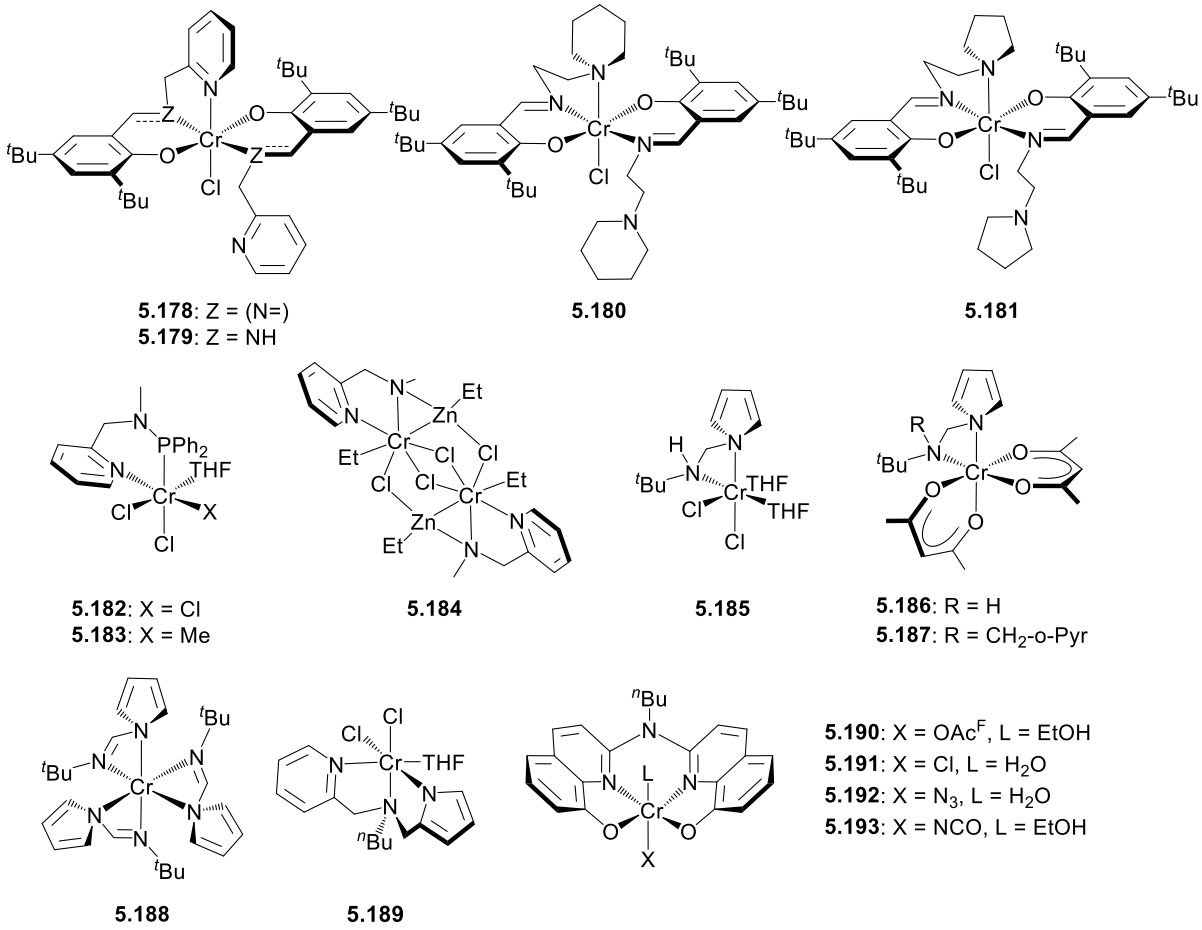

Figure 5.15. Chromium catalysts of bi- and tri-dentate NN'O Schiff base, pyridine-aminophosphine, amino-pyridine, amino-\imino-pyrrole, pyridine-amino-pyrrole and bis(hydroxyquinoline) derivatives.

Initially successfully used to the development of iron catalysts (*vide infra*),[409] the tri- and tetradentate amino-bis(phenolate) ligand scaffolds, with different pendant donor groups such as pyridyl (**5.194**-**5.198**),[410-413] dimethylethyleneamino (**5.199**-**5.200**),[412, 414] methoxyethyl (**5.201**),[415] benzyl (**5.202**-**5.203**)[416] and tetrahydofuranyl (**5.204**),[416] were applied to the synthesis of chromium(III) chloride complexes, which have been reported to initiate the copolymerization of CO_2 with CHO or PO in the presence of DMAP and [PPN]X co-catalysts (Figure 5.16). Examples of high activities for the copolymerization of CHO\CO_2 reaching TOFs of 220 h^{-1} under high pressure were reported by adding one equiv. of DMAP to either **5.194** and **5.199** and high selectivity in PCHC without detectable amounts of CHC with low polydispersities values.[410, 414] Complex **5.164** was also reported to copolymerize PO and CO_2 efficiently in presence of 0.5 equiv. of [PPN]X (X = Cl, N_3) with TOFs up to 48 h^{-1} with good-to-excellent selectivity in PPCs (from 51 to 96%) depending on the reaction conditions (T = 23-25 ºC, P_{CO2} = 37-42 bar).[411]

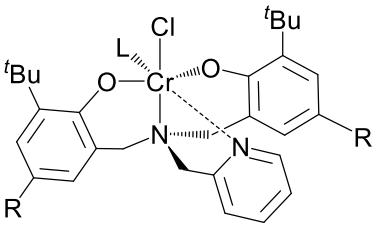

5.194: R = ^{t}Bu, L = THF
5.195: R = ^{t}Bu, L = DMAP
5.196: R = Me, L = THF
5.197: R = OMe, L = THF
5.198: R = OMe, L = DMAP

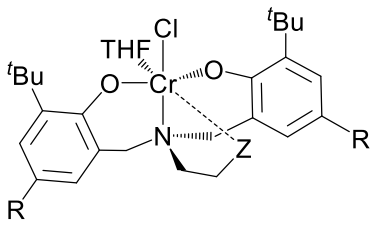

5.199: R = ^{t}Bu, Z = NMe_2
5.200: R = OMe, Z = NMe_2
5.201: R = ^{t}Bu, Z = OMe

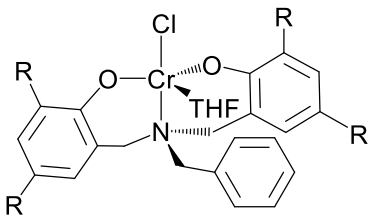

5.202: R = ^{t}Bu
5.203: R = ^{t}Am

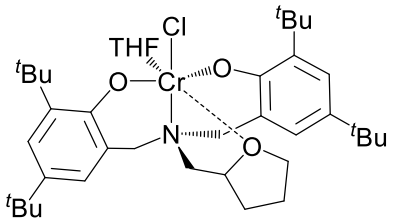

5.204

Figure 5.16. Chromium catalysts of amino bis(phenolate)-type ligands.

5.2.5. Group 7 Metal Catalysts

In 2003, a manganese complex supported by a tetraphenylporphyrin ligand was reported as active catalyst for the copolymerization of CHO with CO_2. Complex (Tpp)MnOAc (**5.205**, Figure 5.17) catalyzed at 80 °C under 51 bar, the copolymerization of CHO/CO_2 to afford selectively PCHC with a TOF up to 16 h^{-1} and high carbonate linkages (98-99 %) but with low molecular weights (M_n = 5800-6700 g mol^{-1}, $Đ$ = 1.3-1.4). Additives such as PPh_3, DMPA and *N*-methylimidazole decelerated the polymerization rates and decreased the content of carbonate linkages. Complex **5.205** was the first example of a catalyst copolymerizing at low pressures (1 bar) and showing high content of carbonate linkages (95% with M_n = 3000 g mol^{-1}, $Đ$ = 1.6), albeit with low activity (TOF = 3 h^{-1}) at 80 °C.[417]

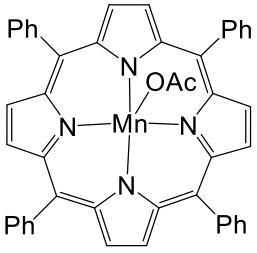

5.205

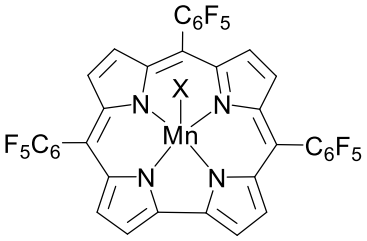

5.206: X = -
5.207: X = Cl

Figure 5.17. Manganese catalysts.

Apart from complex **5.205**, the only other Mn-based catalysts are tri- and tetravalent Mn complexes supported by a trianionic tetradentate corrole-type ligand (**5.206**-**5.207**, Figure 5.17). In combination with a co-catalyst, such as [PPN]X (with X = Cl N_3, OAc and $OC(O)C_6F_5$), $[R_4N]Cl$ (with R = Et, Bu) and $[R_4P]Cl$ (with R = Bu, Ph), complexes **5.206**-**5.207** were found to be active in copolymerization of CHO and PO with CO_2.[418] At 60 °C, complex **5.206** coupled with [PPN]OAc reacted the most efficiently with CHO and 20 bar CO_2 to selectively produce either PCHC (carbonates linkages: 99% with M_n = 20000 g mol^{-1}, $Đ$ = 1.2) or PPC (carbonates linkages: 29% with M_n = 49900 g mol^{-1}, $Đ$ = 1.3) with moderate TOFs of 23 h^{-1} and 69 h^{-1}, respectively, with traces of cyclic

carbonates. When complex **5.206** was activated by other bulky non-coordinating cations ([PPN]X, $[R_4N]Cl$ and $[R_4P]Cl$), a notable decrease in the activity was observed for both epoxide monomers, along with an increase of CPC as side-product of the PO/CO_2 copolymerization, but this was accompanied by an enhanced carbonates linkages content (60-99%).[418]

5.2.6. Group 8 Metal Catalysts

The earlier reports on iron-based catalysts for the epoxides/CO_2 copolymerization involved mostly heterobimetallic systems such as double metal cyanide $Zn_a(Fe(CN)_x)_b$ (DMC) and polyethylene oxide-supported DCMs exhibiting low activity in either CHO/CO_2 or PO/CO_2 copolymerization with moderate carbonates linkages (50-95%).[419-420] Although undoubtedly iron-based catalysts are very attractive in terms of abundance, the use of iron as homogeneous catalysts was primarily disregarded due to the poor understanding of its role as active species in the heterobimetallic systems (including homogeneous models mimicking DCM).[421-422] The first report on homogeneous iron catalysts was reported by the William's group, and composed of a bimetallic trivalent di-Fe compound (**5.208**, Figure 5.18) bearing a bis(phenolate)tetraamine macrocyclic ligand similar to complexes (**5.3**-**5.5**).[423] Di-Fe complex **5.208** alone is able of copolymerizing neat CHO with CO_2 under mild conditions (TOF_{max} = 54 h^{-1} per Fe center at T = 80 °C with P_{CO2} range = 1-10 bar). The polymer obtained at 1 bar CO_2 showed a degree of carbonate linkage close to 66%, while the PCHCs obtained under 10 bar are completely alternated (carbonate linkage > 99%). Attempts to copolymerize CO_2 with PO or SO as monomers with **5.208** afforded only the corresponding cycloaddition products. In contrast, tetra- and tri-valent iron-corrole complexes **5.209**-**5.211** and **5.212** (Figure 5.18), respectively, in presence of co-catalysts were reported by Nozaki and co-workers as active catalysts not only for the copolymerization of CHO with CO_2, but also as effective catalysts for the copolymerization of CO_2 with PO and the far less investigated glycidyl phenyl ether (GPE) monomer.[424] While all [PPN]Cl-activated complexes (**5.209**-**5.212**) gave the copolymer selectively (carbonate linkages: 84-96%) without concomitant formation CHC (TOF_{max} = 109 h^{-1} per Fe center for **5.212**, at T = 80 °C under P_{CO2} = 20 bar), both carbonate linkages reported for the CO_2-based copolymers formed from PO or GPE monomers contained a high degree of ether linkages (71-91%) with only traces of cycloaddition products for PO and none for GPE, independently of the co-catalysts used ([PPN]X-type or DMAP).

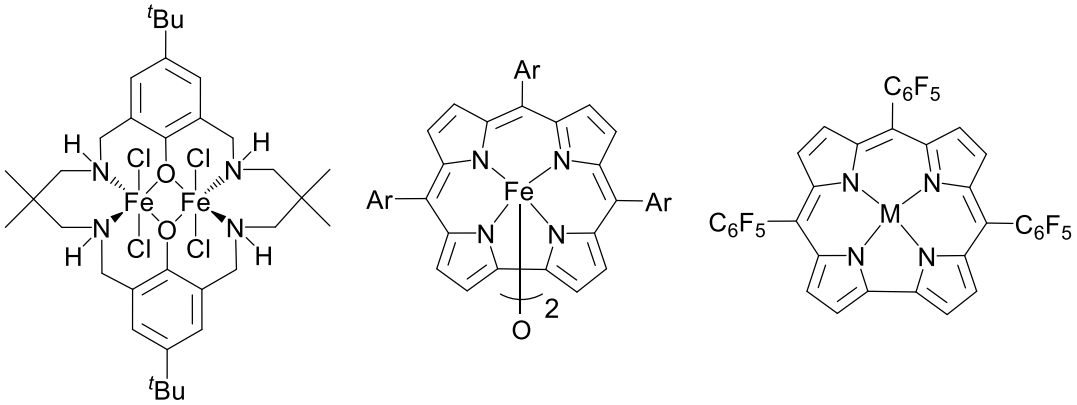

5.208

5.209: Ar = C_6F_5
5.210: Ar = C_6H_5

5.211: M = FeCl
5.212: M = $Fe(OEt_2)_2$

Figure 5.18. Iron catalyst of a bis(phenolate)tetraamine macrocyclic ligand and tetra- and trivalent iron-corrole complexes.

One of the most recent advances on iron-based catalysts can be attributed to Kleij and coworkers, and revolve around tetradentate amino-tris(phenolate) (**5.213**-**5.216**) and pyridylamino-bis(phenolate) (**5.217**-**5.218**) complexes of trivalent iron (Figure 5.19).[409, 425-427] With trivalent iron catalysts (**5.213**-**5.216**) and depending of the amount of [^{n}Bu$_4$N] and [PPN] halide salts used as co-catalysts, a switch in selectivity was observed for forming selectively either PCHC (82-99% with an equimolar amount of onium salt) or CHC (48-96% with 10 equiv. of onium salts) under $ScCO_2$ conditions. Copolymerization of v-CHO with CO_2 was also performed with catalysts (**5.217**-**5.218**) and displayed higher selectivity for polycarbonate formation than for CHO (95% with carbonate linkages >99%).

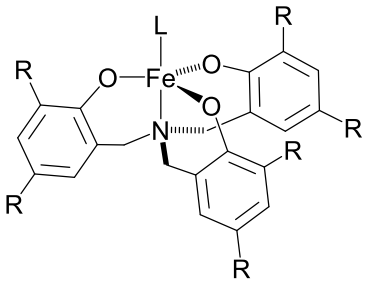

5.213: R = Me
5.214: R = ^{t}Bu
5.215: R = Cl

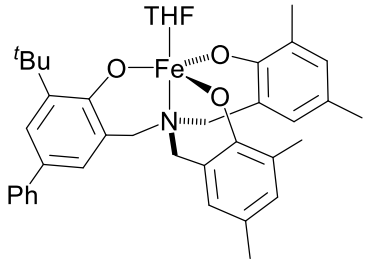

5.216

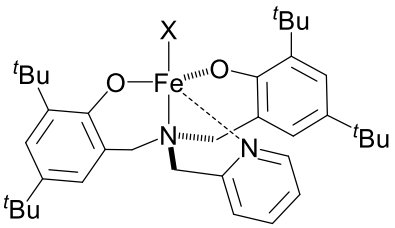

5.217: X = Cl
5.218: X = Br

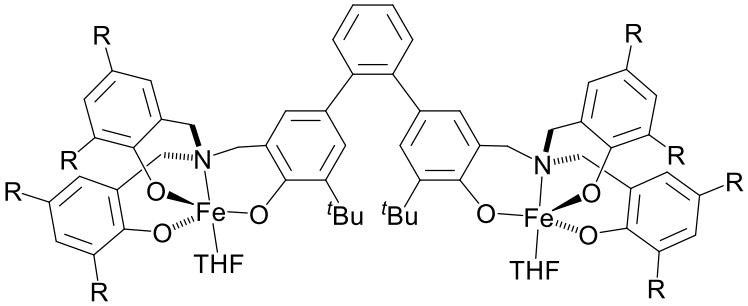

5.219: R = ^{t}Bu
5.220: R = Me

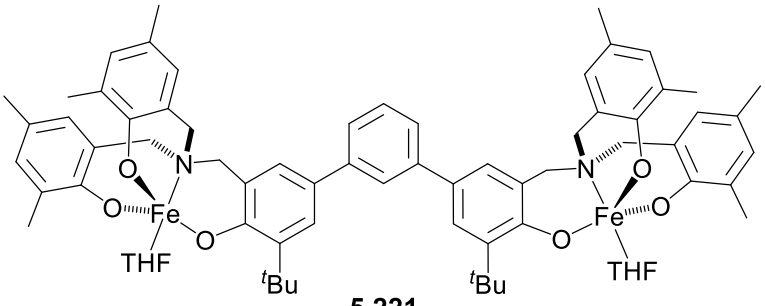

5.221

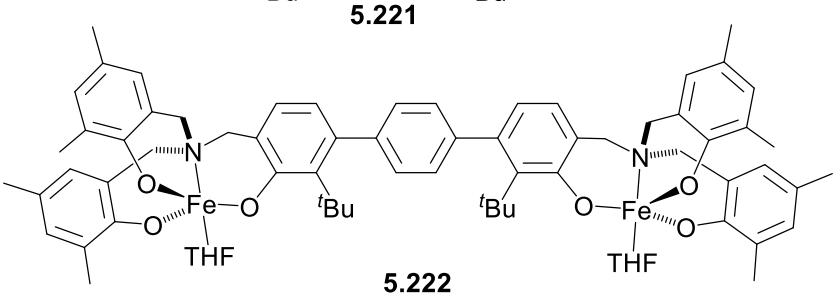

5.222

Figure 5.19. Iron catalysts of amino-phenolate-type ligands.

A subsequent report from Jiang *et al*. presented the use of phenylene-bridged iron(III) bimetallic analogs (**5.219-5.222**, Figure 5.19) of the iron amino-tris(phenolate) complexes for the alternating copolymerization of CHO and CO_2 in presence of 1 equiv. of [PPN]Cl at 90 °C under 45 bar.[427] The bimetallic complex **5.220** exhibited the highest activity, which is relatively similar to the complexes **5.221**-**5.222** and **5.216**, while the less sterically hindered complex **5.219** showed the lowest activity. Under optimized conditions (CHO:**5.220** = 1000:1, 120 °C at 45 bar), complex **5.220** was shown to be the most efficient (TOF = 536 h^{-1}) preserving high selectivity in PCHC (>99%) and carbonate linkages (99%).

In 2012, Zevaco and co-workers reported a series of anionic iron complexes (**5.223**-**5.227**, Figure 5.20) of *N,N*-bis(2-pyridinecarboximide)-1,2-benzene chelating ligands (bpb), having [Et_4N] as counter cation, that were employed as an alternative to binary catalytic systems.[404, 428] These catalysts were studied for CHO/CO_2 copolymerization at 80 °C under 50 bar of CO_2, and at best TOFs inferior to ≈5 h^{-1} and high selectivity for PCHC over CHC (67-99% with carbonate linkage: 86-99%) were reported, showing the small influence of electron donating or withdrawing substituents on bpb ligands (Me ≈ H > Cl ≈ NO_2)[404] or co-ligands (Cl > OAc)[428] employed.

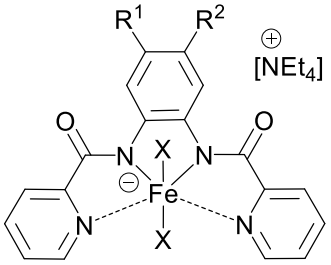

5.223: X = Cl, R^1 = R^2 = H
5.224: X = Cl, R^1 = R^2 = Cl
5.225: X = Cl, R^1 = H, R^2 = NO_2
5.226: X = Cl, R^1 = R^2 = Me
5.227: X = OAc, R^1 = R^2 = H

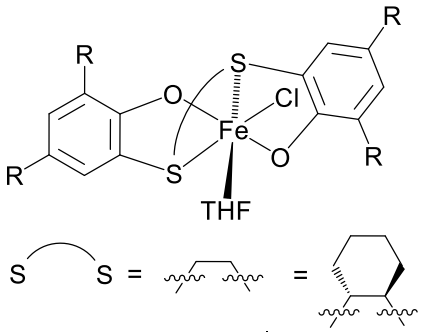

5.228: R = CPh_3
5.229: R = CMe_2Ph
5.230: R = Me

5.231: R = ^{t}Bu

Figure 5.20. Iron catalysts of bis(2-pyridinecarboximide)- and bis-thioether bis(phenolate)-type ligands.

Very recently, bis-thioether bis(phenolate) complexes of iron (**5.228**-**5.231**, Figure 5.20), in combination with [^{n}Bu_4N]Cl or [PPN]Cl, have been shown to display moderate-to-high activity for the alternating copolymerization of CHO with CO_2 producing completely alternated PCHC (T = 80 °C, P_{CO2} = 10 bar).[429] In particular, the presence of a sterically hindered substituent on the ligand backbone, as in complex **5.229**, has led to a higher catalytic activity (TOF = 340 h^{-1}) than the related less crowed complex **5.230** (TOF = 42 h^{-1}).

5.2.7. Group 9 Metal Catalysts

The most studied and successful Group 9 metal catalysts combine a cobalt(III) metal center and tetradentate salen-type ligands or tetraazamacrocycle–porphyrin derivatives. Although mononuclear complexes were the most widely studied species for the copolymerization of CO_2 and various epoxides, dinuclear Co complexes were also shown to be efficient (pre)catalysts. For example, a dinuclear cobalt catalyst of a macrocyclic ancillary ligand preformed well for the production of

CO_2/CHO copolymer under mild conditions and dinuclear salen-cobalt species realized the stereospecific CO_2/EP copolymerization to yield stereocomplexed polycarbonates or crystalline-gradient terpolymers. Dinuclear cobalt-based catalysts supposedly operate through a distinct mechanism to that of single-site complexes.[430]

As stated in the introduction, cobalt catalysts represent one of the major class of catalysts for the copolymerization of CO_2 and epoxides. Several comprehensive reviews are available and critically discuss ligands/catalysts developments, structure/activity relationship and therefore, interested readers are encouraged to consult these reference papers for more informations that can not be detailed here.[313, 315-317, 319]

5.2.8. Group 10 Metal Catalysts

Inspired by the high catalytic performances for the copolymerization of epoxides with CO_2 of salen-type cobalt and chromium complexes, nickel catalysts of salen ligands and derivatives were also examined due to their higher tolerance towards air and availability. In this regard, Ko and co-workers designed and synthesized a series of air-stable binuclear Ni^{II} complexes of benzotriazole-modified salen and salan ligands, bridged through phenoxy and acetate co-ligands (**5.232**-**5.244**, Figure 5.21).[431-434] These catalysts were all found highly active and efficient, without additional co-catalysts, for the copolymerization of CHO and CO_2, leading to a high selectivity in PCHC containing 99% of carbonate linkages. The highest catalytic performances were achieved by the di-nickel-salen catalyst containing electron-withdrawing carboxylate (**5.234**)[434] and the sterically less encumbered a di-nickel-salan catalyst (**5.244**),[433] reaching TOFs of 432 and 328 h^{-1}, respectively, under optimal conditions (CHO:di-Ni = 3200, T = 130-140 °C, P_{CO2} ≈ 20 bar). The di-nickel catalyst **5.234** also exhibited a relatively good selectivity when CPO was used as monomer toward the formation of completely alternated PCPC (71% together with 29% of cyclopentene carbonate), although the activities were very low (TOF < 7 h^{-1}) at high temperature (T = 100 °C) under 20 bar of CO_2 and producing only cyclic carbonate and homopolymer above 100 °C.[434]

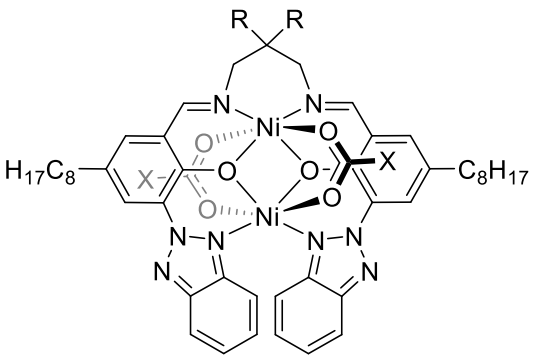

R = H:
5.232: X = Me
5.234: X = CF_3
5.236: X = Ph
5.238: X = 4-CF_3-C_6H_4
5.240: X = 4-OMe-C_6H_4

R = Me:
5.233: X = Me
5.235: X = CF_3
5.237: X = Ph
5.239: X = 4-CF_3-C_6H_4

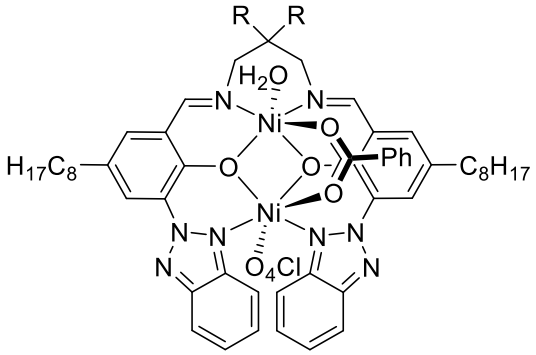

5.241: R = H
5.242: R = Me

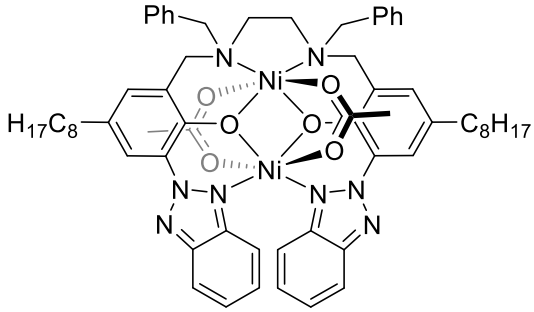

5.243

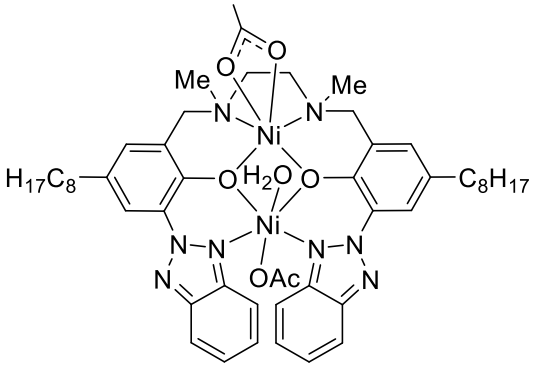

5.244

Figure 5.21. Nickel catalysts of salen and salan ligands.

Variously substituted mono-, di- and tri-nuclear Ni acetate complexes, supported by monoanionic NNO-tridentate Schiff-base ligands (**5.245**-**5.253**, Figure 5.22), were also developed by Ko and co-workers for application in CHO/CO_2 copolymerization catalysis.[435] While mononuclear Ni complexes (**5.245**-**5.246**) produced only traces of polycarbonates, the di- and tri-nuclear Ni species (**5.247**-**5.253**) were much more active catalysts (TOFs up to 114 h^{-1}) and afforded more PCHCs (up to 88%) but still along with CHC as side product under harsh conditions (T = 90-150 °C, P_{CO2} = 20 bar).

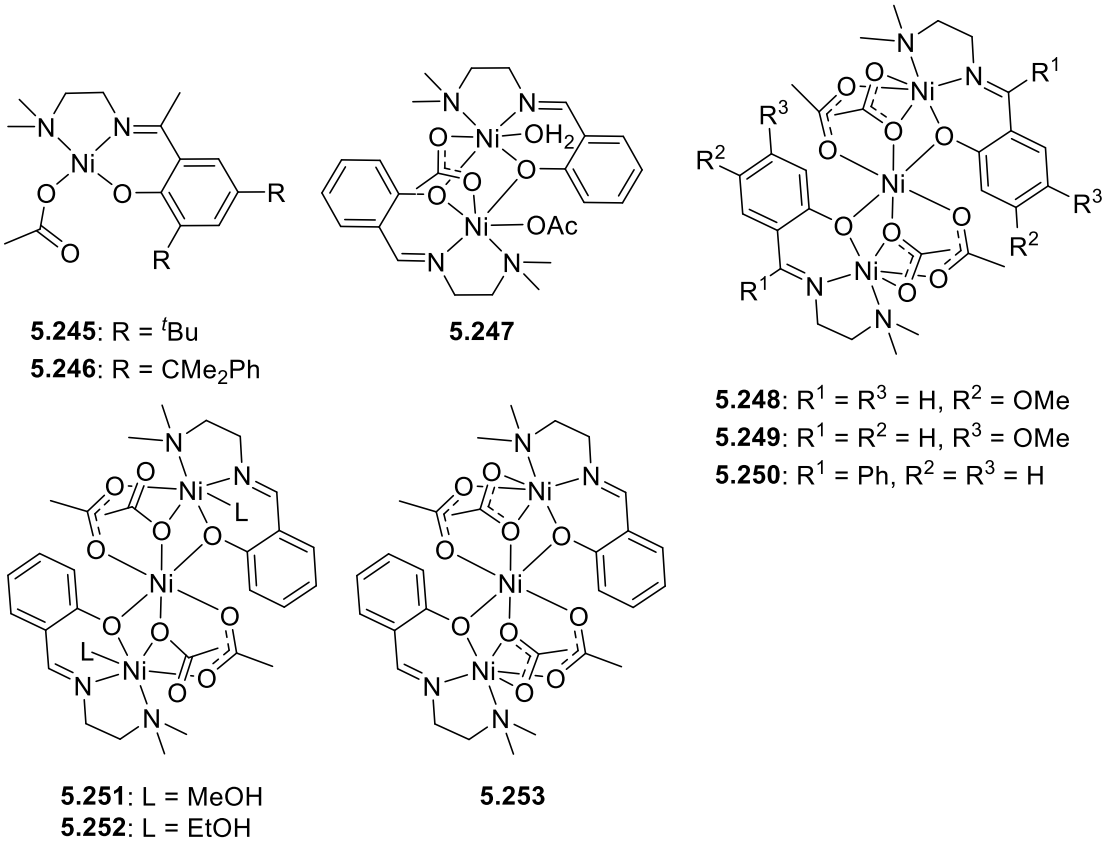

5.245: R = ^{t}Bu
5.246: R = CMe_2Ph

5.247

5.248: $R^1 = R^3 = H$, $R^2 = OMe$
5.249: $R^1 = R^2 = H$, $R^3 = OMe$
5.250: $R^1 = Ph$, $R^2 = R^3 = H$

5.251: L = MeOH
5.252: L = EtOH

5.253

Figure 5.22. Nickel catalysts of tridentate Schiff-base ligands.

5.2.9. Group 11 Metal Catalysts

As for nickel (see section 5.2.8), monoanionic NNO-tridentate Schiff-base ligands were also used to synthesize several mono-, bi- and tri-nuclear copper acetate complexes (**5.254-5.258**, Figure 5.23),[436] which exhibited moderate activity for CHO/CO_2 copolymerization at 120°C under 20 bar of CO_2, affording PCHCs (up to 97% carbonate linkages) with a low-to-moderate selectivity in CHC (16-69%). Di-Cu complex **5.256** performed with the highest activity (TOFs < 19 h^{-1}).

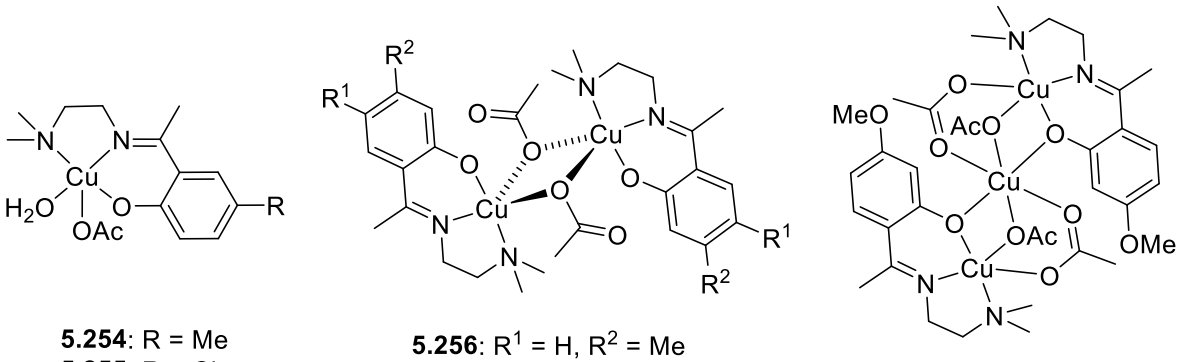

5.254: R = Me
5.255: R = Cl

5.256: R^1 = H, R^2 = Me
5.257: R_1 = Me, R_2 = H

5.258

Figure 5.23. Copper catalysts.

5.2.10. Group 12 Metal Catalysts

Contrary to zinc catalysts, which count among the best performing systems and were therefore intensively studied, no cadmium-based catalyst has been found active for the copolymerization of epoxides and CO_2.

Zinc alkoxide and amide complexes of β-diketiminate type ligands count within the most notable catalysts that were reported for the copolymerization of CO_2 and epoxides. Dinuclear zinc complexes of a bis(phenolate)tetraamine macrocyclic ligand also exhibited remarkable activity in CHO/CO_2 copolymerization at low CO_2 pressure, and for the original production of sequence-controlled copolymers, from a four-component monomer feedstock, composed of caprolactone, CHO, phthalic anhydride (PA), and CO_2.[430, 437]

The developments of zinc-based catalysts, structure/activity relationships, recent achievements in term of produced materials and polymerized monomers etc. were comprehensively reviewed and discussed, and will therefore not be detailed in the present chapter.[313, 316-317, 319]

5.2.11. Group 13 Metal Catalysts

Aluminum catalysts were extensively studied over the last twenty years, and their evolution and catalytic performances were comprehensively reviewed.[313-314, 319-320] Along with salen-aluminum catalysts, which belong to the most performant systems,[315] several other supporting ligand scaffolds, such as porphyrin, β-ketoiminate, amino-phenolate derivatives also realized important achievements in the field.[430]

Despite numerous studies involving salen-aluminum catalysts, only a few isolated (salen)GaX (X = Cl, N_3) complexes have been examined for the copolymerization of CHO with CO_2 and only traces of PCHC were observed.[438] In contrast to the salen-gallium complexes, indium complexes bearing either salen (**5.259**) and phosphasalen (**5.260**-**5.266**) ligands showed some activity (TOFs < 3 h^{-1}) in copolymerization of CHO with CO_2 without any pressure dependence from 1-40 bar of CO_2 (Figure 5.24).[439]

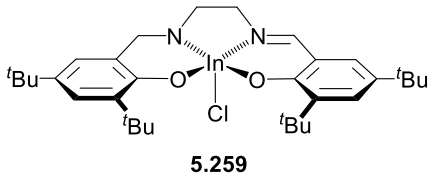

5.259

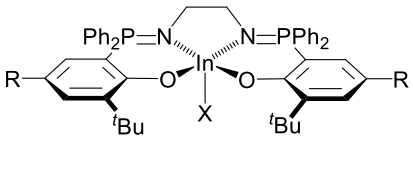

5.260: X = Cl, R = ^{t}Bu
5.261: X = Br, R = ^{t}Bu
5.262: X = OAc, R = ^{t}Bu
5.263: X = NO_3, R = ^{t}Bu
5.264: X = O^{t}Bu, R = ^{t}Bu
5.265: X = O^{t}Bu, R = C_5H_{11}
5.266: X = O^{t}Bu, R = CMe_2Ph

Figure 5.24. Indium catalysts.

Copolymerizations were run at 60 °C for 48 h in neat CHO under 1 bar of CO_2 and in the absence of co-catalyst, complex **5.259** converted 21% CHO monomer to PCHO. In contrast, complex **5.260** yielded polycarbonate containing 66% carbonate linkages, with high selectivity in PCHC (94%). Based on those leads, other (phosphasalen)InX (**5.261**-**5.263**) were investigated and the most active of these catalysts (**5.263**) reached a TOF of 2.5 h^{-1} and yielded a highly alternating PCHC with high selectivity in polymer (83%), high isoselectivity (P_m = 76%), with relatively short molecular weight (M_n = 1.4 kg mol^{-1}) and narrow dispersity ($Đ$ = 1.23).[439] Interestingly, the more sterically hindering *ortho*-substituents in complexes **5.264**-**5.266** led to an enhanced activity (TOFs up to 15 h^{-1}), improving greatly the polymer selectivity (90-95%) with high content of carbonate linkage (>99%) and high isoselectivity (P_m = 78-86%).

5.2.12. Group 14 Metal Catalysts

Tetravalent germanium and tin complexes (**5.267-5.268**, Figure 5.25) bearing the boxdipy ligand, which are structurally similar to tetravalent titanium and zirconium complexes (**5.72-5.73**, Figure 5.8), have been reported as active catalysts for CHO and PO with CO_2 copolymerization in presence of [PPN]X salts.[357] Copolymerizations of CHO/CO_2 were run at 60 °C for 12 h in neat CHO under 20 bar of CO_2 and the germanium complex **5.267** (+ 1 equiv. of [PPN]Cl) converted efficiently CHO/CO_2 to PCHC with a TOF of 60 h^{-1} (99% carbonate linkages with M_n = 14 kg mol^{-1}) and a narrow dispersity ($Đ$ = 1.12), while the tin complex **5.268** (+ 1 equiv. of [PPN]Cl) displayed a low activity (TOF = 17 h^{-1}) and gave PCHC with low carbonate linkages (75%). Similar trends for the copolymerization of PO and CO_2 were observed with both complexes, except that both exhibited a much higher level of CPC (7-68%) as side product along with the concomitant formation of poly(propylene oxide) (carbonate linkage: 87-97%).[357]

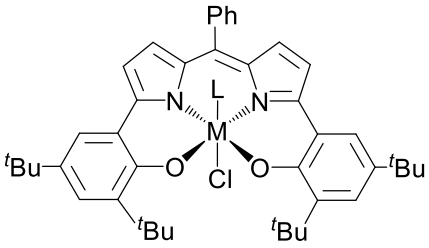

5.267: M = Ge, L = -
5.268: M = Sn, L = THF

Figure 5.25. Germanium and tin catalysts.

6. Summary and Outlook

Coordination compounds are undoubtedly compounds of importance in the field of polymerization. As summarized in this chapter, they are present and effective in the areas of coordination polymerization, radical polymerization and ring-opening (co)polymerization, in which they already have achieved many breakthroughs. However, some general and more specific (for each technique) opportunities for further developments can also be identified.

Over the last two decades, interest in the metal-catalyzed coordination polymerization of polar and non-polar vinyl monomers remained very high, especially due to the unique ability of this technique to produce the corresponding polymeric materials with a high level of stereocontrol. The development of new catalysts, with the objectives of improving catalytic activities and (stereo)selectivities, is still an important area of research, and it clearly appears that these properties are directly related to catalyst structure (metal centers, oxidation states, ligands, etc.). Unfortunately, no single or universal catalyst can meet all demanding needs. Identified remaining challenges in this area would be, for example, effective and (stereo)controlled random copolymerization of polar and non-polar vinyl monomers with the production of high molecular weight materials or the incorporation of biorenewable vinyl monomers for the production of more sustainable polymers.

Copper-catalyzed atom transfer radical polymerization is a mature technique that allows the production of well-defined polymeric materials of various architectures with very efficient catalysts that can be used at ppm levels and work even in water or in aerobic conditions. However, the supremacy of copper catalysts was recently challenged by iron catalysts, which are very attractive

(cost, abundance, toxicity) and, for some of them, also very efficient. ATRP works very well for the so-called more activated monomers, but the controlled polymerization of less activated remains challenging. This challenge (for radical polymerization techniques) was overcome, in some instances, by the more recently developed organometallic-mediated radical polymerization techniques, which use all the tools of coordination chemistry (metal coordination sphere, ligand design, redox properties of metal centers etc.) to ensure a controlled polymerization. The black spot of both metal mediated radical techniques is that they face undesired metal catalyzed radical termination reactions. Further efforts have to be dedicated to kinetic and mechanistic studies, which should allow the design of more efficient and selective catalysts.

Over the last two decades, significant improvements have been accomplished in the ring-opening polymerization of bio-based cyclic esters (e.g. lactide) and the alternating copolymerization of epoxides with CO_2, enabling a promising approach towards sustainable polyesters and polycarbonates, respectively, to be built. For the CO_2/epoxide copolymerization, such major improvements in term of activity, selectivity, controlling the polycarbonates properties (molecular weight, polydispersity, regio- and stereo-chemistry) and mechanistic studies have been mostly achieved by two leading type of mono- and bi-metallic homogeneous catalysts, i.e. the bulky zinc β-diketiminate and the cobalt/chromium salen-type catalysts. In the last decade, recent efforts have been particularly centered on boosting the activity and the selectivity by the development of single component and bimetallic catalysts, avoiding the use of cocatalysts as additives, and directed towards the development of more sustainable catalysts using inexpensive, less toxic and abundant metal centers such as iron and aluminum. To a lesser extent, other metal centers from Group 2 to 14, including lanthanides, have shown some interesting activity selectively forming the expected polycarbonates. Such diversification in catalyst development has brought a new impetus to the field, not only in the variety of ligands and metals used, but also in the use of epoxides from renewable resources, the introduction of functional groups (unsaturated bond) for further functionalization of the polymeric chains, and the development of controlled block and random terpolymerization. In addition, among the new emergent catalysts some of them have shown interesting prospects in the ability to operate under very mild conditions (below 1 bar of CO_2 for instance) and to tolerate impurities (including water, oxygen, amines and thiols) in the CO_2 gas feed.

Various metal catalysts, ranging from Group 1 to 13, now readily achieve a controlled polymerization of lactide, however the control of the microstructure of the produced material remains difficult to predict.

Despite these recent advances, the future challenges are many as it stands today. To enable the polycarbonates to broaden their current applications, further developments will be necessary for tuning and matching the thermal and mechanical properties for competing with petroleum-based polymers. This is also true for most of the polyesters made by ROP. It can be attained by using more efficient catalysts, i.e. allowing a better control of the molecular weights, the microstructures, by sequential monomers addition, and functionalization of chain ends, for instance. Future improvements of catalytic systems will indubitably be gained by developing more robust and impurity tolerant catalysts able to work under realistic and economically viable industrial conditions. Another area of research for enhancing the polycarbonates applicability is to develop efficient catalysts able to copolymerize a wider range of epoxides than now, particularly from biorenewable epoxides for making more sustainable polycarbonates that are currently difficult to obtain. Finally,

another important aspect for engineering more sustainable polymers, albeit in a nascent field, is to comprehend their biodegradability conditions in various environments.

7. Acknowledgement

C.F and S.D are grateful to the Centre National de la Recherche Scientifique (CNRS) for recurrent funding. E.L.R. acknowledges financial support from FRINATEK-NFR (240333) and the University of Bergen.

8. References

1. Kaminsky, W.; Funck, A.; Haehnsen, H. *Dalton Trans.* **2009,** (41), 8803-8810.
2. Domski, G. J.; Rose, J. M.; Coates, G. W.; Bolig, A. D.; Brookhart, M. *Prog. Polym. Sci.* **2007,** *32* (1), 30-92.
3. Tritto, I.; Boggioni, L.; Ferro, D. R. *Coord. Chem. Rev.* **2006,** *250* (1-2), 212-241.
4. Gromada, J.; Carpentier, J.-F.; Mortreux, A. *Coord. Chem. Rev.* **2004,** *248* (3-4), 397-410.
5. Wang, B. *Coord. Chem. Rev.* **2006,** *250* (1-2), 242-258.
6. Prashar, S.; Antiñolo, A.; Otero, A. *Coord. Chem. Rev.* **2006,** *250* (1-2), 133-154.
7. Kirillov, E.; Carpentier, J.-F. *Chem. Rec.* **2020**, DOI:10.1002/tcr.202000142.
8. Laur, E.; Louyriac, E.; Dorcet, V.; Welle, A.; Vantomme, A.; Miserque, O.; Brusson, J.-M.; Maron, L.; Carpentier, J.-F.; Kirillov, E. *Macromolecules* **2017,** *50* (17), 6539–6551.
9. Louyriac, E.; Laur, E.; Welle, A.; Vantomme, A.; Miserque, O.; Brusson, J.-M.; Maron, L.; Carpentier, J.-F.; Kirillov, E. *Macromolecules* **2017,** *50* (24), 9577–9588.
10. Gibson, V. C.; Spitzmesser, S. K. *Chem. Rev.* **2003,** *103* (1), 283-316.
11. Britovsek, G. J. P.; Gibson, V. C.; Wass, D. F. *Angew. Chem. Int. Ed.* **1999,** *38* (4), 428-447.
12. McKnight, A. L.; Waymouth, R. M. *Chem. Rev.* **1998,** *98* (7), 2587–2598.
13. Lin, F.; Wang, X.; Pan, Y.; Wang, M.; Liu, B.; Luo, Y.; Cui, D. *ACS Catal.* **2016,** *6* (1), 176-185.
14. Wang, T.; Liu, D.; Cui, D. *Macromolecules* **2019,** *52* (24), 9555-9560.
15. Jiang, Y.; Kang, X.; Zhang, Z.; Li, S.; Cui, D. *ACS Catal.* **2020,** *10* (9), 5223-5229.
16. Collins, R. A.; Russell, A. F.; Mountford, P. *Appl. Petrochem. Res.* **2015,** *5*, 153-171.
17. Chen, E. Y. X. *Chem. Rev.* **2009,** *109* (11), 5157-5214.
18. Coates, G. W.; Hustad, P. D.; Reinartz, S. *Angew. Chem. Int. Ed.* **2002,** *41* (13), 2236-2257.
19. Takeuchi, D. *Dalton Trans.* **2010,** *39*, 311-328.
20. Lv, K.; Cui, D. *Organometallics* **2010,** *29* (13), 2987-2993.
21. Yao, C.; Liu, D.; Li, P.; Wu, C.; Li, S.; Liu, B.; Cui, D. *Organometallics* **2014,** *33* (3), 684-691.
22. Tolpygin, A. O.; Glukhova, T. A.; Cherkasov, A. V.; Fukin, G. K.; Aleksanyan, D. V.; Cui, D.; Trifonov, A. A. *Dalton Trans.* **2015,** *44* (37), 16465-16474.
23. Rad'kov, V. Y.; Skvortsov, G. G.; Lyubov, D. M.; Cherkasov, A. V.; Fukin, G. K.; Shavyrin, A. S.; Cui, D.; Trifonov, A. A. *Eur. J. Inorg. Chem.* **2012,** *2012* (13), 2289-2297.
24. Paolucci, G.; Bortoluzzi, M.; Napoli, M.; Longo, P.; Bertolasi, V. *J. Mol. Catal. A: Chem.* **2010,** *317* (1-2), 54-60.
25. Mountford, P.; Clot, E.; Tredget, C. S. *Organometallics* **2008,** *27* (14), 3458-3473.
26. Howe, R. G.; Tredget, C. S.; Lawrence, S. C.; Subongkoj, S.; Cowley, A. R.; Mountford, P. *Chem. Commun.* **2006,** (2), 223-225.
27. Ward, B. D.; Bellemin-Laponnaz, S.; Gade, L. H. *Angew. Chem. Int. Ed.* **2005,** *44* (11), 1668-1671.
28. Lukešová, L.; Ward, B. D.; Bellemin-Laponnaz, S.; Wadepohl, H.; Gade, L. H. *Dalton Trans.* **2007,** (9), 920-922.
29. Liu, H.; He, J.; Liu, Z.; Lin, Z.; Du, G.; Zhang, S.; Li, X. *Macromolecules* **2013,** *46* (9), 3257-3265.
30. Wang, L.; Liu, D.; Cui, D. *Organometallics* **2012,** *31* (17), 6014-6021.

31. Zhang, P.; Liao, H.; Wang, H.; Li, X.; Yang, F.; Zhang, S. *Organometallics* **2017,** *36* (13), 2446-2451.
32. Ge, S.; Meetsma, A.; Hessen, B. *Organometallics* **2007,** *26* (22), 5278-5284.
33. Ge, S.; Bambirra, S.; Meetsma, A.; Hessen, B. *Chem. Commun.* **2006,** (31), 3320-3322.
34. Lawrence, S. C.; Ward, B. D.; Dubberley, S. R.; Kozak, C. M.; Mountford, P. *Chem. Commun.* **2003,** (23), 2880-2881.
35. Yang, Y.; Lv, K.; Wang, L.; Wang, Y.; Cui, D. *Chem. Commun.* **2010,** *46* (33), 6150-6152.
36. Li, S.; Cui, D.; Li, D.; Hou, Z. *Organometallics* **2009,** *28* (16), 4814-4822.
37. Gao, W.; Cui, D. *J. Am. Chem. Soc.* **2008,** *130* (14), 4984-4991.
38. Zhang, L.; Suzuki, T.; Luo, Y.; Nishiura, M.; Hou, Z. *Angew. Chem. Int. Ed.* **2007,** *46* (11), 1909-1913.
39. Wang, L.; Cui, D.; Hou, Z.; Li, W.; Li, Y. *Organometallics* **2011,** *30* (4), 760-767.
40. Wang, Y.; Duan, J.-B.; Liu, Z.-X.; Xu, T.-Q. *Polym. Chem.* **2020,** *11* (20), 3434-3438
41. Yan, C.; Xu, T.-Q.; Lu, X.-B. *Macromolecules* **2018,** *51* (6), 2240-2246.
42. Mou, Z.; Zhuang, Q.; Xie, H.; Luo, Y.; Cui, D. *Dalton Trans.* **2018,** *47* (42), 14985-14991
43. Xu, T.-Q.; Yang, G.-W.; Lu, X.-B. *ACS Catal.* **2016,** *6* (8), 4907-4913.
44. Kronast, A.; Reiter, D.; Altenbuchner, P. T.; Vagin, S. I.; Rieger, B. *Macromolecules* **2016,** *49* (17), 6260-6267.
45. Chen, J.; Gao, Y.; Marks, T. J. *Angew. Chem. Int. Ed.* **2020,** *59* (35), 14726-14735.
46. Peng, D.; Yan, X.; Yu, C.; Zhang, S.; Li, X. *Polym. Chem.* **2016,** *7* (15), 2601-2634.
47. Yuan, S.-F.; Yan, Y.; Solan, G. A.; Ma, Y.; Sun, W.-H. *Coord. Chem. Rev.* **2020,** *411*, 213254.
48. Makio, H.; Terao, H.; Iwashita, A.; Fujita, T. *Chem. Rev.* **2011,** *111* (3), 2363-2449.
49. Makio, H.; Fujita, T. *Acc. Chem. Res.* **2009,** *42* (10), 1532-1544.
50. Matsugi, T.; Fujita, T. *Chem. Soc. Rev.* **2008,** *37* (6), 1264-1277
51. Budagumpi, S.; Keri, R. S.; Biffis, A.; Patil, S. A. *Appl. Catal., A* **2017,** *535*, 32-60.
52. Gao, Y.; Christianson, M. D.; Wang, Y.; Chen, J.; Marshall, S.; Klosin, J.; Lohr, T. L.; Marks, T. J. *J. Am. Chem. Soc.* **2019,** *141*, 7822−7830.
53. Zhao, X.; Chen, Z.; Li, H.; Ma, Y. *Macromolecules* **2020,** *53*, 3806−3813.
54. Gao, Y.; Mouat, A. R.; Motta, A.; Macchioni, A.; Zuccaccia, C.; Delferro, M.; Marks, T. J. *ACS Catal.* **2015,** *5* (9), 5272–5282.
55. Yuan, S.; Wang, L.; Zhang, Q.; Sun, W. *Prog. Chem.* **2017,** *29* (12), 1462-1470.
56. Chen, Z.; Li, J.-F.; Tao, W.-J.; Sun, X.-L.; Yang, X.-H.; Tang, Y. *Macromolecules* **2013,** *46* (7), 2870–2875.
57. Liu, C.-C.; Liu, Q.; Yiu, S.-M.; Chan, M. C. W. *Organometallics* **2019,** *38* (15), 2963–2971.
58. Nakata, N.; Toda, T.; Ishii, A. *Polym. Chem.* **2011,** *2* (8), 1597-1610.
59. Janas, Z. *Coord. Chem. Rev.* **2010,** *254* (17-18), 2227-2233.
60. Faisca Phillips, A. M.; Suo, H.; Guedes da Silva, M. d. F. C.; Pombeiro, A. J. L.; Sun, W.-H. *Coord. Chem. Rev.* **2020,** *416*, 213332.
61. Wu, J.-Q.; Li, Y.-S. *Coord. Chem. Rev.* **2011,** *255* (19-20), 2303-2314.
62. Nomura, K.; Zhang, S. *Chem. Rev.* **2011,** *111* (3), 2342-2362.
63. Bariashir, C.; Huang, C.; Solan, G. A.; Sun, W.-H. *Coord. Chem. Rev.* **2019,** *385*, 208-229.
64. McGuinness, D. *Chem. Rev.* **2011,** *111* (3), 2321-2341.
65. Agapie, T. *Coord. Chem. Rev.* **2011,** *255* (7-8), 861-880.
66. Dagorne, S.; Fliedel, C. *Top. Organomet. Chem.* **2013,** *41*, 125-172.
67. Burcher, B.; Breuil, P.-A. R.; Magna, L.; Olivier-Bourbigou, H. *Top. Organomet. Chem.* **2015,** *50*, 217-257.
68. Champouret, Y.; Hashmi, O. H.; Visseaux, M. *Coord. Chem. Rev.* **2019,** *390*, 127-170.
69. Olivier-Bourbigou, H.; Breuil, P. A. R.; Magna, L.; Michel, T.; Pastor, M. F. E.; Delcroix, D. *Chem. Rev.* **2020,** *120* (15), 7919-7983.

70. Bekmukhamedov, G. E.; Sukhov, A. V.; Kuchkaev, A. M.; Yakhvarov, D. G. *Catalysts* **2020,** *10* (5), 498.
71. Fliedel, C.; Poli, R. *Coord. Chem. Rev.* **2018,** *355*, 1-26.
72. Fliedel, C.; Ghisolfi, A.; Braunstein, P. *2016* **2016,** *116* (16), 9237-9304.
73. Speiser, F.; Braunstein, P.; Saussine, L. *Acc. Chem. Res.* **2005,** *38* (784-793).
74. Su, W.-F., Radical chain polymerization. In *Principles of polymer design and synthesis. Lecture notes in chemistry*, Su, W.-F., Ed. Springer, Berlin, Heidelberg: 2013; Vol. 82, pp 137-183.
75. Braunecker, W. A.; Matyjaszewski, K. *Prog. Polym. Sci.* **2007,** *32* (1), 93-146.
76. Matyjaszewski, K.; Davis, T. P., *Handbook of Radical Polymerization*. Wiley: 2002.
77. Matyjaszewski, K.; Gnanou, Y.; Leibler, L., *Macromolecular engineering: Precise synthesis, materials properties, applications*. Wiley-VCH Verlag GmbH: 2007.
78. Fischer, H. *Chem. Rev.* **2001,** *101*, 3581-3610.
79. Inoue, S. *J. Polym. Sci., Part A: Polym. Chem.* **2000,** *38*, 2861-2871.
80. Aida, T. *Prog. Polym. Sci.* **1994,** *19*, 469-528.
81. Fliedel, C.; Poli, R. *J. Organomet. Chem.* **2019,** *880*, 241-252.
82. Poli, R. *Angew. Chem. Int. Ed.* **2006,** *45* (31), 5058-5070.
83. Debuigne, A.; Jérôme, C.; Detrembleur, C. *Polymer* **2017,** *115*, 285-307.
84. Poli, R. *Chem. Eur. J.* **2015,** *21* (19), 6988-7001.
85. Wang, J.-S.; Matyjaszewski, K. *J. Am. Chem. Soc.* **1995,** *117* (20), 5614-5615.
86. Kato, M.; Kamigaito, M.; Sawamoto, M.; Higashimura, T. *Macromolecules* **1995,** *28* (5), 1721-1723.
87. Ribelli, T. G.; Lorandi, F.; Fantin, M.; Matyjaszewski, K. *Macromol. Rapid Commun.* **2019,** *40* (1), e1800616.
88. Matyjaszewski, K. *Macromolecules* **2012,** *45* (10), 4015-4039.
89. Matyjaszewski, K.; Xia, J. *Chem. Rev.* **2001,** *101*, 2921-2990.
90. Matyjaszewski, K. *Adv. Mater.* **2018,** *30* (23), e1706441.
91. Matyjaszewski, K.; Tsarevsky, N. V. *Nat. Chem.* **2009,** *1* (4), 276-288.
92. Dadashi-Silab, S.; Matyjaszewski, K. *Molecules* **2020,** *25* (7), 1648.
93. Xue, Z.; He, D.; Xie, X. *Polym. Chem.* **2015,** *6* (10), 1660-1687.
94. Krys, P.; Matyjaszewski, K. *Eur. Polym. J.* **2017,** *89*, 482-523.
95. Wang, J.-S.; Matyjaszewski, K. *Macromolecules* **1995,** *28*, 7901-7910.
96. Wang, J.-S.; Matyjaszewski, K. *Macromolecules* **1995,** *28*, 7572-7573.
97. Matyjaszewski, K.; Coca, S.; Gaynor, S. G.; Wei, M.; Woodworth, B. E. *Macromolecules* **1997,** *30*, 7348-7350.
98. Zhang, Y.; Wang, Y.; Matyjaszewski, K. *Macromolecules* **2011,** *44* (4), 683-685.
99. Matyjaszewski, K.; Tsarevsky, N. V.; Braunecker, W. A.; Dong, H.; Huang, J.; Jakubowski, W.; Kwak, Y.; Nicolay, R.; Tang, W.; Yoon, J. A. *Macromolecules* **2007,** *40*, 7795-7806.
100. Pan, X.; Fantin, M.; Yuan, F.; Matyjaszewski, K. *Chem. Soc. Rev.* **2018,** *47* (14), 5457-5490.
101. Wang, W.; Zhao, J.; Zhou, N.; Zhu, J.; Zhang, W.; Pan, X.; Zhang, Z.; Zhu, X. *Polym. Chem.* **2014,** *5* (11), 3533-3546.
102. Dadashi-Silab, S.; Matyjaszewski, K. *Macromolecules* **2018,** *51* (11), 4250-4258.
103. Percec, V.; Guliashvili, T.; Ladislaw, J. S.; Wistrand, A.; Stjerndahl, A.; Sienkowska, M. J.; Monteiro, M. J.; Sahoo, S. *J. Am. Chem. Soc.* **2006,** *128*, 14156-14165.
104. Rosen, B. M.; Percec, V. *Chem. Rev.* **2009,** *109*, 5069-5119.
105. Ribelli, T. G.; Krys, P.; Cong, Y.; Matyjaszewski, K. *Macromolecules* **2015,** *48* (23), 8428-8436.
106. Lorandi, F.; Fantin, M.; Isse, A. A.; Gennaro, A. *Polymer* **2015,** *72*, 238-245.
107. Konkolewicz, D.; Wang, Y.; Krys, P.; Zhong, M.; Isse, A. A.; Gennaro, A.; Matyjaszewski, K. *Polym. Chem.* **2014,** *5* (15), 4396-4417.
108. Konkolewicz, D.; Krys, P.; Góis, J. R.; Mendonça, P. V.; Zhong, M.; Wang, Y.; Gennaro, A.; Isse, A. A.; Fantin, M.; Matyjaszewski, K. *Macromolecules* **2014,** *47* (2), 560-570.

109. Konkolewicz, D.; Wang, Y.; Zhong, M.; Krys, P.; Isse, A. A.; Gennaro, A.; Matyjaszewski, K. *Macromolecules* **2013,** *46* (22), 8749-8772.
110. Boyer, C.; Corrigan, N. A.; Jung, K.; Nguyen, D.; Nguyen, T. K.; Adnan, N. N.; Oliver, S.; Shanmugam, S.; Yeow, J. *Chem. Rev.* **2016,** *116* (4), 1803-1949.
111. Anastasaki, A.; Nikolaou, V.; Nurumbetov, G.; Wilson, P.; Kempe, K.; Quinn, J. F.; Davis, T. P.; Whittaker, M. R.; Haddleton, D. M. *Chem. Rev.* **2016,** *116* (3), 835-877.
112. Li, M.; Jahed, N. M.; Min, K.; Matyjaszewski, K. *Macromolecules* **2004,** *37*, 2434-2441.
113. Gromada, J.; Matyjaszewski, K. *Macromolecules* **2001,** *34*, 7664-7671.
114. Jakubowski, W.; Matyjaszewski, K. *Macromolecules* **2005,** *38*, 4139-4146.
115. Min, K.; Gao, H.; Matyjaszewski, K. *J. Am. Chem. Soc.* **2005,** *127*, 3825-3830.
116. Bai, L.; Zhang, L.; Cheng, Z.; Zhu, X. *Polym. Chem.* **2012,** *3* (10), 2685-2697.
117. Jakubowski, W.; Min, K.; Matyjaszewski, K. *Macromolecules* **2006,** *39*, 39-45.
118. Jakubowski, W.; Matyjaszewski, K. *Angew. Chem. Int. Ed.* **2006,** *45*, 4482–4486.
119. Matyjaszewski, K.; Jakubowski, W.; Min, K.; Tang, W.; Huang, J.; Braunecker, W. A.; Tsarevsky, N. V. *Proc. Natl. Acad. Sci. USA* **2006,** *103* (42), 15309-15314.
120. Min, K.; Gao, H.; Matyjaszewski, K. *Macromolecules* **2007,** *40*, 1789-1791.
121. Enciso, A. E.; Fu, L.; Russell, A. J.; Matyjaszewski, K. *Angew. Chem. Int. Ed.* **2018,** *57* (4), 933–936.
122. Zhou, Y.-N.; Li, J.-J.; Wu, Y.-Y.; Luo, Z.-H. *Chem. Rev.* **2020,** *120* (5), 2950-3048.
123. Magenau, A. J. D.; Strandwitz, N. C.; Gennaro, A.; Matyjaszewski, K. *Science* **2011,** *332* (6025), 81-84.
124. Bortolamei, N.; Isse, A. A.; Magenau, A. J. D.; Gennaro, A.; Matyjaszewski, K. *Angew. Chem. Int. Ed.* **2011,** *50* (48), 11391-11394.
125. Park, S.; Chmielarz, P.; Gennaro, A.; Matyjaszewski, K. *Angew. Chem. Int. Ed.* **2015,** *54* (8), 2388-2392.
126. Chmielarz, P.; Fantin, M.; Park, S.; Isse, A. A.; Gennaro, A.; Magenau, A. J. D.; Sobkowiak, A.; Matyjaszewski, K. *Prog. Polym. Sci.* **2017,** *69*, 47-78.
127. Shanmugam, S.; Xu, J.; Boyer, C. *Macromol. Rapid Commun.* **2017,** *38* (13), 1700143.
128. Pan, X.; Tasdelen, M. A.; Laun, J.; Junkers, T.; Yagci, Y.; Matyjaszewski, K. *Prog. Polym. Sci.* **2016,** *62*, 73-125.
129. Dadashi-Silab, S.; Doran, S.; Yagci, Y. *Chem. Rev.* **2016,** *116* (17), 10212-10275.
130. Corrigan, N.; Shanmugam, S.; Xu, J.; Boyer, C. *Chem. Soc. Rev.* **2016,** *45* (22), 6165-6212.
131. Chen, M.; Zhong, M.; Johnson, J. A. *Chem. Rev.* **2016,** *116* (17), 10167-10211.
132. De Neve, J.; Haven, J. J.; Maes, L.; Junkers, T. *Polym. Chem.* **2018,** *9* (38), 4692-4705.
133. Wang, Z.; Pan, X.; Yan, J.; Dadashi-Silab, S.; Xie, G.; Zhang, J.; Wang, Z.; Xia, H.; Matyjaszewski, K. *ACS Macro Lett.* **2017,** *6* (5), 546-549.
134. Wang, Z.; Pan, X.; Li, L.; Fantin, M.; Yan, J.; Wang, Z.; Wang, Z.; Xia, H.; Matyjaszewski, K. *Macromolecules* **2017,** *50* (20), 7940-7948.
135. Mohapatra, H.; Kleiman, M.; Esser-Kahn, A. P. *Nat. Chem.* **2017,** *9* (2), 135-139.
136. Wang, Z.; Wang, Z.; Pan, X.; Fu, L.; Lathwal, S.; Olszewski, M.; Yan, J.; Enciso, A. E.; Wang, Z.; Xia, H.; Matyjaszewski, K. *ACS Macro Lett.* **2018,** *7* (3), 275-280.
137. Wang, Z.; Lorandi, F.; Fantin, M.; Wang, Z.; Yan, J.; Wang, Z.; Xia, H.; Matyjaszewski, K. *ACS Macro Lett.* **2019,** *8* (2), 161-165.
138. Xue, Z.; Nguyen, T. B.; Noh, S. K.; Lyoo, W. S. *Angew. Chem. Int. Ed.* **2008,** *47* (34), 6426-6429.
139. Khan, M. Y.; Chen, X.; Lee, S. W.; Noh, S. K. *Macromol. Rapid Commun.* **2013,** *34* (15), 1225-1230.
140. Wang, Y.; Kwak, Y.; Matyjaszewski, K. *Macromolecules* **2012,** *45* (15), 5911-5915.
141. Yang, D.; Wang, J.; Han, J.; Khan, M. Y.; Xie, X.; Xue, Z. *J. Polym. Sci., Part A: Polym. Chem.* **2017,** *55* (23), 3842-3850.
142. Wang, J.; Xie, X.; Xue, Z.; Fliedel, C.; Poli, R. *Polym. Chem.* **2020,** *11* (7), 1375-1385.

143. Wang, J.; Han, J.; Xie, X.; Xue, Z.; Fliedel, C.; Poli, R. *Macromolecules* **2019,** *52* (14), 5366-5376.
144. Lanzalaco, S.; Fantin, M.; Scialdone, O.; Galia, A.; Isse, A. A.; Gennaro, A.; Matyjaszewski, K. *Macromolecules* **2017,** *50* (1), 192-202.
145. Tang, W.; Kwak, Y.; Braunecker, W.; Tsarevsky, N. V.; Coote, M. L.; Matyjaszewski, K. *J. Am. Chem. Soc.* **2008,** *130* (32), 10702-10713.
146. Braunecker, W. A.; Tsarevsky, N. V.; Gennaro, A.; Matyjaszewski, K. *Macromolecules* **2009,** *42* (17), 6348-6360.
147. Tang, W.; Matyjaszewski, K. *Macromolecules* **2006,** *39*, 4953-4959.
148. Zerk, T. J.; Bernhardt, P. V. *Coord. Chem. Rev.* **2018,** *375*, 173-190.
149. Patten, T. E.; Xia, J.; Abernathy, T.; Matyjaszewski, K. *Science* **1996,** *272* (5263), 866-868.
150. Magenau, A. J. D.; Kwak, Y.; Schröder, K.; Matyjaszewski, K. *ACS Macro Lett.* **2012,** *1* (4), 508-512.
151. Kickelbick, G.; Matyjaszewski, K. *Macromol. Rapid Commun.* **1999,** *20*, 341-346.
152. Matyjaszewski, K.; Göbelt, B.; Paik, H.-j.; Horwitz, C. P. *Macromolecules* **2001,** *34*, 430-440.
153. Tang, H.; Radosz, M.; Shen, Y. *AlChE J.* **2009,** *55* (3), 737-746.
154. Haddleton, D. M.; Jasieczek, C. B.; Hannon, M. J.; Shooter, A. J. *Macromolecules* **1997,** *30*, 2190-2193.
155. Tang, W.; Nanda, A. K.; Matyjaszewski, K. *Macromol. Chem. Phys.* **2005,** *206* (12), 1171-1177.
156. Fliedel, C.; Rosa, V.; Santos, C. I.; Gonzalez, P. J.; Almeida, R. M.; Gomes, C. S.; Gomes, P. T.; Lemos, M. A.; Aullon, G.; Welter, R.; Aviles, T. *Dalton Trans.* **2014,** *43* (34), 13041-13054.
157. Xia, J.; Matyjaszewski, K. *Macromolecules* **1997,** *30*, 7697-7700.
158. Xia, J.; Gaynor, S. G.; Matyjaszewski, K. *Macromolecules* **1998,** *31*, 5958-5959.
159. Pintauer, T.; Matyjaszewski, K. *Coord. Chem. Rev.* **2005,** *249* (11-12), 1155-1184.
160. Inoue, Y.; Matyjaszewski, K. *Macromolecules* **2004,** *37*, 4014-4021.
161. Inoue, Y.; Matyjaszewski, K. *Macromolecules* **2003,** *36*, 7432-7438.
162. Xia, J.; Matyjaszewski, K. *Macromolecules* **1999,** *32*, 2434-2437.
163. Xia, J.; Zhang, X.; Matyjaszewski, K. *ACS Symp. Ser.* **2000,** *760*, 207-223.
164. Elsen, A. M.; Burdyńska, J.; Park, S.; Matyjaszewski, K. *Macromolecules* **2012,** *45* (18), 7356-7363.
165. Eckenhoff, W. T.; Pintauer, T. *Inorg. Chem.* **2010,** *49* (22), 10617-10626.
166. Kaur, A.; Ribelli, T. G.; Schroder, K.; Matyjaszewski, K.; Pintauer, T. *Inorg. Chem.* **2015,** *54* (4), 1474-1486.
167. Schröder, K.; Mathers, R. T.; Buback, J.; Konkolewicz, D.; Magenau, A. J. D.; Matyjaszewski, K. *ACS Macro Lett.* **2012,** *1* (8), 1037-1040.
168. Matyjaszewski, K.; Enciso, A. E.; Lorandi, F.; Mehmood, A.; Fantin, M.; Szczepaniak, G.; Janesko, B. G. *Angew. Chem. Int. Ed.* **2020,** *in press*, 10.1002/anie.202004724.
169. Ribelli, T. G.; Fantin, M.; Daran, J. C.; Augustine, K. F.; Poli, R.; Matyjaszewski, K. *J. Am. Chem. Soc.* **2018,** *140* (4), 1525-1534.
170. Carmo dos Santos, N. A.; Lorandi, F.; Badetti, E.; Wurst, K.; Isse, A. A.; Gennaro, A.; Licini, G.; Zonta, C. *Polymer* **2017,** *128*, 169-176.
171. Nishiura, C.; Williams, V.; Matyjaszewski, K. *Macromol. Res.* **2017,** *25* (6), 504-512.
172. Tang, H.; Arulsamy, N.; Radosz, M.; Shen, Y.; Tsarevsky, N. V.; Braunecker, W. A.; Tang, W.; Matyjaszewski, K. *J. Am. Chem. Soc.* **2006,** *128*, 16277-16285.
173. Tsarevsky, N. V.; Braunecker, W. A.; Tang, W.; Brooks, S. J.; Matyjaszewski, K.; Weisman, G. R.; Wong, E. H. *J. Mol. Catal. A: Chem.* **2006,** *257* (1-2), 132-140.
174. Mazzotti, G.; Benelli, T.; Lanzi, M.; Mazzocchetti, L.; Giorgini, L. *Eur. Polym. J.* **2016,** *77*, 75-87.
175. Lu, X.; Gong, S.; Meng, L.; Li, C.; Yang, S.; Zhang, L. *Polymer* **2007,** *48* (10), 2835-2842.
176. Wang, X.-Y.; Chen, Z.-H.; Sun, X.-L.; Tang, Y. *Polymer* **2019,** *178*, 121630.

177. Chen, Z.-H.; Wang, X.-Y.; Sun, X.-L.; Li, J.-F.; Zhu, B.-H.; Tang, Y. *Macromolecules* **2019,** *52* (24), 9792-9798.
178. Wang, X.-Y.; Sun, X.-L.; Chen, Z.-H.; Wang, F.; Wang, S. R.; Tang, Y. *Polym. Chem.* **2018,** *9* (32), 4309-4315.
179. Schaubach, S.; Wang, X.-Y.; Li, J.-F.; Sun, X.-L.; Wang, S. R.; Tang, Y. *Polym. Chem.* **2018,** *9* (38), 4711-4715.
180. Wang, X.-Y.; Sun, X.-L.; Wang, F.; Tang, Y. *ACS Catal.* **2017,** *7* (7), 4692-4696.
181. Hong, S. C.; Shin, K. E.; Noh, S. K.; Lyoo, W. S. *Macromol. Res.* **2005,** *13* (5), 391-396.
182. Bantu, B.; Wang, D.; Wurst, K.; Buchmeiser, M. R. *Tetrahedron* **2005,** *61* (51), 12145-12152.
183. Ando, T.; Kamigaito, M.; Sawamoto, M. *Macromolecules* **1997,** *30* (16), 4507-4510.
184. Matyjaszewski, K.; Wei, M.; Xia, J.; McDermott, N., E. *Macromolecules* **1997,** *30*, 8161-8164.
185. Schroeder, H.; Matyjaszewski, K.; Buback, M. *Macromolecules* **2015,** *48* (13), 4431-4437.
186. Aoshima, H.; Satoh, K.; Umemura, T.; Kamigaito, M. *Polym. Chem.* **2013,** *4* (12), 3554–3562.
187. Uchiike, C.; Terashima, T.; Ouchi, M.; Ando, T.; Kamigaito, M.; Sawamoto, M. *Macromolecules* **2007,** *40*, 8658-8662.
188. Uchiike, C.; Ouchi, M.; Ando, T.; Kamigaito, M.; Sawamoto, M. *J. Polym. Sci., Part A: Polym. Chem.* **2008,** *46* (20), 6819-6827.
189. Xue, Z.; Oh, H. S.; Noh, S. K.; Lyoo, W. S. *Macromol. Rapid Commun.* **2008,** *29* (23), 1887-1894.
190. Xue, Z.; Lee, B. W.; Noh, S. K.; Lyoo, W. S. *Polymer* **2007,** *48* (16), 4704-4714.
191. Xue, Z.; He, D.; Noh, S. K.; Lyoo, W. S. *Macromolecules* **2009,** *42* (8), 2949-2957.
192. Ishio, M.; Terashima, T.; Ouchi, M.; Sawamoto, M. *Macromolecules* **2010,** *43* (2), 920-926.
193. Ishio, M.; Terashima, T.; Ouchi, M.; Sawamoto, M. *Polym. J.* **2010,** *42* (1), 17-24.
194. Shaver, M. P.; Allan, L. E. N.; Gibson, V. C. *Organometallics* **2007,** *26* (19), 4725-4730.
195. O'Reilly, R. K.; Shaver, M. P.; Gibson, V. C.; White, A. J. P. *Macromolecules* **2007,** *40* (21), 7441-7452.
196. Allan, L. E. N.; Shaver, M. P.; White, A. J. P.; Gibson, V. C. *Inorg. Chem.* **2007,** *46* (21), 8963-8970.
197. Shaver, M. P.; Allan, L. E. N.; Rzepa, H. S.; Gibson, V. C. *Angew. Chem. Int. Ed.* **2006,** *45* (8), 1241-1244.
198. Gibson, V. C.; O'Reilly, R. K.; Wass, D. F.; White, A. J. P.; Williams, D. J. *Macromolecules* **2003,** *36* (8), 2591-2593.
199. Gibson, V. C.; O'Reilly, R. K.; Reed, W.; Wass, D. F.; White, A. J. P.; Williams, D. J. *Chem. Commun.* **2002,** (17), 1850-1851.
200. O'Reilly, R. K.; Gibson, V. C.; White, A. J. P.; Williams, D. J. *J. Am. Chem. Soc.* **2003,** *125* (28), 8450-8451.
201. Nakanishi, S.-i.; Kawamura, M.; Kai, H.; Jin, R.-H.; Sunada, Y.; Nagashima, H. *Chem. Eur. J.* **2014,** *20* (19), 5802-5814.
202. Allan, L. E. N.; MacDonald, J. P.; Nichol, G. S.; Shaver, M. P. *Macromolecules* **2014,** *47* (4), 1249-1257.
203. Allan, L. E. N.; MacDonald, J. P.; Reckling, A. M.; Kozak, C. M.; Shaver, M. P. *Macromol. Rapid Commun.* **2012,** *33* (5), 414-418.
204. Wang, G.; Zhu, X.; Zhu, J.; Cheng, Z. *J. Polym. Sci., Part A: Polym. Chem.* **2006,** *44* (1), 483-489.
205. Guo, T.; Zhang, L.; Jiang, H.; Zhang, Z.; Zhu, J.; Cheng, Z.; Zhu, X. *Polym. Chem.* **2011,** *2* (10), 2385-2390.
206. Zhang, L.; Miao, J.; Cheng, Z.; Zhu, X. *Macromol. Rapid Commun.* **2010,** *31* (3), 275-280.
207. Ouchi, M.; Sawamoto, M. *Macromolecules* **2017,** *50* (7), 2603-2614.
208. Ouchi, M.; Terashima, T.; Sawamoto, M. *Chem. Rev.* **2009,** *109* (11), 4963–5050.

209. Bai, L.; Zhang, L.; Zhang, Z.; Tu, Y.; Zhou, N.; Cheng, Z.; Zhu, X. *Macromolecules* **2010,** *43* (22), 9283-9290.
210. Bai, L.; Zhang, L.; Zhang, Z.; Zhu, J.; Zhou, N.; Cheng, Z.; Zhu, X. *J. Polym. Sci., Part A: Polym. Chem.* **2011,** *49* (18), 3970-3979.
211. Bai, L.; Zhang, L.; Zhang, Z.; Zhu, J.; Zhou, N.; Cheng, Z.; Zhu, X. *J. Polym. Sci., Part A: Polym. Chem.* **2011,** *49* (18), 3980-3987.
212. Wang, Y.; Matyjaszewski, K. *Macromolecules* **2011,** *44* (6), 1226-1228.
213. Mukumoto, K.; Wang, Y.; Matyjaszewski, K. *ACS Macro Lett.* **2012,** *1* (5), 599-602.
214. Wang, Y.; Zhang, Y.; Parker, B.; Matyjaszewski, K. *Macromolecules* **2011,** *44* (11), 4022-4025.
215. Ishio, M.; Katsube, M.; Ouchi, M.; Sawamoto, M.; Inoue, Y. *Macromolecules* **2009,** *42* (1), 188-193.
216. Deng, Z.; Guo, J.; Qiu, L.; Zhou, Y.; Xia, L.; Yan, F. *Polym. Chem.* **2012,** *3* (9), 2436-2443.
217. Okada, S.; Park, S.; Matyjaszewski, K. *ACS Macro Lett.* **2014,** *3* (9), 944-947.
218. Wang, Y.; Matyjaszewski, K. *Macromolecules* **2010,** *43* (9), 4003-4005.
219. Yang, D.; He, D.; Liao, Y.; Xue, Z.; Zhou, X.; Xie, X. *J. Polym. Sci., Part A: Polym. Chem.* **2014,** *52* (7), 1020-1027.
220. Xue, Z.; Zhou, J.; He, D.; Wu, F.; Yang, D.; Ye, Y. S.; Liao, Y.; Zhou, X.; Xie, X. *Dalton Trans.* **2014,** *43*, 16528-16533.
221. Ding, M.; Jiang, X.; Peng, J.; Zhang, L.; Cheng, Z.; Zhu, X. *Green Chem.* **2015,** *17* (1), 271-278.
222. di Lena, F.; Matyjaszewski, K. *Prog. Polym. Sci.* **2010,** *35*, 959-1021.
223. Kamigaito, M.; Ando, T.; Sawamoto, M. *Chem. Rev.* **2001,** *101*, 36893746.
224. Poli, R. *Eur. J. Inorg. Chem.* **2011,** (10), 1513-1530.
225. Thevenin, L.; Fliedel, C.; Matyjaszewski, K.; Poli, R. *Eur. J. Inorg. Chem.* **2019,** *2019* (42), 4489-4499.
226. Allan, L. E. N.; Perry, M. R.; Shaver, M. P. *Prog. Polym. Sci.* **2012,** *37* (1), 127-156.
227. Hurtgen, M.; Detrembleur, C.; Jerome, C.; Debuigne, A. *Polym. Rev.* **2011,** *51* (2), 188-213.
228. Poli, R.; Allan, L. E. N.; Shaver, M. P. *Prog. Polym. Sci.* **2014,** *39* (10), 1827-1845.
229. Demarteau, J.; Debuigne, A.; Detrembleur, C. *Chem. Rev.* **2019,** *119* (12), 6906-6955.
230. Debuigne, A.; Poli, R.; Jerome, C.; Jerome, R.; Detrembleur, C. *Prog. Polym. Sci.* **2009,** *34* (3), 211-239.
231. Wayland, B. B.; Poszmik, G.; Mukerjee, S. L.; Fryd, M. *J. Am. Chem. Soc.* **1994,** *116* (17), 7943-7944.
232. Langlotz, B. K.; Fillol, J. L.; Gross, J. H.; Wadepohl, H.; Gade, L. H. *Chem. Eur. J.* **2008,** *14* (33), 10267-10279.
233. Debuigne, A.; Caille, J. R.; Jerome, R. *Angew. Chem. Int. Ed.* **2005,** *44* (7), 1101-1104.
234. Debuigne, A.; Champouret, Y.; Jerome, R.; Poli, R.; Detrembleur, C. *Chem. Eur. J.* **2008,** *14* (13), 4046-4059.
235. Hurtgen, M.; Debuigne, A.; Jerome, C.; Detrembleur, C. *Macromolecules* **2010,** *43* (2), 886-894.
236. Bryaskova, R.; Detrembleur, C.; Debuigne, A.; Jerome, R. *Macromolecules* **2006,** *39* (24), 8263-8268.
237. Poli, R., Organometallic Mediated Radical Polymerization. In *Reference Module in Materials Science and Engineering* Hashmi, S., Ed. Elsevier: 2016.
238. Santhosh, K.; Gnanou, Y.; Champouret, Y.; Daran, J. C.; Poli, R. *Chem. Eur. J.* **2009,** *15* (19), 4874-4885.
239. Kaneyoshi, H.; Matyjaszewski, K. *Macromolecules* **2005,** *38* (20), 8163-8169.
240. Santhosh, K. K. S.; Li, Y. G.; Gnanou, Y.; Baisch, U.; Champouret, Y.; Poli, R.; Robson, K. C. D.; McNeil, W. S. *Chem. Asian J.* **2009,** *4* (8), 1257-1265.
241. Liao, C.-M.; Hsu, C.-C.; Wang, F.-S.; Wayland, B. B.; Peng, C.-H. *Polym. Chem.* **2013,** *4* (10), 3098-3104

242. Asandei, A. D.; Moran, I. W. *J. Am. Chem. Soc.* **2004,** *126* (49), 15932-15933.
243. Perry, M. R.; Allan, L. E. N.; Decken, A.; Shaver, M. P. *Dalton Trans.* **2013,** *42* (25), 9157-9165
244. Allan, L. E. N.; Cross, E. D.; Francis-Pranger, T. W.; Hanhan, M. E.; Jones, M. R.; Pearson, J. K.; Perry, M. R.; Storr, T.; Shaver, M. P. *Macromolecules* **2011,** *44* (11), 4072-4081.
245. Shaver, M. P.; Hanhan, M. E.; Jones, M. R. *Chem. Commun.* **2010,** *46* (12), 2127-2129.
246. Champouret, Y.; Baisch, U.; Poli, R.; Tang, L.; Conway, J. L.; Smith, K. M. *Angew. Chem. Int. Ed.* **2008,** *47* (32), 6069-6072.
247. Xue, Z. G.; Poli, R. *J. Polym. Sci., Part A: Polym. Chem.* **2013,** *51* (16), 3494-3504.
248. Place, E. S.; George, J. H.; Williams, C. K.; Stevens, M. M. *Chem. Soc. Rev.* **2009,** *38* (4), 1139-1151.
249. Jérôme, C.; Lecomte, P. *Adv. Drug Deliv. Rev.* **2008,** *60* (9), 1056-1076.
250. Nair, L. S.; Laurencin, C. T. *Prog. Polym. Sci.* **2007,** *32* (8-9), 762-798.
251. Vert, M. *Biomacromolecules* **2005,** *6* (2), 538-546.
252. Albertsson, A.-C.; Varma, I. K. *Biomacromolecules* **2003,** *4* (6), 1466-1486.
253. Gruber, P. R.; Kolstad, J. J.; Hall, E. S.; Eichen Conn, R. S.; Ryan, C. M. *(Cargill Incorporated)* **2000,** *US Patent*, 6 143 863.
254. Gruber, P. R.; Hall, E. S.; Kolstad, J. J.; Iwen, M. L.; Benson, R. D.; Borchardt, R. L. *(Cargill Incorporated)* **1993,** *US Patent*, 5 258 488.
255. Slomkowski, S.; Penczek, S.; Duda, A. *Polym. Adv. Technol.* **2014,** *25* (5), 436–447.
256. Endo, T., General Mechanisms in Ring-Opening Polymerization. Dubois, P.; Coulembier, O.; Raquez, J. M., Eds. Wiley: Weinheim, 2009.
257. Gao, J.; Zhu, D.; Zhang, W.; Solan, G. A.; Ma, Y.; Sun, W.-H. *Inorganic Chemistry Frontiers* **2019,** *6* (10), 2619-2652
258. Tian, L.-L.; Wu, B.-B.; Wang, Z.-X. *Journal of Macromolecular Science, Part A: Pure and Applied Chemistry* **2017,** *54* (12), 944-950.
259. Sutar, A. K.; Maharana, T.; Dutta, S.; Chen, C.-T.; Lin, C.-C. *Chem. Soc. Rev.* **2010,** *39* (5), 1724-1746
260. Wu, J.; Yu, T.-L.; Chen, C.-T.; Lin, C.-C. *Coord. Chem. Rev.* **2006,** *250* (5-6), 602-626.
261. Macromolecular ResearchDevaine-Pressing, K.; Oldenburg, F. J.; Menzel, J. P.; Springer, M.; Dawe, L. N.; Kozak, C. M. *Dalton Trans.* **2020,** *49* (5), 1531-1544.
262. Durango-García, C. J.; Rufino-Felipe, E.; López-Cardoso, M.; Muñoz-Hernández, M.-A.; Montiel-Palma, V. *J. Mol. Struct.* **2018,** *1164*, 248-258.
263. Binda, P. I.; Hill, B. R.; Skelton, B. W. *J. Coord. Chem.* **2018,** *71* (7), 941-951.
264. Yao, C.; Yang, Y.; Xu, S.; Ma, H. *Dalton Trans.* **2017,** *46* (18), 6087-6097
265. Saunders, L. N.; Dawe, L. N.; Kozak, C. M. *J. Organomet. Chem.* **2014,** *749*, 34-40.
266. Dai, Z.; Sun, Y.; Xiong, J.; Pan, X.; Wu, J. *ACS Macro Lett.* **2015,** *4* (5), 556-560.
267. Zhang, J.; Xiong, J.; Sun, Y.; Tang, N.; Wu, J. *Macromolecules* **2014,** *47* (22), 7789-7796.
268. Redshaw, C. *Dalton Trans.* **2016,** *45* (22), 9018-9030.
269. Chisholm, M. H. *Inorg. Chim. Acta* **2009,** *362* (12), 4284-4290.
270. Chisholm, M. H.; Gallucci, J. C.; Phomphrai, K. *Inorg. Chem.* **2005,** *44* (22), 8004-8010.
271. McKeown, P.; McCormick, S. N.; Mahon, M. F.; Jones, M. *Polym. Chem.* **2018,** *9* (44), 5339-5347.
272. Hung, W.-C.; Lin, C.-C. *Inorg. Chem.* **2009,** *48* (2), 728-734.
273. Garcés, A.; Sánchez-Barba, L. F.; Fernández-Baeza, J.; Otero, A.; Lara-Sánchez, A.; Rodríguez, A. M. *Organometallics* **2017,** *36* (4), 884-897.
274. Wang, H.; Guo, J.; Yang, Y.; Ma, H. *Dalton Trans.* **2016,** *45* (27), 10942-10953.
275. Poirier, V.; Roisnel, T.; Carpentier, J.-F.; Sarazin, Y. *Dalton Trans.* **2009,** (44), 9820-9827.
276. Hu, J.; Kan, C.; Wang, H.; Ma, H. *Macromolecules* **2018,** *51* (14), 5304-5312.
277. Rosen, T.; Goldberg, I.; Venditto, V.; Kol, M. *J. Am. Chem. Soc.* **2016,** *138* (37), 12041-12044.

278. Liu, B.; Roisnel, T.; Guégan, J.-P.; Carpentier, J.-F.; Sarazin, Y. *Chem. Eur. J.* **2012,** *18* (20), 6289–6301.
279. Chisholm, M. H.; Gallucci, J.; Phomphrai, K. *Chem. Commun.* **2003,** (1), 48-49
280. Le Roux, E. *Coord. Chem. Rev.* **2016,** *306* (1), 65-85.
281. Sauer, A.; Kapelski, A.; Fliedel, C.; Dagorne, S.; Kol, M.; Okuda, J. *Dalton Trans.* **2013,** *42* (25), 9007-9023.
282. Gendler, S.; Segal, S.; Goldberg, I.; Goldschmidt, Z.; Kol, M. *Inorg. Chem.* **2006,** *45* (12), 4783-4790.
283. Romain, C.; Heinrich, B.; Bellemin-Laponnaz, S.; Dagorne, S. *Chem. Commun.* **2012,** *48* (16), 2213-2215.
284. Schäfer, P. M.; Herres-Pawlis, S. *ChemPlusChem* **2020,** *85* (5), 1044-1052.
285. Dagorne, S. *Synthesis* **2018,** *50* (18), 3662-3670.
286. dos Santos Vieira, I.; Herres-Pawlis, S. *Eur. J. Inorg. Chem.* **2012,** *2012* (5), 765-774.
287. Wheaton, C. A.; Hayes, P. G. *Comments Inorg. Chem.* **2011,** *32* (3), 127-162.
288. Wheaton, C. A.; Hayes, P. G.; Ireland, B. J. *Dalton Trans.* **2009,** (25), 4832-4846.
289. O'Keefe, B. J.; Hillmyer, M. A.; Tolman, W. B. *J. Chem. Soc., Dalton Trans.* **2001,** (15), 2215-2224.
290. Williams, C. K.; Breyfogle, L. E.; Choi, S. K.; Nam, W.; Young Jr., V. G.; Hillmyer, M. A.; Tolman, W. B. *J. Am. Chem. Soc.* **2003,** *125* (37), 11350-11359.
291. Cheng, M.; Attygalle, A. B.; Lobkovsky, E. B.; Coates, G. W. *J. Am. Chem. Soc.* **1999,** *121* (49), 11583-11584.
292. Fliedel, C.; Rosa, V.; Alves, F. M.; Martins, A. M.; Avilés, T.; Dagorne, S. *Dalton Trans.* **2015,** *44* (27), 12376-12387.
293. Fliedel, C.; Vila-Viçosa, D.; Calhorda, M. J.; Dagorne, S.; Avilés, T. *ChemCatChem* **2014,** *6* (5), 1357-1367.
294. Wheaton, C. A.; Hayes, P. G. *Chem. Commun.* **2010,** *46* (44), 8404-8406.
295. Kan, C.; Hu, J.; Huang, Y.; Wang, H.; Ma, H. *Macromolecules* **2017,** *50* (20), 7911-7919.
296. Ebrahimi, T.; Aluthge, D. C.; Hatzikiriakos, S. G.; Mehrkhodavandi, P. *Macromolecules* **2016,** *49* (23), 8812-8824.
297. Abbina, S.; Du, G. *ACS Macro Lett.* **2014,** *3* (7), 689-692.
298. Spassky, N.; Wisniewski, M.; Pluta, C.; Le Borgne, A. *Macromol. Chem. Phys.* **1996,** *197* (9), 2627-2637.
299. Aida, T.; Inoue, S. *Acc. Chem. Res.* **1996,** *29* (1), 39-48.
300. Wei, Y.; Wang, S.; Zhou, S. *Dalton Trans.* **2016,** *45* (11), 4471-4485.
301. Cameron, D. J. A.; Shaver, M. P. *Chem. Soc. Rev.* **2011,** *40* (3), 1761-1776.
302. Thomas, C. M. *Chem. Soc. Rev.* **2010,** *39* (1), 165-173
303. Arbaoui, A.; Redshaw, C. *Polym. Chem.* **2010,** *1* (6), 801-826
304. Labet, M.; Thielemans, W. *Chem. Soc. Rev.* **2009,** *38* (12), 3484-3504.
305. Platel, R. H.; Hodgson, L. M.; Williams, C. K. *Polym. Rev.* **2008,** *48* (1), 11-63.
306. Dove, A. P. *Chem. Commun.* **2008,** (48), 6446-6470
307. Dechy-Cabaret, O.; Martin-Vaca, B.; Bourissou, D. *Chem. Rev.* **2004,** *104* (12), 6147-6176.
308. Press, K.; Goldberg, I.; Kol, M. *Angew. Chem. Int. Ed.* **2015,** *54*, 14858-14861.
309. Hador, R.; Botta, A.; Venditto, V.; Lipstman, S.; Goldberg, I.; Kol, M. *Angew. Chem. Int. Ed.* **2019,** *58* (41), 14679–14685.
310. Dagorne, S.; Normand, M.; Kirillov, E.; Carpentier, J.-F. *Coord. Chem. Rev.* **2013,** *257* (11-12), 1869-1886.
311. Yu, I.; Acosta-Ramirez, A.; Mehrkhodavandi, P. *J. Am. Chem. Soc.* **2012,** *134* (30), 12758-12773.
312. Specklin, D.; Fliedel, C.; Hild, F.; Mameri, S.; Karmazin, L.; Bailly, C.; Dagorne, S. *Dalton Trans.* **2017,** *46* (38), 12824-12834.

313. Coates, G. W.; Moore, D. R. *Angew. Chem. Int. Ed.* **2004,** *43* (48), 6618-6639.
314. Darensbourg, D. J.; Mackiewicz, R. M.; Phelps, A. L.; Billodeaux, D. R. *Acc. Chem. Res.* **2004,** *37* (11), 836-844.
315. Darensbourg, D. J. *Chem. Rev.* **2007,** *107* (6), 2388-2410.
316. Kember, M. R.; Buchard, A.; Williams, C. K. *Chem. Comm.* **2011,** *47* (1), 141-163.
317. Klaus, S.; Lehenmeier, M. W.; Anderson, C. E.; Rieger, B. *Coord. Chem. Rev.* **2011,** *255* (13–14), 1460-1479.
318. Trott, G.; Saini, P. K.; Williams, C. K. *Phil. Trans. R. Soc. A* **2016,** *374* (2061).
319. Kozak, C. M.; Ambrose, K.; Anderson, T. S. *Coord. Chem. Rev.* **2018,** *376*, 565-587.
320. Andrea, K. A.; Plommer, H.; Kerton, F. M. *Eur. Polym. J.* **2019,** *120*, 109202.
321. North, M.; Editor, *Sustainable Catalysis: With Non-endangered Metals*. RSC Green Chemistry: 2015; Vol. 38, p 480.
322. Chamberlain, B. M.; Cheng, M.; Moore, D. R.; Ovitt, T. M.; Lobkovsky, E. B.; Coates, G. W. *J. Am. Chem. Soc.* **2001,** *123* (14), 3229-3238.
323. Chisholm, M. H.; Huffman, J. C.; Phomphrai, K. *J. Chem. Soc., Dalton Trans.* **2001,** (3), 222-224.
324. Kobayashi, M.; Inoue, S.; Tsuruta, T. *Polym. Sci. Jpn.* **1975,** *8*, 1.
325. Soga, K.; Uenishi, K.; Hosoda, S.; Ikeda, S. *Makromol. Chem.* **1977,** *178* (3), 893-897.
326. Xiao, Y.; Wang, Z.; Ding, K. *Macromolecules* **2006,** *39*, 1128-137.
327. Kember, M. R.; Williams, C. K. *J. Am. Chem. Soc.* **2012,** *134* (38), 15676-15679.
328. Chapman, A. M.; Keyworth, C.; Kember, M. R.; Lennox, A. J. J.; Williams, C. K. *ACS Catal.* **2015,** *5* (3), 1581-1588.
329. Winkler, M.; Romain, C.; Meier, M. A. R.; Williams, C. K. *Green Chem.* **2015,** *17* (1), 300-306.
330. Saini, P. K.; Romain, C.; Williams, C. K. *Chem. Commun.* **2014,** *50* (32), 4164-4167.
331. Trott, G.; Garden, J. A.; Williams, C. K. *Chem. Sci.* **2019,** *10* (17), 4618-4627.
332. Chen, X.; Shen, Z.; Zhang, Y. *Macromolecules* **1991,** *24* (19), 5305-5308.
333. Liu, B.; Zhao, X.; Wang, X.; Wang, F. *J. Polym. Sci. A Polym. Chem.* **2001,** *39* (16), 2751-2754.
334. Wu, J.; Shen, Z. *Polym. J.* **1990,** *22* (4), 326-330.
335. Wu, J.; Shen, Z. *J. Polym. Sci. A Polym. Chem.* **1990,** *28* (7), 1995-1997.
336. Cui, D.; Nishiura, M.; Hou, Z. *Macromolecules* **2005,** *38* (10), 4089-4095.
337. Lazarov, B. B.; Hampel, F.; Hultzsch, K. C. *Z. Anorg. Allg. Chem.* **2007,** *633* (13-14), 2367-2373.
338. Cui, D.; Nishiura, M.; Tardif, O.; Hou, Z. *Organometallics* **2008,** *27* (11), 2428-2435.
339. Vitanova, D. V.; Hampel, F.; Hultzsch, K. C. *J. Organomet. Chem.* **2005,** *690* (23), 5182-5197.
340. Zhang, Z.; Cui, D.; Liu, X. *J. Polym. Sci. A Polym. Chem.* **2008,** *46* (20), 6810-6818.
341. Decortes, A.; Haak, R. M.; Martín, C.; Belmonte, M. M.; Martin, E.; Benet-Buchholz, J.; Kleij, A. W. *Macromolecules* **2015,** *48* (22), 8197-8207.
342. Ho, C.-H.; Chuang, H.-J.; Lin, P.-H.; Ko, B.-T. *J. Polym. Sci. Part A: Polym. Chem.* **2017,** *55* (2), 321-328.
343. Shen, Z.; Chen, X.; Zhang, Y. *Macromol. Chem. Phys.* **1994,** *195* (6), 2003-2011.
344. Tan, C.-S.; Hsu, T.-J. *Macromolecules* **1997,** *30* (11), 3147-3150.
345. Hsu, T.-J.; Tan, C.-S. *Polymer* **2001,** *42* (12), 5143-5150.
346. Guo, J.-T.; Wang, X.-Y.; Xu, Y.-S.; Sun, J.-W. *J. Appl. Polym. Sci.* **2003,** *87* (14), 2356-2359.
347. Quan, Z.; Wang, X.; Zhao, X.; Wang, F. *Polymer* **2003,** *44* (19), 5605-5610.
348. Qin, J.; Xu, B.; Zhang, Y.; Yuan, D.; Yao, Y. *Green Chem.* **2016,** *18* (15), 4270-4275.
349. Nagae, H.; Aoki, R.; Akutagawa, S.-n.; Kleemann, J.; Tagawa, R.; Schindler, T.; Choi, G.; Spaniol, T. P.; Tsurugi, H.; Okuda, J.; Mashima, K. *Angew. Chem. Int. Ed.* **2018,** *57* (9), 2492-2496.
350. Nagae, H.; Aoki, R.; Akutagawa, S.-n.; Kleemann, J.; Tagawa, R.; Schindler, T.; Choi, G.; Spaniol, T. P.; Tsurugi, H.; Okuda, J.; Mashima, K. *Angew. Chem.* **2018,** *130* (9), 2518-2522.
351. Hua, L.; Li, B.; Han, C.; Gao, P.; Wang, Y.; Yuan, D.; Yao, Y. *Inorg. Chem.* **2019,** *58* (13), 8775-8786.

352. Dechy-Cabaret, O.; Martin-Vaca, B.; Bourissou, D. *Chem. Rev.* **2004,** *104* (12), 6147-6176.
353. Sauer, A.; Kapelski, A.; Fliedel, C.; Dagorne, S.; Kol, M.; Okuda, J. *Dalton Trans.* **2013,** *42* (25), 9007-9023.
354. Slomkowski, S.; Penczek, S.; Duda, A. *Polym. Adv. Technol.* **2014,** *25* (5), 436-447.
355. Le Roux, E., Chapter 6 Titanium-based Catalysts for Polymer Synthesis. In *Sustainable Catalysis: With Non-endangered Metals, Part 1*, The Royal Society of Chemistry: 2015; pp 116-139.
356. Le Roux, E. *Coord. Chem. Rev.* **2016,** *306*, 65-85.
357. Nakano, K.; Kobayashi, K.; Nozaki, K. *J. Am. Chem. Soc.* **2011,** *133* (28), 10720-10723.
358. Quadri, C. C.; Le Roux, E. *Dalton Trans.* **2014,** *43* (11), 4242-4246.
359. Hessevik, J.; Lalrempuia, R.; Nsiri, H.; Tornroos, K. W.; Jensen, V. R.; Le Roux, E. *Dalton Trans.* **2016,** *45*, 14734-14744.
360. Lalrempuia, R.; Breivik, F.; Törnroos, K. W.; Le Roux, E. *Dalton Trans.* **2017,** *46* (25), 8065-8076.
361. Quadri, C. C.; Lalrempuia, R.; Hessevik, J.; Törnroos, K. W.; Le Roux, E. *Organometallics* **2017,** *36* (22), 4477-4489.
362. Lalrempuia, R.; Underhaug, J.; Törnroos, K. W.; Le Roux, E. *Chem. Commun.* **2019,** *55* (50), 7227-7230.
363. Wang, Y.; Qin, Y.; Wang, X.; Wang, F. *Catal. Sci. Technol.* **2014,** *4* (11), 3964-3972.
364. Wang, Y.; Qin, Y.; Wang, X.; Wang, F. *ACS Catal.* **2015,** *5* (1), 393-396.
365. Mandal, M.; Chakraborty, D. *J. Polym. Sci. Part A: Polym. Chem.* **2016,** *54* (6), 809-824.
366. Mandal, M.; Ramkumar, V.; Chakraborty, D. *Polym. Chem.* **2019,** *10* (25), 3444-3460.
367. Mandal, M.; Chakraborty, D.; Ramkumar, V. *RSC Adv.* **2015,** *5* (36), 28536-28553.
368. Mandal, M.; Monkowius, U.; Chakraborty, D. *New J. Chem.* **2016,** *40* (11), 9824-9839.
369. Chuang, H.-J.; Ko, B.-T. *Dalton Trans.* **2015,** *44* (2), 598-607.
370. Su, C.-K.; Chuang, H.-J.; Li, C.-Y.; Yu, C.-Y.; Ko, B.-T.; Chen, J.-D.; Chen, M.-J. *Organometallics* **2014,** *33* (24), 7091-7100.
371. Garden, J. A.; White, A. J. P.; Williams, C. K. *Dalton Trans.* **2017,** *46* (8), 2532-2541.
372. Darensbourg, D. J. *J. Chem. Educ.* **2017,** *94* (11), 1691-1695.
373. Kruper, W. J.; Dellar, D. D. *J. Org. Chem.* **1995,** *60* (3), 725-727.
374. Mang, S.; Cooper, A. I.; Colclough, M. E.; Chauhan, N.; Holmes, A. B. *Macromolecules* **2000,** *33* (2), 303-308.
375. Stamp, L. M.; Mang, S. A.; Holmes, A. B.; Knights, K. A.; de Miguel, Y. R.; McConvey, I. F. *Chem. Commun.* **2001,** (23), 2502-2503.
376. Chatterjee, C.; Chisholm, M. H. *Inorg. Chem.* **2012,** *51* (21), 12041-12052.
377. Chukanova, O. M.; Belov, G. P. *Kinet. Catal.* **2017,** *58* (4), 397-401.
378. Darensbourg, D. J.; Yarbrough, J. C. *J. Am. Chem. Soc.* **2002,** *124* (22), 6335-6342.
379. Darensbourg, D. J.; Yarbrough, J. C.; Ortiz, C.; Fang, C. C. *J. Am. Chem. Soc.* **2003,** *125* (25), 7586-7591.
380. Eberhardt, R.; Allmendinger, M.; Rieger, B. *Macromol. Rapid Commun.* **2003,** *24* (2), 194-196.
381. Darensbourg, D. J.; Mackiewicz, R. M.; Billodeaux, D. R. *Organometallics* **2005,** *24* (1), 144-148.
382. Darensbourg, D. J.; Phelps, A. L. *Inorg. Chem.* **2005,** *44* (13), 4622-4629.
383. Li, B.; Zhang, R.; Lu, X.-B. *Macromolecules* **2007,** *40* (7), 2303-2307.
384. Darensbourg, D. J.; Poland, R. R.; Escobedo, C. *Macromolecules* **2012,** *45* (5), 2242-2248.
385. Luinstra, G. A.; Haas, G. R.; Molnar, F.; Bernhart, V.; Eberhardt, R.; Rieger, B. *Chem. – A Eur. J.* **2005,** *11* (21), 6298-6314.
386. Rao, D.-Y.; Li, B.; Zhang, R.; Wang, H.; Lu, X.-B. *Inorg. Chem.* **2009,** *48* (7), 2830-2836.
387. Nakano, K.; Nakamura, M.; Nozaki, K. *Macromolecules* **2009,** *42* (18), 6972-6980.
388. Li, B.; Wu, G.-P.; Ren, W.-M.; Wang, Y.-M.; Rao, D.-Y.; Lu, X.-B. *J. Polym. Sci. A Polym. Chem.* **2008,** *46* (18), 6102-6113.

389. Darensbourg, D. J.; Ulusoy, M.; Karroonnirum, O.; Poland, R. R.; Reibenspies, J. H.; Çetinkaya, B. *Macromolecules* **2009,** *42* (18), 6992-6998.
390. Han, B.; Zhang, L.; Kyran, S. J.; Liu, B.; Duan, Z.; Darensbourg, D. J. *J. Polym. Sci. Part A: Polym. Chem.* **2016,** *54* (13), 1938-1944.
391. Si, G.; Zhang, L.; Han, B.; Zhang, H.; Li, X.; Liu, B. *RSC Adv.* **2016,** *6* (27), 22821-22826.
392. Darensbourg, D. J.; Chung, W.-C.; Wilson, S. J. *ACS Catal.* **2013,** *3* (12), 3050-3057.
393. Darensbourg, D. J.; Chung, W.-C. *Macromolecules* **2014,** *47* (15), 4943-4948.
394. Darensbourg, D. J.; Chung, W.-C.; Arp, C. J.; Tsai, F.-T.; Kyran, S. J. *Macromolecules* **2014,** *47* (21), 7347-7353.
395. Vagin, S. I.; Reichardt, R.; Klaus, S.; Rieger, B. *J. Am. Chem. Soc.* **2010,** *132* (41), 14367-14369.
396. Liu, Y.; Zhou, H.; Guo, J.-Z.; Ren, W.-M.; Lu, X.-B. *Angew. Chem. Int. Ed.* **2017,** *56* (17), 4862-4866.
397. Liu, Y.; Guo, J.-Z.; Lu, H.-W.; Wang, H.-B.; Lu, X.-B. *Macromolecules* **2018,** *51* (3), 771-778.
398. Hongfa, C.; Tian, J.; Andreatta, J.; Darensbourg, D. J.; Bergbreiter, D. E. *Chem. Commun.* **2008,** (8), 975-977.
399. Wang, J.; Shan, X.; Shan, S.; Su, H.; Wu, S.; Jia, Q. *Catal. Commun.* **2015,** *59*, 116-121.
400. Darensbourg, D. J.; Fitch, S. B. *Inorg. Chem.* **2007,** *46* (14), 5474-5476.
401. Darensbourg, D. J.; Fitch, S. B. *Inorg. Chem.* **2008,** *47* (24), 11868-11878.
402. Darensbourg, D. J.; Fitch, S. B. *Inorg. Chem.* **2009,** *48* (18), 8668-8677.
403. Cuesta-Aluja, L.; Djoufak, M.; Aghmiz, A.; Rivas, R.; Christ, L.; Masdeu-Bultó, A. M. *J. Mol. Catal. A Chem.* **2014,** *381*, 161-170.
404. Adolph, M.; Zevaco, T. A.; Altesleben, C.; Walter, O.; Dinjus, E. *Dalton Trans.* **2014,** *43* (8), 3285-3296.
405. Iksi, S.; Aghmiz, A.; Rivas, R.; González, M. D.; Cuesta-Aluja, L.; Castilla, J.; Orejón, A.; El Guemmout, F.; Masdeu-Bultó, A. M. *J. Mol. Catal. A Chem.* **2014,** *383-384*, 143-152.
406. Gurnham, J.; Gambarotta, S.; Korobkov, I.; Jasinska-Walc, L.; Duchateau, R. *Organometallics* **2014,** *33* (17), 4401-4409.
407. Elmas, S.; Subhani, M. A.; Harrer, M.; Leitner, W.; Sundermeyer, J.; Müller, T. E. *Catal. Sci. Technol.* **2014,** *4* (6), 1652-1657.
408. Hartweg, M.; Sundermeyer, J. *Eur. Polym. J.* **2019,** *120*, 109245.
409. Whiteoak, C. J.; Martin, E.; Belmonte, M. M.; Benet-Buchholz, J.; Kleij, A. W. *Adv. Synth. Catal.* **2012,** *354* (2-3), 469-476.
410. Dean, R. K.; Dawe, L. N.; Kozak, C. M. *Inorg. Chem.* **2012,** *51* (16), 9095-9103.
411. Dean, R. K.; Devaine-Pressing, K.; Dawe, L. N.; Kozak, C. M. *Dalton Trans.* **2013,** *42* (25), 9233-9244.
412. Devaine-Pressing, K.; Dawe, L. N.; Kozak, C. M. *Polym. Chem.* **2015,** *6* (35), 6305-6315.
413. Devaine-Pressing, K.; Kozak, C. M. *ChemSusChem* **2017,** *10* (6), 1266-1273.
414. Ni, K.; Kozak, C. M. *Inorg. Chem.* **2018,** *57* (6), 3097-3106.
415. Ni, K.; Paniez-Grave, V.; Kozak, C. M. *Organometallics* **2018,** *37* (15), 2507-2518.
416. Chen, H.; Dawe, L. N.; Kozak, C. M. *Catal. Sci. Technol.* **2014,** *4* (6), 1547-1555.
417. Sugimoto, H.; Ohshima, H.; Inoue, S. *J. Polym. Sci. A Polym. Chem.* **2003,** *41* (22), 3549-3555.
418. Robert, C.; Ohkawara, T.; Nozaki, K. *Chem. Eur. J.* **2014,** *20* (16), 4789-4795.
419. W. J. Kruper; D. J. Smart Carbon dioxide oxirane copolymers prepared using double metal cyanide complexes US Patent 4 500 704, The Dow Chemical Co., 15 August 1983, 1983.
420. Chen, L.-B. *Makromol. Chem. Macromol. Symp.* **1992,** *59* (1), 75-82.
421. Darensbourg, D. J.; Adams, M. J.; Yarbrough, J. C. *Inorg. Chem.* **2001,** *40* (26), 6543-6544.
422. Darensbourg, D. J.; Adams, M. J.; Yarbrough, J. C.; Phelps, A. L. *Inorg. Chem.* **2003,** *42* (24), 7809-7818.
423. Buchard, A.; Kember, M. R.; Sandeman, K. G.; Williams, C. K. *Chem. Commun.* **2011,** *47* (1), 212-214.

424. Nakano, K.; Kobayashi, K.; Ohkawara, T.; Imoto, H.; Nozaki, K. *J. Am. Chem. Soc.* **2013,** *135* (23), 8456-8459.
425. Taherimehr, M.; Al-Amsyar, S. M.; Whiteoak, C. J.; Kleij, A. W.; Pescarmona, P. P. *Green Chem.* **2013,** *15* (11), 3083-3090.
426. Taherimehr, M.; Sertã, J. P. C. C.; Kleij, A. W.; Whiteoak, C. J.; Pescarmona, P. P. *ChemSusChem* **2015,** *8* (6), 1034-1042.
427. Shi, Z.; Jiang, Q.; Song, Z.; Wang, Z.; Gao, C. *Polym. Chem.* **2018,** *9* (38), 4733-4743.
428. Adolph, M.; Zevaco, T. A.; Walter, O.; Dinjus, E.; Döring, M. *Polyhedron* **2012,** *48* (1), 92-98.
429. Della Monica, F.; Maity, B.; Pehl, T.; Buonerba, A.; De Nisi, A.; Monari, M.; Grassi, A.; Rieger, B.; Cavallo, L.; Capacchione, C. *ACS Catal.* **2018,** *8* (8), 6882-6893.
430. Huang, J.; Worch, J. C.; Dove, A. P.; Coulembier, O. *ChemSusChem* **2020,** *13* (3), 469-487.
431. Li, C.-H.; Chuang, H.-J.; Li, C.-Y.; Ko, B.-T.; Lin, C.-H. *Polym. Chem.* **2014,** *5* (17), 4875-4878.
432. Yu, C.-Y.; Chuang, H.-J.; Ko, B.-T. *Catal. Sci. Technol.* **2016,** *6* (6), 1779-1791.
433. Lin, P.-M.; Chang, C.-H.; Chuang, H.-J.; Liu, C.-T.; Ko, B.-T.; Lin, C.-C. *ChemCatChem* **2016,** *8* (5), 984-991.
434. Huang, L.-S.; Tsai, C.-Y.; Chuang, H.-J.; Ko, B.-T. *Inorg. Chem.* **2017,** *56* (11), 6141-6151.
435. Tsai, C.-Y.; Cheng, F.-Y.; Lu, K.-Y.; Wu, J.-T.; Huang, B.-H.; Chen, W.-A.; Lin, C.-C.; Ko, B.-T. *Inorg. Chem.* **2016,** *55* (16), 7843-7851.
436. Tsai, C.-Y.; Huang, B.-H.; Hsiao, M.-W.; Lin, C.-C.; Ko, B.-T. *Inorg. Chem.* **2014,** *53* (10), 5109-5116.
437. Zhu, Y.; Romain, C.; Williams, C. K. *Nature* **2016,** *540* (7633), 354-362.
438. Darensbourg, D. J.; Billodeaux, D. R. *C. R. Chim.* **2004,** *7* (8), 755-761.
439. Thevenon, A.; Cyriac, A.; Myers, D.; White, A. J. P.; Durr, C. B.; Williams, C. K. *J. Am. Chem. Soc.* **2018,** *140* (22), 6893-6903.